ON ASTRONOMIC, PHOTOGRAMMETRIC AND TRIGONOMETRIC REFRACTION

BY

AXEL LEIJONHUFVUD

STOCKHOLM 1950

Upberg
Diss. Uppsala
1950

Digitized by the Internet Archive
in 2026

https://archive.org/details/IA41550013_0049

ON ASTRONOMIC, PHOTOGRAMMETRIC AND TRIGONOMETRIC REFRACTION

INAUGURAL DISSERTATION

BY

AXEL LEIJONHUFVUD
Fil. Lic., Sthlm

By due permission of the faculty of philosophy of the university of Uppsala to be publicly discussed in lecture hall 11 of the University House, sept. 23rd, 1950, at 10 A. M., for the degree of doctor of philosophy

R. UNIV.
BIBLIOTHEEK
LEIDEN

ON ASTRONOMIC, PHOTOGRAMMETRIC AND TRIGONOMETRIC REFRACTION

BY

AXEL LEIJONHUFVUD

STOCKHOLM 1950

R. UNIV.
BIBLIOTHEEK
LEIDEN

STOCKHOLM 1950
KUNGL. BOKTRYCKERIET P. A. NORSTEDT & SÖNER
501534

CONTENTS.

Page

Preface 5

I. *Astronomic refraction* 7

Approximations 7

Development of optical density 9

Discussion of lapse-rates 11

Series for the I.C.A.N.-atmosphere 12

Variation with pressure 14

Variation with temperature 15

Variation with lapse-rate 17

Variation with humidity 18

Summary 21

II. *Photogrammetric refraction* 23

The parameter function 23

The parameter of the photogrammetric ray 25

Refraction along the photogrammetric ray 26

Effect of curvature 34

Cancellation effect 36

Effect of variation in conditions 36

Errors at 4 000 m and relative errors 40

A method for measurements 45

III. *Trigonometric refraction* 46

A. Hypothesis based upon known observations of surface inversion ... 46

Initial formulae 46

Lapse-rates at Leafield 46

Discussion of surface inversion 47

Computation of typical stages 48

Result 52

B. Theory based on measurements 56

Experiment stations 56

Taking measurements 56

Effective height 65

Amplitudes 66

Absolute refraction 67

Insolation functions 68

General formulae 69

Diagrams for solution 69

Literature 75

Appendix: Tables 76

PREFACE.

The Director-in-Chief of the Geographical Survey Office of Sweden, V. Hernlund, *Fil. Lic.*, and the management of the office have obligingly supported this work.

For his kind interest in connection with the experiments, I am grateful to the Chief of the Royal Swedish Air Force, General B. Nordenskiöld.

I am especially indebted to the Professor of the Astronomic Observatory of Saltsjöbaden, B. Lindblad, *Fil. Dr.*, the Professor of the Division of Photogrammetry of the Royal Institute of Technology at Stockholm, B. Hallert, *Tekn. Dr.*, and to the Professors of the Geographical Survey Office, G. A. Rune, *Fil. Dr.*, and L. Asplund, *Tekn. Dr.*, for advice regarding chapters I, II and III respectively.

Mr. R. Mc Naughton has made a valuable linguistic revision.

To all others who have encouraged the work I owe a debt of gratitude.

†1—501534

I. Astronomic refraction.

Approximations.

The zone of zenith-distance treated is from 0° to 60°.
If

R = astronomic refraction,
K = a function of atmospheric conditions,
z = observed zenith-distance, regarded as the true distance and
$R = K \cdot \operatorname{tg} z$,

we have defined two errors, ε_1 and ε_2.

The error ε_1, when using the observed zenith-distance as the true distance, can be written

$$\varepsilon_1 = R \frac{\Delta \operatorname{tg} z}{\operatorname{tg} z}$$

and has the following values:

z°	10	20	30	40	50	60
ε_1''	0.000	0.000	0.000	0.000	— 0.001	— 0.001

at 0° and 760 mm, which is why we disregard it for these steep rays.

The error ε_2, when using the expression $R = K \operatorname{tg} z$, is the effect of the curvature of atmospheric layers.

Denomination,

r = Radius vector from the centre of the earth to the ray.
r_1 = » » » » » » » » » » instrument.
n = index of refraction in the ray.
n_1 = » » » at the instrument.
z_1 = zenith-distance at the instrument.

We have, according to Pernter and Exner [1]

$$r_1 n_1 \sin z_1 = \text{constant} = c;$$

then

$$R = \int_1^{n_1} \frac{c}{\sqrt{n^2 r^2 - c^2}} \cdot \frac{dn}{n}$$

and

$$\varepsilon_2 = K \operatorname{tg} z_1 - \int_1^{n_1} \frac{c}{\sqrt{n^2 r^2 - c^2}} \cdot \frac{dn}{n}$$

Calculated according to E. and B. Strömgren's tables, based on observations at Poulkowa [2], we obtain

z°	10	20	30	40	50	60
ε_2''	0.00	+ 0.01	+ 0.02	+ 0.05	+ 0.14	+ 0.36

As is shown below, ε_2 corresponds to the effect of variations in absolute temperature at sea level no larger than

z°	10	20	30	40	50	60
T° C	0.0	0.0	0.1	0.2	0.7	1.8

resulting from the lack of homogeneity of the air-mass, which lies well within the spread of this factor at ground level. This is one reason to disregard ε_2.

Moreover, as the limits of integration will shrink with increasing height (h) at the same rate for R and ε_2,

$$\lim_{h \to 10} R \approx \tfrac{1}{3} (R)_{h=0} \quad .$$ (see page 12)

gives

$$\lim_{h \to 10} \varepsilon_2 \approx \tfrac{1}{3} (\varepsilon_2)_{h=0}$$

and a method to compute ε_2, if necessary, with the data given above.

For these reasons, however, it seems acceptable to disregard ε_2 and its customary development to the advantage of the more important development of optical density with variations.

Development of optical density.

Let a = gas constant
g = constant of gravity
g_o = » » » mean, at sea level
T = absolute temperature
T_o = » » at sea level
p = pressure
p_o = » at sea level
θ = density
θ_o = » at sea level
β = numerical value of lapse-rate of temperature, in degrees C/100 m.
h = height in hundreds of *dynamic* meters.

For a dry atmosphere with the lapse-rate β the fundamental equation, as formed for the troposphere by Brunt [3], is

$$\frac{T_o - \beta h}{T_o} = \left(\frac{p}{p_o}\right)^{\frac{a\beta}{g}}$$

The value of p is

$$p = p_o \left(\frac{T_o - \beta h}{T_o}\right)^{\frac{g}{a\beta}}$$

This formula is only valid below the tropopause. The troposphere is the zone concerned for photogrammetric surveying and also the highest for ordinary astronomic observations. It will then be sufficient to deal with altitudes up to 10 km.

Accepting the two approximations ε_1 and ε_2 above, and assuming a linear lapse-rate in the troposphere, treated in more detail below, we can use a very simple form of the refraction integral, used by Newcomb [17 a]

$$R = c \int_0^{\theta_o} \operatorname{tg} z \, d\theta$$

where $c = 0.22607$ for the D-line.

Thus

$$K = 0.22607\, \theta_o$$

$$= 0.22607 \frac{0.35111}{T} \cdot \frac{p}{p_o (1 + \lambda t)} \cdot \frac{g}{g_o}.$$

Furthermore, as in the premises dynamic height is used, for which

$$h_{\text{dyn}} = 10^{-1} \int_0^h g \, dh_{\text{length}},$$

we obtain the result $\frac{g}{g_o} = 1$.

Then

$$K = 0.00010444 \frac{p}{T} \quad (R \text{ in radians})$$

$$K = 21.54 \frac{p}{T}. \qquad (R \text{ in seconds of arc})$$

In the series only the first term is used for the value at ground level. (See Series for I.C.A.N. atmosphere on page 12).

With the value 21.54 for the constant in K we obtain the normal refraction 56".84. This theoretical value ought to be compared with the observed values in Greenwich, Cape and Leiden, reduced by Oort [28], and in Kiel by Harzer [27] after very careful computations.

Taking the mean of

	Greenwich	Cape	Leiden	Kiel	Theor
Weight	3	1	1	1	1
	57".94	58".03	57".80	58".21	56".84

we get

57".82

which means

$$K = 21.91 \frac{p}{T}.$$

As

$$T = T_o - \beta h,$$

we can write

$$K = 21.91 \frac{p_o}{T_o - \beta h} \left(\frac{T_o - \beta h}{T_o} \right)^{\frac{g}{\alpha \beta}},$$

or reduced, with h in km,

$$K = 21.91 \frac{p_o}{T_o} \left(1 - \frac{10 \beta h}{T_o} \right)^{\left(\frac{g}{\alpha \beta} - 1 \right)},$$

with which the development of optical density in the troposphere is determined without any pressure or temperatures other than the initial ones at

ground level, at a given lapse-rate, for dry air. This expression is not suitable for practical use and has to be developed into series, varying in accordance with the values of all variables, including humidity.

Discussion of lapse-rates.

Recent researches in the higher atmosphere by Jaumotte [4], Köhler [31], and others show that the termic conditions in the troposphere to a certain extent conform to Ivory's hypothesis, but in the lower stratosphere to Newton's hypothesis.

Modifications of the former hypothesis were made early by Bouguer, Simpson and Bradley, and of the latter the best-known modification was by Bessel. It is natural that none of these classical theories cover the results of modern soundings, as seen in the formulae for p and T in the troposphere related by Brunt [3] above.

In 1931 Plummer [30] suggested one »nitrogen» atmosphere between 2.6 and 19.7 km and one »oxygen» atmosphere below 2.6 km. In reality the proportions between nitrogen and oxygen have proved to be constant with height to an astonishing degree as shown by Paneth [29].

It is of utmost importance here to note the differences between mean annual lapse-rate, cloud inversion, and lapse-rate for a clear day or night. The three types are shown in the following schematical figure:

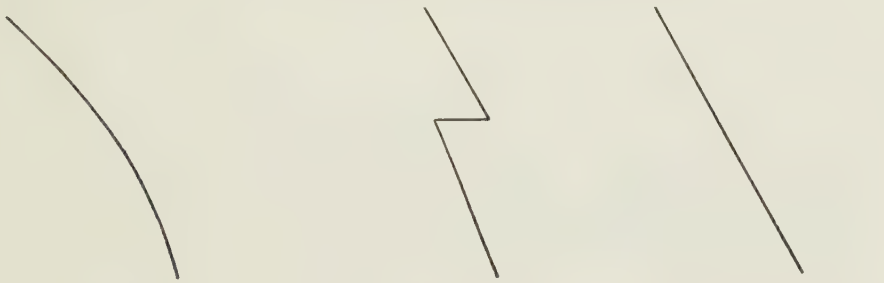

Mean annual lapse-rate | Cloud inversion | Lapse-rate for clear day or night

The works of Gast [5], Hughes [6] and Ramsayer [7] are based on the first type, partly using Dines' annual means over Lindesberg. As this type is a mean of the climatical data of the two others, it is not accepted in this essay for the following reason:

An astronomic or photogrammetric observation (from air-craft) is never made with mean annual lapse-rate and very seldom with cloud inversion.

This fact not only permits but obliges us to use linear lapse-rate for astronomical and photogrammetrical purposes.

For trigonometric refraction it is necessary to consider the ground inversion as shown in the chapter on that subject.

There are several values suggested for the lapse-rate of temperature, from Ivory's 0.525, Bauernfeind's 0.543, Schmidt's and Bauernfeind's 0.57 and Radau's [26] 0.515 to the value accepted for a »normal atmosphere» by the International Comission for Air Navigation, 0.65° C per 100 m.

This atmosphere is called the I.C.A.N. atmosphere and has initial values of pressure of about 760 mm and an absolute temperature of 288. In the following series both the initial values and the lapse-rate are varied to all possible values.

Series of the I.C.A.N.-atmosphere.

For the I.C.A.N. atmosphere we get the formula

$$K = 21.91 \frac{760}{288}\left(1 - \frac{6.5h}{288}\right)^{\frac{3.4165}{0.65}-1}.$$

Using a function-series of the Mac Laurin type, where

$$f(x) = f(x)_o + \frac{x}{1!}\frac{df(x)_o}{dx} + \frac{x^2}{2!}\frac{d^2f(x)_o}{dx^2} + \frac{x^3}{3!}\frac{d^3f(x)_o}{dx^3} + \ldots + \frac{x^n}{n!}\frac{d^nf(x)_o}{dx^n}$$

we obtain

$$K = 57.818 - \frac{5.5539}{1!}h + \frac{0.4081}{2!}h^2 - \frac{0.0208}{3!}h^3 + \frac{0.0006}{4!}h^4 - \frac{0.000003}{5!}h^5 + \ldots$$

As the term h^5 only reaches 0.″0043 when $h = 10$ km and $z = 60°$, it can be disregarded. With the same conditions h^4 reaches 0.″43. With decimals for 0.″01 at 10 km we get

$$K = 57.82 - 5.554\,h + 0.2040\,h^2 - 0.00347\,h^3 + 0.000025\,h^4$$

which gives, when $z = 45° = 50^c$,

h^{km} ..	0	1	2	3	4	5	6	7	8	9	10
R'' ...	57.82	52.47	47.50	42.90	38.65	34.73	31.12	27.81	24.77	21.99	19.46

A comparison between these values and the results of Gast [5], Hughes [6] and Ramsayer [7] is made in the following table and fig. 1, where the I.C.A.N. values are used as the axis.

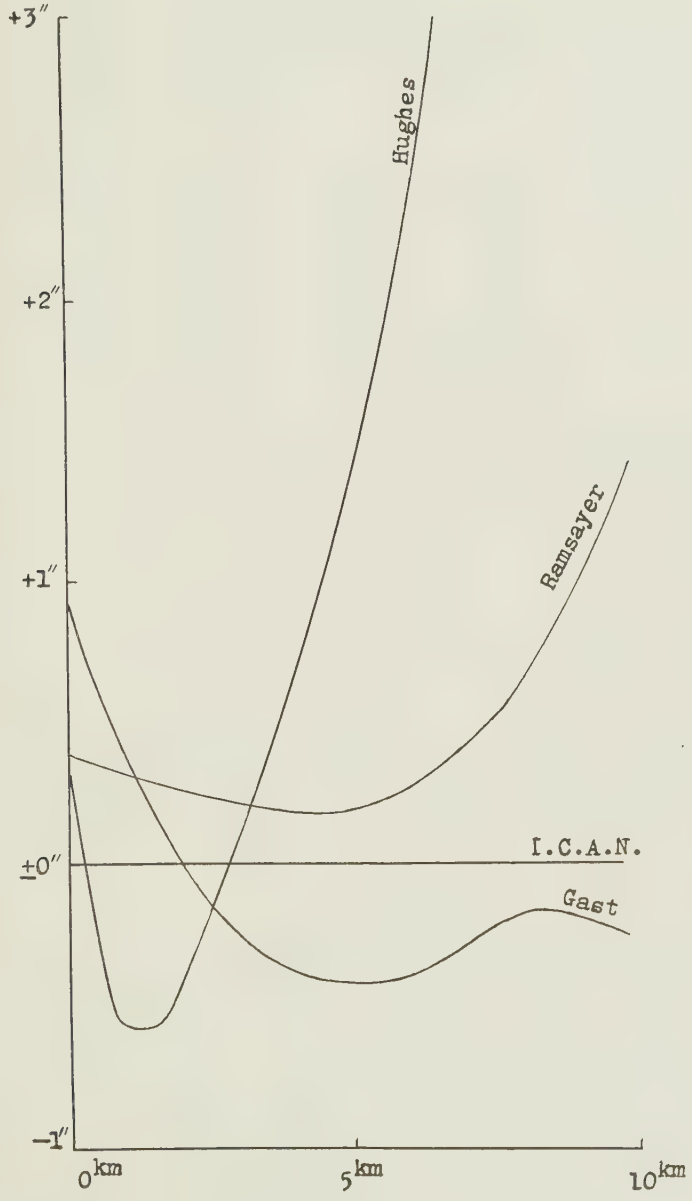

Fig. 1.

	Gast	Hughes (Ramsayer)	Ramsayer	I.C.A.N.
P mm	762	760	760	760
$T°$ A	281	283	283	288
$\beta°$ C	0.4—0.8		0.5—0.7	0.65
Height				
0 km	58.8	58.2	58.2	57.82
1	52.8	51.9	52.8	52.47
2	47.5	47.1	47.8	47.50
3	42.6	43.0	43.1	42.90
4	38.3	39.3	38.9	38.65
5	34.3	36.3	34.9	34.73
6	30.7	33.5	31.4	31.12
7	27.5	31.3	28.2	27.81
8	24.6	29.4	25.4	24.77
9	21.8	27.8	23.0	21.99
10	19.2	26.6	20.9	19.46

The differences are, with the exception of Hughes' values above 5 km, not excessive under normal conditions. They become more evident in varying the elements and, as demonstrated in chapter II, in application to photogrammetric refraction.

Variation with pressure.

Varying the pressure at the rate of — 30 mm, — 10 mm, + 10 mm and + 30 mm, we obtain the series

P_o mm	T_o °A	β °C	$K \approx$
730	288	0.65	$55.54 - 5.335\,h + 0.1960\,h^2 - 0.00333\,h^3 + 0.000025\,h^4$
750	288	0.65	$57.06 - 5.481\,h + 0.2014\,h^2 - 0.00342\,h^3 + 0.000025\,h^4$
770	288	0.65	$58.58 - 5.627\,h + 0.2068\,h^2 - 0.00352\,h^3 + 0.000025\,h^4$
790	288	0.65	$60.10 - 5.773\,h + 0.2122\,h^2 - 0.00360\,h^3 + 0.000025\,h^4$

T_o and β constant,

Variation of $R_{z=45°}$ with pressure at ground level; amplitudes.

h	730	750	760	770	790	Total ampl.	Ampl. per mm
	"						
0 km	55.54	57.06	58.82	58.58	60.10	4.56	0.076
1	50.40	51.78	52.47	53.16	54.54	4.14	0.069
2	45.63	46.88	47.50	48.13	49.37	3.74	0.062
3	41.21	42.34	42.90	43.47	44.60	3.39	0.057
4	37.13	38.15	38.65	39.16	40.18	3.05	0.051
5	33.36	34.66	34.73	35.19	36.11	2.75	0.046
6	29.90	30.72	31.12	31.53	32.36	2.46	0.041
7	26.72	27.45	27.81	28.18	28.91	2.19	0.037
8	23.80	24.46	24.77	25.10	25.76	1.96	0.033
9	21.14	21.72	21.99	22.29	22.87	1.73	0.029
10	18.71	19.22	19.46	19.72	20.24	1.53	0.026

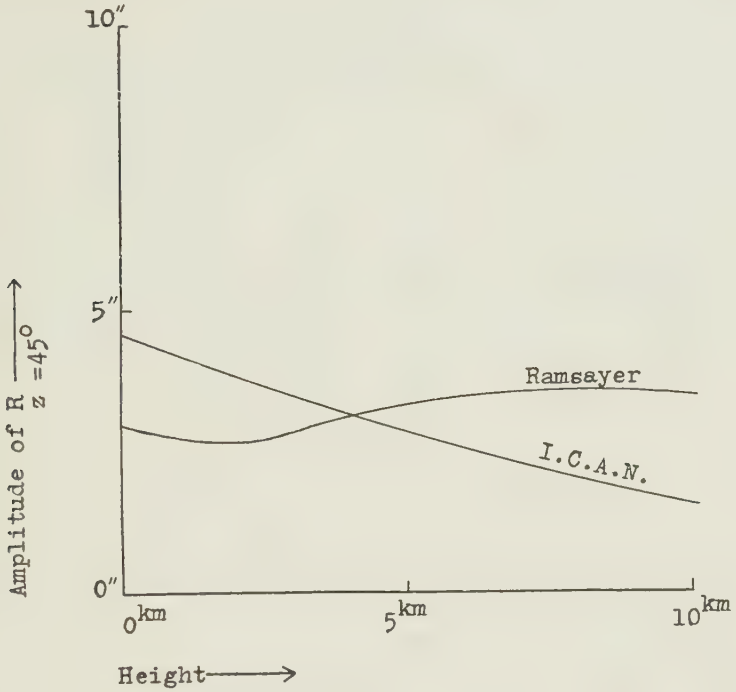

Fig. 2.

The amplitude of R at the different heights for a variation in pressure of 60 mm when $h = 0$ is indicated in fig. 2, which also shows the values for a 40 mm variation when $h = 0$ and corresponding differences at other heights after Ramsayer.

Variation with temperature.

Temperature is varied in the same way, at the rate of — 30° C, — 10° C, + 10° C and + 30° C.

P_o mm	T_o °A	β °C	$K \approx$
760	258	0.65	$64.54 - 6.919\,h + 0.2838\,h^2 - 0.00538\,h^3 + 0.000042\,h^4$
760	278	0.65	$59.90 - 5.960\,h + 0.2268\,h^2 - 0.00398\,h^3 + 0.000029\,h^4$
760	298	0.65	$55.88 - 5.187\,h + 0.1842\,h^2 - 0.00302\,h^3 + 0.000021\,h^4$
760	318	0.65	$52.36 - 4.555\,h + 0.1516\,h^2 - 0.00233\,h^3 + 0.000017\,h^4$

P_0 and β constant,

Variation of $R_{z=45°}$ with temperature at ground level; amplitudes.

h	258	278	288	298	318	Total ampl.	Ampl. per mm
	"						
0 km	64.54	59.90	57.82	55.88	52.36	12.18	0.203
1	57.90	54.16	52.47	50.87	47.95	9.95	0.166
2	51.79	48.86	47.50	46.22	43.84	7.95	0.132
3	46.20	43.96	42.90	41.90	40.00	6.20	0.103
4	41.07	39.44	38.65	37.89	36.42	4.65	0.077
5	36.39	35.29	34.73	34.19	33.09	3.30	0.054
6	32.14	31.48	31.12	30.76	30.01	2.13	0.035
7	28.27	28.00	27.81	27.61	27.15	1.12	0.019
8	24.77	24.82	24.77	24.71	24.50	0.97	0.004
9	21.61	21.92	21.99	22.05	22.06	0.45	0.007
10	18.77	19.29	19.46	19.62	19.81	1.04	0.017

Fig. 3.

The amplitude of R for a variation in temperature of 60° C when $h = 0$ is indicated in fig. 3, together with the values for a 62° — variation when $h = 0$, and corresponding differences at other heights after Ramsayer.

The investigations by Dines [25] in correlation between variables at different heights show that the correlation between temperature at ground and at tropopause is small.

Even the correlation between mean temp. from 1 to 9 km and temp. at tropopause is only 0.37.

As astronomic refraction is most sensitive to variations in the layers immediately above the observation point, we have to expect that refraction immediately below the tropopause will be independent of variations in temperature at ground level, which seems to agree with the obtained result.

Variation with lapse-rate.

The lapse-rate of temperature is varied — 0°.30 C, — 0°.10 C, + 0°.10 C and + 0°.30 C from the standard value (numerically 0°.65 C/100 m).

P_o mm	T_o °A	β °C	$K \approx$
760	288	0.35	$57.82 - 6.154\,h + 0.2902\,h^2 - 0.00795\,h^3 + 0.000138\,h^4$
760	288	0.55	$57.82 - 5.756\,h + 0.2315\,h^2 - 0.00473\,h^3 + 0.000050\,h^4$
760	288	0.75	$57.82 - 5.352\,h + 0.1780\,h^2 - 0.00240\,h^3 + 0.000008\,h^4$
760	288	0.95	$57.82 - 4.951\,h + 0.1304\,h^2 - 0.00085\,h^3$

P_o and T_o constant,

Variation of $R_{z=45°}$ with lapse-rate; amplitudes.

h	0.35	0.55	0.65	0.75	0.95	Total ampl.	Ampl. per 0°.01
	"						
0 km	57.82	57.82	57.82	57.82	57.82	0.00	0.000
1	51.95	52.29	52.47	52.64	53.00	1.05	0.018
2	46.61	47.20	47.50	47.81	48.43	1.82	0.030
3	41.77	42.51	42.90	43.30	44.12	2.35	0.039
4	37.37	38.21	38.65	39.11	40.05	2.68	0.045
5	33.40	34.27	34.73	35.22	36.22	2.02	0.047
6	29.80	30.66	31.12	31.61	32.62	2.82	0.047
7	26.57	27.37	27.81	28.27	29.26	2.69	0.045
8	23.66	24.37	24.77	25.20	26.12	2.46	0.041
9	21.05	21.65	21.99	22.37	23.20	2.15	0.036
10	18.73	19.18	19.46	19.78	20.50	1.77	0.030

The influence of lapse-rate is compared with that of absolute temperature in fig. 4.

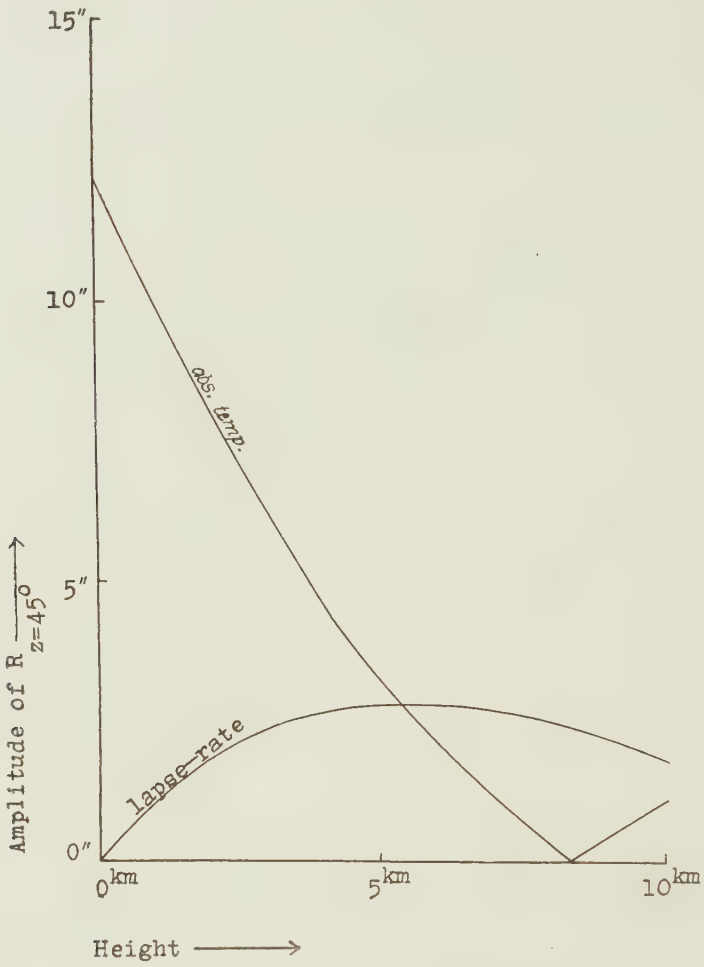

Fig. 4.

Variation with humidity.

According to Dalton's law, vapour pressure is independent of dry air pressure in the same mixture. This fact turns the study of optical density with regard to humidity, into a study of temperature.

Brunt [8] has given one of the later methods to obtain the relationship between temperature and optical density, and compares the results of Gladstone and Dale [9], Jamin [10], Lorentz [11] and Pérard [12], giving the following equation:

$$T'' = T\left(1 + \frac{\mu_1 - \mu_2}{\mu_1 - 1} \cdot \frac{e}{p}\right).$$

where

e = pressure of water vapour in mm
μ_1 = index of refraction of the dry air
μ_2 = » » » » » water vapour
T = absolute temperature of dry air
T'' = temperature at which the mixture has the same index of refraction as the dry air at T.

This temperature is called »optical temperature» in the following discussion. It is to be noted that Brunt gives one value of μ_2, based on Kaye and Laby's tables [13], namely 1.000257.

Lorentz's own measurements gave 1.000250. The result of this difference is slight but obvious, as proved in the tables below. μ_1 is in both cases 1.000292.

The maximum pressure of water vapour, known as saturation pressure, is dependent upon temperature and gives an upper limit to optical temperature, at each temperature.

As seen from the tables and figures, humidity has influence only at high temperatures, and the amplitude for variations has been chosen at 100 % relative humidity, to get observable results on refraction.

The series for saturated air have been computed with optical temperature, and the results individually compared with corresponding series for dry air.

Only the series for 298° A and 318° A have been computed with both values of μ_2.

μ_2	e_{max} mb	T_o opt. °A	P_o mm	T_o °A	β °C	$K \approx$
1.00257	1.91	258.06	760	258	0.65	$64.53 - 6.918\ h + 0.2837\ h^2 - 0.00537\ h^3 + 0.000042\ h^4$
	8.72	278.29	760	278	0.65	$59.84 - 5.949\ h + 0.2262\ h^2 - 0.00397\ h^3 + 0.000029\ h^4$
	17.05	288.59	760	288	0.65	$57.70 - 5.530\ h + 0.2028\ h^2 - 0.00343\ h^3 + 0.000025\ h^4$
	31.68	299.13	760	298	0.65	$55.67 - 5.148\ h + 0.1821\ h^2 - 0.00298\ h^3 + 0.000021\ h^4$
	95.84	321.65	760	318	0.65	$51.77 - 4.453\ h + 0.1465\ h^2 - 0.00223\ h^3 + 0.000012\ h^4$
1.00250	31.68	299.36	760	298	0.65	$55.62 - 5.140\ h + 0.1816\ h^2 - 0.00297\ h^3 + 0.000021\ h^4$
	95.84	322.39	760	318	0.65	$51.65 - 4.432\ h + 0.1454\ h^2 - 0.00220\ h^3 + 0.000012\ h^4$

Variation of $R_{z=45°}$ with humidity.

h km	$\mu_2 = 1.000257$										$\mu_2 = 1.000250$	
	258°		278°		288°		298°		318°		298°	318°
	$e = 0$	$e =$ max	$e = 0$	$e =$ max	$e = 0$	$e =$ max	$e = 0$	$e =$ max	$e = 0$	$e =$ max	$e =$ max	$e =$ max
	″											
0	64.54	64.53	59.90	59.84	57.82	57.70	55.88	55.67	52.36	51.77	55.62	51.65
1	57.90	57.89	54.16	54.11	52.47	52.37	50.87	50.70	47.95	47.46	50.66	47.36
2	51.79	51.79	48.86	48.82	47.50	47.42	46.22	46.08	43.84	43.43	46.04	43.35
3	46.20	46.19	43.96	43.92	42.90	42.84	41.90	41.79	40.00	39.67	41.76	39.60
4	41.07	41.06	39.44	39.42	38.65	38.61	37.89	37.81	36.42	36.16	37.78	36.11
5	36.39	36.39	35.29	35.27	34.73	34.71	34.19	34.12	33.09	32.90	34.10	32.85
6	32.14	32.13	31.48	31.47	31.12	31.11	30.76	30.72	30.01	29.86	30.70	29.83
7	28.27	28.26	28.00	27.99	27.81	27.81	27.61	27.58	27.15	27.04	27.57	27.02
8	24.77	24.77	24.82	24.81	24.77	24.79	24.71	24.70	24.50	24.43	24.69	24.42
9	21.66	21.61	21.92	21.92	21.99	22.02	22.05	22.05	22.06	22.01	22.04	22.01
10	18.77	18.77	19.29	19.29	19.46	19.50	19.62	19.63	19.81	19.78	19.62	19.79

Amplitudes.

h km	$\mu_2 = 1.000257$										$\mu_2 = 1.000250$	
	258°		278°		288°		298°		318°		298°	318°
	total ampl.	ampl. per %	total ampl.	ampl. per %	total ampl.	ampl. per %	total ampl.	ampl. per %	total ampl.	ampl. per %	total ampl.	total ampl.
	″											
0	0.01		0.06	0.001	0.12	0.001	0.21	0.002	0.59	0.006	0.26	0.71
1	0.01		0.05		0.10	0.001	0.17	0.002	0.49	0.005	0.21	0.59
2			0.04		0.08	0.001	0.14	0.001	0.41	0.004	0.18	0.49
3	0.01		0.04		0.06	0.001	0.11	0.001	0.33	0.003	0.14	0.40
4	0.01		0.02		0.04		0.08	0.001	0.26	0.003	0.11	0.31
5			0.02		0.02		0.07	0.001	0.19	0.002	0.09	0.24
6	0.01		0.01		0.01		0.04		0.15	0.002	0.06	0.18
7	0.01		0.01				0.02		0.11	0.001	0.04	0.13
8			0.01		0.02		0.01		0.07	0.001	0.02	0.08
9					0.03				0.05		0.01	0.05
10					0.04		0.01		0.03			0.02

Fig. 5 shows the influence of maximal variations in humidity at different temperatures, with the values for $\mu_2 = 1.000250$ in dotted lines.

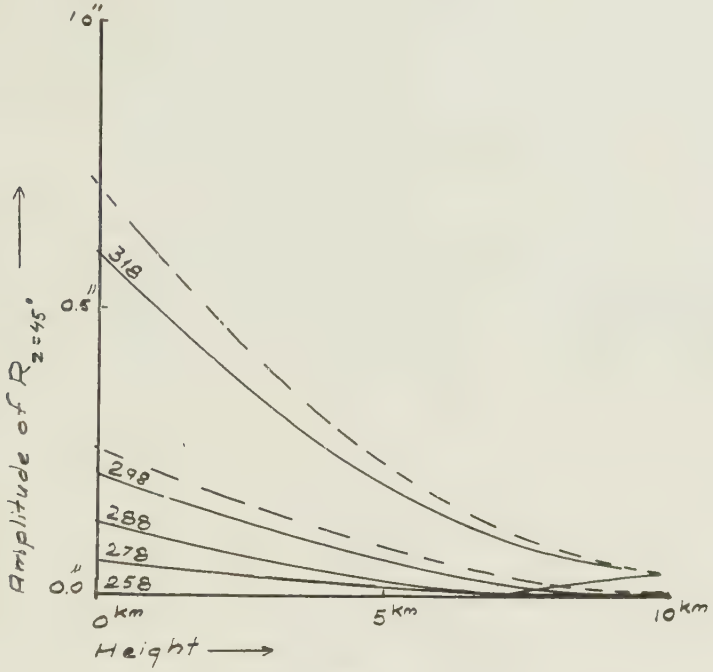

Fig. 5.

Summary.

These amplitudes ought to be compared with the spread values obtained by Bauschinger [14], Courvoisier [15] and later by Bohrmann [16], about $\pm 0''.2$ when $z = 30°$ and about $\pm 0''.5$ when $z = 60°$. This error, here called ε_3, is about $\pm 0.008 \cdot z$.

In the foregoing discussion, β was varied but assumed constant up to $h = 10$ km in each instance.

Other conditions demand two postulates for the computation, a sounding or other temperature measurements of equal value and a function $F(h)$, deduced from these, to replace β.

If $F(h)$ is known and optical temperature is used with regard to humidity, a more strict formula can be obtained:

$$R = 21.91 \frac{p_o}{T''} \left(1 - \frac{10\,h \cdot F(h)}{T''}\right)^{\frac{g}{aF(h)}} - \varepsilon_1 - \varepsilon_2 \pm \varepsilon_3$$

where

$$T'' = T\left(1 + \frac{\mu_1 - \mu_2}{\mu_1 - 1} \cdot \frac{e}{p}\right)$$

Temperature has obviously the largest effect upon refraction. The older developments of density with height were made without knowlidge of temperature and pressure lapse-rates, and thus were regarded as hypotheses.

This is the case with the hypothesis made by de Ball [17 b],

$$t_o - t = C\,(r_o - r)\,,$$

where t_o, r_o are the initial values of temperature and density and t, r are corresponding values for a certain height, with C a constant.

This constant varies in reality between 31 and 43 from 5 to 10 km. in the standard atmosphere.

II. Photogrammetric refraction.

The parameter function.

Each photogrammetric ray in the zone from $z = 0°$ to $z = 60°$ can be regarded as the beginning of an astronomic ray of the types treated in the previous section. If the function for the ray-path is known up to a height of 10 km, it would be possible to obtain the photogrammetric ray-path as well.

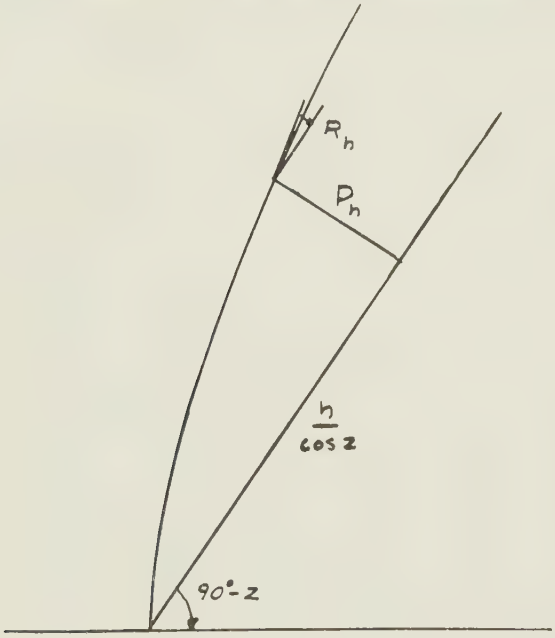

Fig. 6.

For this purpose we introduce the function for the distance between an astronomic ray in the atmosphere and in a vacuum and call it P. As seen from fig. 6, the vacuum-ray and the parameter P together give a system for the determination of the ray-path.

In this system, where the parameter corresponding to a certain height h has the distance from origin of $\frac{h}{\cos z}$ and each apparent direction in the ray-path is a tangent to the P-curve,

$$\frac{dP}{dh}\cos z = \operatorname{tg} R$$

and

$$P = \frac{1}{\cos z}\int \operatorname{tg} R\,dh + c$$

which means that P is an integral function to R.

An integration of standard series for R in radians, and z in degrees centesimal,

$$P = 10^{-7}\,\frac{\operatorname{tg} z}{\cos z}\int (2\,803.11 - 269.258\,h + 9.8899\,h^2 - 0.16823\,h^3 + \\ + 0.001212\,h^4)\,dh + C,$$

gives

$$C = 0 \quad \text{when } P = 0; \quad h = 0$$

and

$$P = 10^{-7}\frac{\operatorname{tg} z}{\cos z}(2\,803.11\,h - 134.629\,h^2 + 3.2966\,h^3 - 0.04205\,h^4 + \\ + 0.000242\,h^5).$$

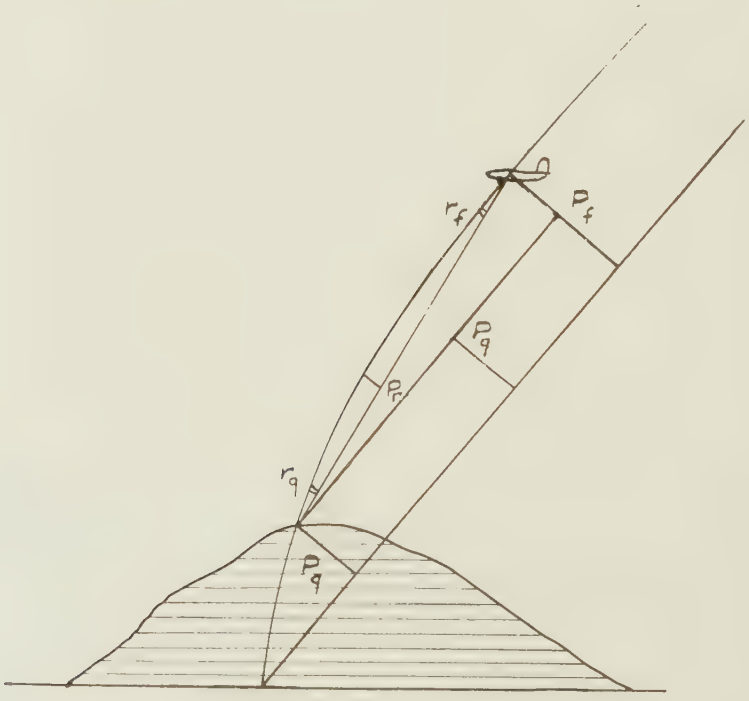

Fig. 7.

P is measured in km.

When $z = 50^c$ and $h = 10$ km, P has the value 2.47 m.

This is valid for a ground level of 0 km.

Over a ground level of h_g km the parameter at the flight level h_f is the difference between the two parameters $P_f - P_g$, as seen from figure 7.

The table below shows the values of

$$10^{+3} \frac{\cos z}{\operatorname{tg} z} (P_f - P_g)$$

for ground levels between 0.0 km and 2.5 km.

(For direct computations, however, it is necessary to use 6 decimal places.)

$$10^{+3} \frac{\cos z}{\operatorname{Tg} z} (P_f - P_g)$$

h_f	h_g					
	0.0 km	0.5	1.0	1.5	2.0	2.5
0.0 km	0.000 m					
0.5	0.137	0.000				
1.0	0.267	0.130	0.000			
1.5	0.391	0.254	0.124	0.000		
2.0	0.509	0.373	0.242	0.118	0.000	
2.5	0.622	0.455	0.354	0.230	0.112	0.000
3.0	0.728	0.592	0.461	0.337	0.219	0.107
3.5	0.830	0.693	0.563	0.438	0.320	0.208
4.0	0.926	0.789	0.659	0.535	0.417	0.304
4.5	1.017	0.880	0.750	0.626	0.508	0.396
5.0	1.104	0.967	0.836	0.712	0.594	0.482
5.5	1.186	1.049	0.918	0.794	0.676	0.564
6.0	1.263	1.126	0.996	0.872	0.754	0.642
6.5	1.337	1.200	1.069	0.945	0.827	0.715
7.0	1.406	1.269	1.139	1.015	0.897	0.784
7.5	1.471	1.335	1.204	1.080	0.962	0.850
8.0	1.533	1.396	1.266	1.142	1.024	0.912
8.5	1.592	1.455	1.324	1.200	1.082	0.970
9.0	1.646	1.510	1.379	1.255	1.137	1.025
9.5	1.698	1.561	1.431	1.307	1.189	1.077
10.0	1.747	1.610	1.480	1.356	1.238	1.125

The parameter of the photogrammetric ray.

If this parameter is called P_r, and the astronomic parameter at the same height h as before is called P, h for this individual ray can have values between the ground level h_g and the flight level h_f.

Furthermore, it is readily seen from fig. 7 that

$$P_r = P - P_g - \frac{h - h_g}{h_f - h_g}(P_f - P_g).$$

The maximal value of P_r is to be found at the height where

$$\frac{dP_r}{dh} = 0;$$

that is,

$$\frac{dP}{dh} = \frac{P_f - P_g}{h_f - h_g},$$

but

$$\frac{dP}{dh} = \frac{\operatorname{tg} R}{\cos z};$$

then

$$0.000004848 \cdot 57.818\ (1 - 0.02257\ h)^{4.256}\ \frac{\operatorname{tg} z}{\cos z} = \frac{P_f - P_g}{h_f - h_g},$$

when R is in " and z is in ^{c}.

This gives the height in km, where (P_r) max is situated, as

$$h = 44.3066 - 302.8843 \left(\frac{\cos z}{\operatorname{tg} z}\ \frac{P_f - P_g}{h_f - h_g}\right)^{0.235}.$$

If the nadir distance = 50^c

h_f km	1	2	3	4	5	6	7	8	9	10
h km	0.4965	0.9872	1.4715	1.9488	2.4192	2.8826	3.3385	3.7867	4.2274	4.6600
$(P_r)_{\max}$ m	0.005	0.018	0.034	0.060	0.089	0.122	0.162	0.204	0.249	0.294

Refraction along the photogrammetric ray.

Differentiating the expression for P_r, we find

$$\frac{dP_r}{dh} = \frac{dP}{dh} - \frac{P_r - P_g}{h_f - h_g}$$

but, when R is measured in radians,

$$\frac{dP}{dh} = \frac{R}{\cos z};$$

then

$$\frac{dP_r}{dh} = \frac{R}{\cos z} - \frac{P_f - P_g}{h_f - h_g}.$$

If r is the refraction in the photogrammetric ray-path, measured in radians, then also

$$r = \frac{d P_r}{dh} \cos z$$

and

$$r = \left(\frac{R}{\cos z} - \frac{P_f - P_g}{h_f - h_g} \right) \cos z,$$

measured in "

$$r = \left[R - \varrho \frac{\frac{\cos z}{\operatorname{tg} z} (P_f - P_g)}{h_f - h_g} \right] \operatorname{tg} z \qquad \varrho = 636\,620$$

where R and $\frac{\cos z}{\operatorname{tg} z}(P_f - P_g)$ are already tabulated in the precedent.

The refraction values at ground and at flight level, called ground refraction and photogrammetric refraction, are the limits where

$$r_g = \lim_{h \to h_g} r$$

and

$$r_f = \lim_{h \to h_f} r$$

respectively, of which the latter has the negative sign.

The following table shows the ground refraction and photogrammetric refraction over various ground levels, up to a flight level of 10.0 km, for zenith distance or nadir distance of 50°.

h km	Ground at											
	0 km		0.5 km		1.0 km		1.5 km		2.0 km		2.5 km	
	r_g	r_f	r_g	r_f	r_g	r_f	r_g	r_f	r_g	r_f	r_g	r_f
	"	"										
0	0.0	0.0										
0.5	4.2	4.2	0.0	0.0								
1.0	8.4	8.2	4.1	4.0	0.0	0.0						
1.5	12.4	11.9	8.1	7.9	3.9	3.9	0.0	0.0				
2.0	16.3	15.5	11.9	11.5	7.8	7.6	3.8	3.7	0.0	0.0		
2.5	20.2	18.9	15.7	14.9	11.5	11.1	7.5	7.3	3.6	3.6	0.0	0.0
3.0	23.9	22.2	19.4	18.2	15.1	14.4	11.1	10.6	7.2	7.0	3.5	3.5
3.5	27.5	25.2	23.0	21.3	18.7	17.5	14.6	13.8	10.6	10.2	6.9	6.7
4.0	31.1	28.1	26.5	24.2	22.2	20.5	18.0	16.8	14.0	13.3	10.2	9.8
4.5	34.6	30.8	29.9	27.0	25.5	23.3	21.3	19.7	17.3	16.2	13.5	12.8
5.0	37.9	33.3	33.3	29.6	28.8	25.9	24.6	22.4	20.5	18.9	16.6	15.6
5.5	41.2	35.7	36.5	32.0	32.0	28.4	27.7	24.9	23.6	21.5	19.7	18.2
6.0	44.4	38.0	39.7	34.3	35.1	30.8	30.8	27.3	26.6	23.9	22.7	20.6
6.5	47.6	40.1	42.8	36.5	38.2	33.0	33.8	29.5	29.6	26.2	25.6	23.0
7.0	50.6	42.0	45.8	38.5	41.1	35.0	36.7	31.6	32.4	28.3	28.4	25.1
7.5	53.6	43.9	48.7	40.3	44.0	36.9	39.5	33.6	35.2	30.3	31.2	27.2
8.0	56.4	45.6	51.5	42.1	46.8	38.7	42.3	35.4	38.0	32.2	33.8	29.1
8.5	59.3	47.1	54.3	43.7	49.5	40.4	45.0	37.1	40.6	33.9	36.5	30.8
9.0	62.0	48.6	57.0	45.2	52.2	41.9	47.6	38.7	43.2	35.6	39.0	32.5
9.5	64.7	49.9	59.6	46.6	54.8	43.3	50.1	40.1	45.7	37.0	41.5	34.0
10.0	67.2	51.2	62.2	47.8	57.3	44.6	52.6	41.5	48.1	38.4	43.9	35.5

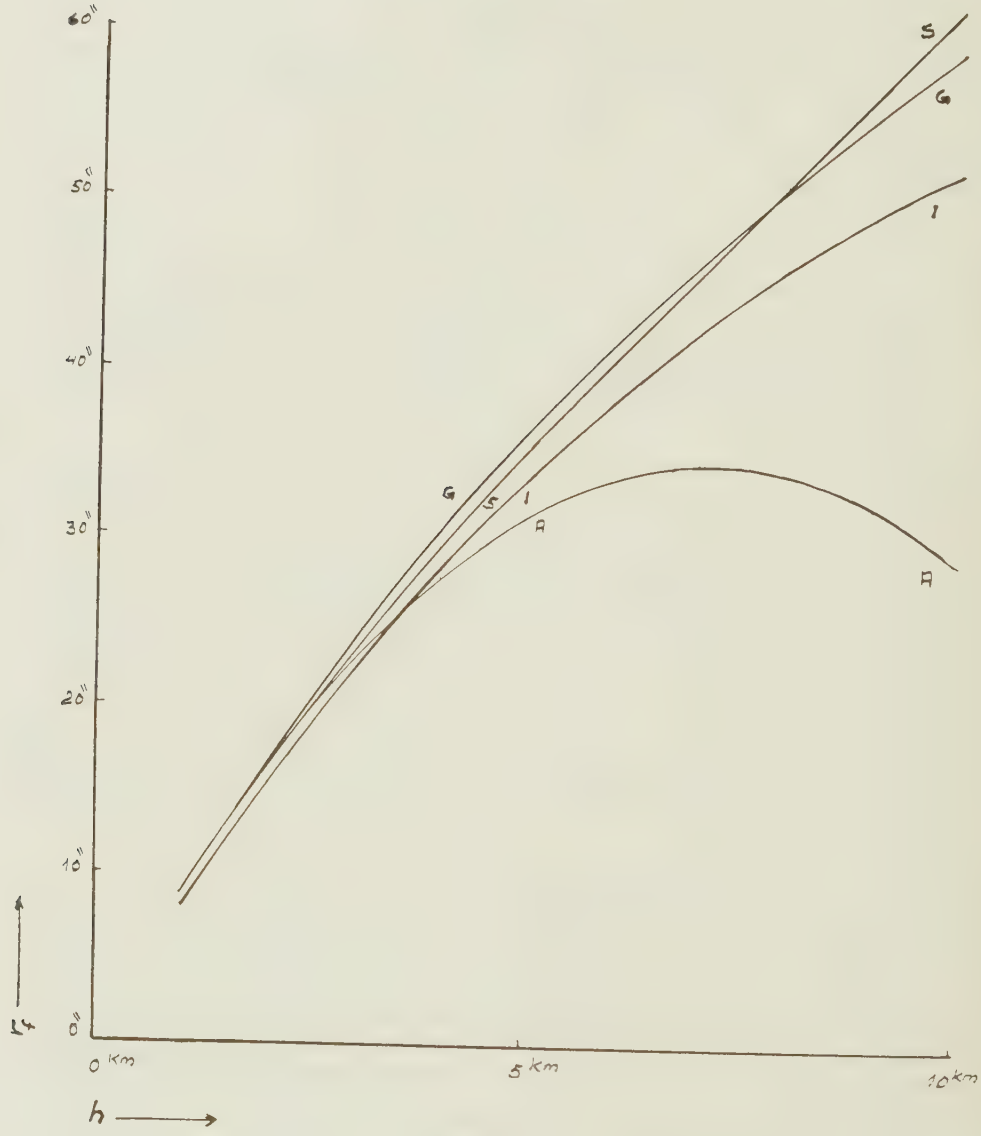

Fig. 8

A comparison between these and the values obtained by Aschenbrenner [18], Schütte [19] and Gast [5] for the nadir distance of 50^c follows:

r_f-values.

h	I	A	S	G
1	8.2	8.9	8.9	8.7
2	15.5	16.5	16.6	16.6
3	22.2	22.7	23.2	23.7
4	28.1	27.6	29.3	30.1
5	33.3	31.1	35.0	36.0
6	38.0	33.3	40.4	41.2
7	42.0	34.1	45.5	45.9
8	45.6	33.7	50.6	50.3
9	48.6	31.8	55.7	54.5
10	51.2	28.7	60.8	58.3

and can also be seen in fig. 8.

r_g-values.

h	I	A	S	G
1	8.4	9.2	8.9	9.8
2	16.3	17.8	16.6	18.3
3	23.9	25.7	23.2	26.3
4	31.1	32.9	29.3	33.2
5	37.9	39.5	35.0	39.7
6	44.4	45.3	40.4	45.5
7	50.6	50.6	45.5	50.7
8	56.4	55.1	50.6	55.2
9	62.0	59.0	55.7	59.7
10	67.2	62.2	60.8	63.9

see fig. 9.

I = Values with I.C.A.N. atmosphere.
A = » after Aschenbrenner.
S = » » Schütte.
G = » » Gast.

Schütte approximates $r_f \approx r_g$, which gives maximum of r_f and minimum values of r_g, as seen from the figures.

The principal test of the sum $r_f + r_g$ is that it should be equal to $R_g - R_f$, demonstrated geometrically by Schütte [19].

This test gives good result for the values, I, S and G. For A it seems improbable above 5 km. Thus, for a height of 10 km the sums are

I = 118.4
A = 90.9
S = 121.6
G = 122.2

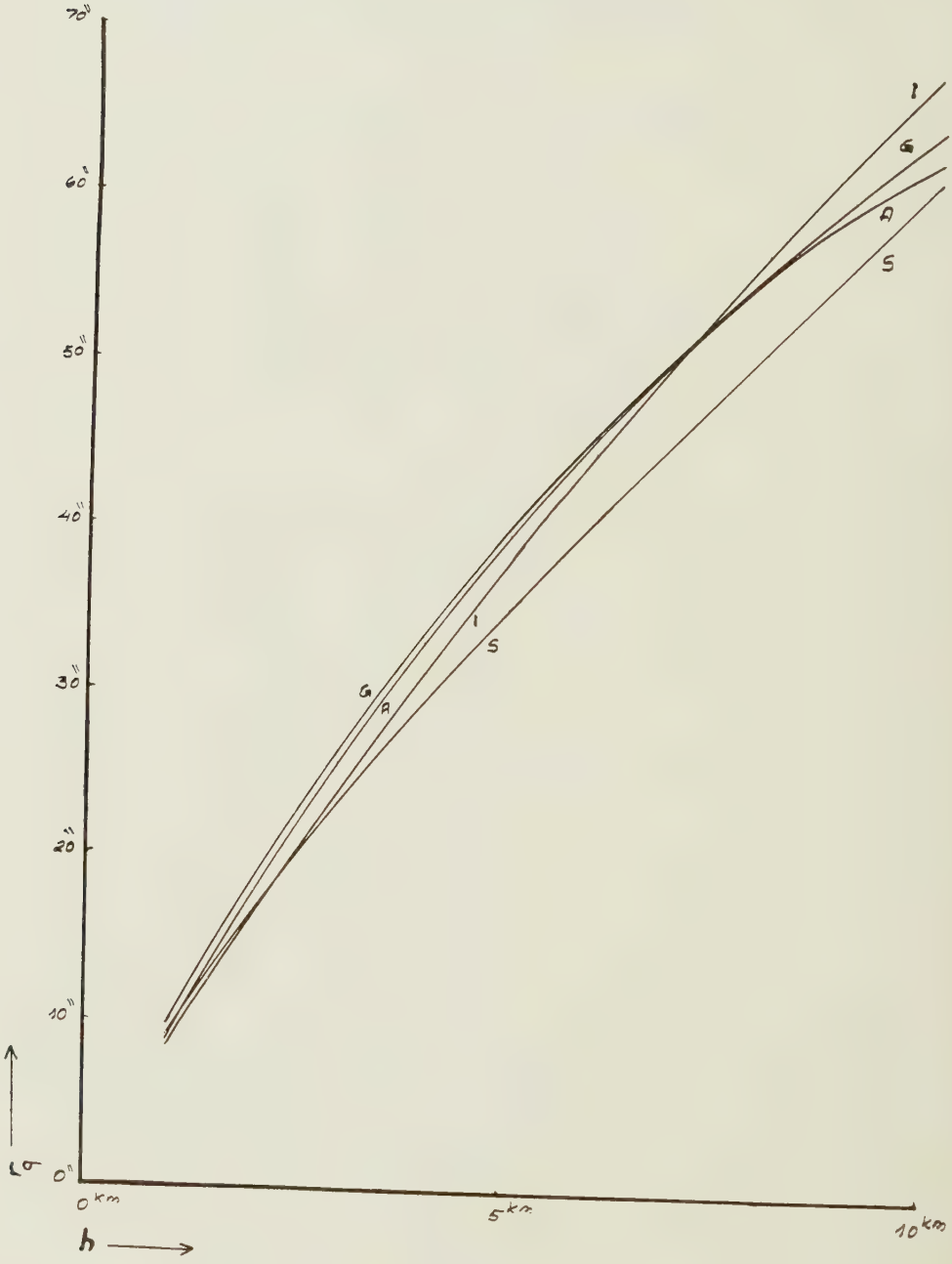

Fig. 9.

Ih the tables below r_f over ground levels between 0.0 km and 2.5 km and r_g are developed for every fifth centesimal degree.

Photogrammetric refraction at altitudes above a ground level of:

0 km.

km	5^c	10	15	20	25	30	35	40	45	50	55	60	65
	"												
0.5	0.3	0.7	1.0	1.4	1.7	2.1	2.6	3.1	3.6	4.2	4.9	5.8	6.9
1.0	0.6	1.3	2.0	2.7	3.4	4.2	5.0	6.0	7.0	8.2	9.6	11.3	13.4
1.5	0.9	1.9	2.9	3.9	4.9	6.1	7.3	8.6	10.2	11.9	13.9	16.4	19.4
2.0	1.2	2.5	3.7	5.0	6.4	7.9	9.5	11.3	13.2	15.5	18.1	21.3	25.3
2.5	1.5	3.0	4.5	6.1	7.8	9.6	11.6	13.7	16.1	18.9	22.1	26.0	30.8
3.0	1.7	3.5	5.3	7.2	9.2	11.3	13.6	16.1	19.0	22.2	26.0	30.6	36.2
3.5	2.0	4.0	6.0	8.2	10.4	12.8	15.4	18.3	21.5	25.2	29.5	34.7	41.1
4.0	2.2	4.5	6.7	9.1	11.6	14.3	17.2	20.4	24.0	28.1	32.9	38.7	45.9
4.5	2.4	4.9	7.4	10.0	12.8	15.7	18.9	22.4	26.3	30.8	36.1	42.4	50.3
5.0	2.6	5.3	8.0	10.8	13.8	17.0	20.4	24.2	28.4	33.3	39.0	45.8	54.3
5.5	2.8	5.7	8.6	11.6	14.8	18.2	21.9	25.9	30.5	35.7	41.8	49.1	58.3
6.0	3.0	6.0	9.1	12.3	15.7	19.4	23.3	27.6	32.5	38.0	44.5	52.3	62.0
6.5	3.2	6.4	9.6	13.0	16.6	20.4	24.6	29.1	34.2	40.1	47.0	55.2	65.4
7.0	3.3	6.7	10.1	13.6	17.4	21.4	25.7	30.5	35.9	42.0	49.2	57.8	68.5
7.5	3.5	7.0	10.5	14.3	18.2	22.4	26.9	31.9	37.5	43.9	51.4	60.4	71.6
8.0	3.6	7.2	10.9	14.8	18.9	23.2	27.9	33.1	38.9	45.6	53.4	62.8	74.4
8.5	3.7	7.5	11.3	15.3	19.5	24.0	28.9	34.2	40.2	47.1	55.1	64.8	76.9
9.0	3.8	7.7	11.7	15.8	20.1	24.8	29.8	35.3	41.5	48.6	56.9	66.9	79.3
9.5	3.9	7.9	12.0	16.2	20.7	25.4	30.6	36.3	42.6	49.9	58.4	68.7	81.4
10.0	4.0	8.1	12.3	16.6	21.2	26.1	31.4	37.2	43.7	51.2	59.9	70.5	83.6

0.5 km.

km	5^c	10	15	20	25	30	35	40	45	50	55	60	65
	"												
1.0	0.3	0.6	1.0	1.3	1.7	2.0	2.5	2.9	3.4	4.0	4.7	5.5	6.5
1.5	0.6	1.3	1.9	2.6	3.3	4.0	4.8	5.7	6.7	7.9	9.2	10.9	12.9
2.0	0.9	1.8	2.8	3.7	4.8	5.9	7.0	8.4	9.8	11.5	13.5	15.8	18.8
2.5	1.2	2.4	3.6	4.8	6.2	7.6	9.1	10.8	12.7	14.9	17.4	20.5	24.3
3.0	1.4	2.9	4.4	5.9	7.5	9.3	11.2	13.2	15.5	18.2	21.3	25.1	29.7
3.5	1.7	3.4	5.1	6.9	8.8	10.9	13.1	15.5	18.2	21.3	24.9	29.3	34.8
4.0	1.9	3.8	5.8	7.9	10.0	12.3	14.8	17.6	20.7	24.2	28.3	33.3	39.5
4.5	2.1	4.3	6.5	8.8	11.2	13.8	16.5	19.6	23.1	27.0	31.6	37.2	44.1
5.0	2.3	4.7	7.1	9.6	12.3	15.1	18.1	21.5	25.3	29.6	34.7	40.7	48.3
5.5	2.5	5.1	7.7	10.4	13.3	16.3	19.6	23.2	27.3	32.0	37.5	44.0	52.2
6.0	2.7	5.4	8.2	11.1	14.2	17.5	21.0	24.9	29.3	34.3	40.2	47.2	56.0
6.5	2.9	5.8	8.8	11.9	15.1	18.9	22.4	26.5	31.2	36.5	42.7	50.2	59.6
7.0	3.0	6.1	9.2	12.5	15.9	19.6	23.6	28.0	32.9	38.5	45.1	53.0	62.8
7.5	3.2	6.4	9.7	13.1	16.7	20.5	24.7	29.3	34.4	40.3	47.2	55.5	65.8
8.0	3.3	6.7	10.1	13.7	17.4	21.5	25.8	30.6	36.0	42.1	49.3	57.9	68.7
8.5	3.4	6.9	10.5	14.2	18.1	22.3	26.8	31.7	37.3	43.7	51.2	60.1	71.3
9.0	3.6	7.2	10.9	14.7	18.7	23.0	27.7	32.8	38.6	45.2	52.9	62.2	73.8
9.5	3.7	7.4	11.2	15.1	19.3	23.7	28.6	33.9	39.8	46.6	54.6	64.1	76.0
10.0	3.8	7.6	11.5	15.5	19.8	24.4	29.3	34.7	40.8	47.8	56.0	65.8	78.0

Photogrammetric refraction at altitudes above a ground level of:

1.0 km.

km	5°	10	15	20	25	30	35	40	45	50	55	60	65
	"												
1.5	0.3	0.6	0.9	1.3	1.6	2.0	2.4	2.8	3.3	3.9	4.6	5.4	6.4
2.0	0.6	1.2	1.8	2.5	3.1	3.9	4.7	5.5	6.5	7.6	8.9	10.5	12.4
2.5	0.9	1.8	2.7	3.6	4.6	5.7	6.8	8.1	9.5	11.1	13.0	15.3	18.1
3.0	1.1	2.3	3.5	4.7	6.0	7.3	8.8	10.5	12.3	14.4	16.7	19.8	23.5
3.5	1.4	2.8	4.2	5.7	7.2	8.9	10.7	12.7	14.9	17.5	20.5	24.1	28.6
4.0	1.6	3.2	4.9	6.7	8.5	10.4	12.6	14.9	17.5	20.5	24.0	28.2	33.5
4.5	1.8	3.7	5.6	7.6	9.7	11.9	14.3	16.9	19.9	23.3	27.3	32.1	38.0
5.0	2.0	4.1	6.2	8.4	10.7	13.2	15.9	18.8	22.1	25.9	30.3	35.6	42.3
5.5	2.2	4.5	6.8	9.2	11.8	14.5	17.4	20.6	24.3	28.4	33.3	39.1	46.3
6.0	2.4	4.9	7.4	10.0	12.8	15.7	18.9	22.4	26.3	30.8	36.1	42.4	50.3
6.5	2.6	5.2	7.9	10.7	13.7	16.8	20.2	24.0	28.2	33.0	38.6	45.4	53.9
7.0	2.8	5.5	8.4	11.4	14.5	17.8	21.4	25.4	29.9	35.0	41.0	48.2	57.1
7.5	2.9	5.8	8.9	12.0	15.3	18.8	22.6	26.8	31.5	36.9	43.2	50.8	60.2
8.0	3.0	6.1	9.3	12.6	16.0	19.7	23.7	28.1	33.1	38.7	45.2	53.3	63.2
8.5	3.2	6.4	9.7	13.1	16.7	20.6	24.8	29.4	34.5	40.4	47.3	55.6	65.9
9.0	3.3	6.6	10.1	13.6	17.4	21.3	25.7	30.4	35.8	41.9	49.1	57.7	68.4
9.5	3.4	6.9	10.4	14.1	17.9	22.1	26.5	31.5	37.0	43.3	50.7	59.6	70.7
10.0	3.5	7.1	10.7	14.5	18.5	22.7	27.3	32.4	38.1	44.6	52.2	61.4	72.8

1.5 km.

km	5°	10	15	20	25	30	35	40	45	50	55	60	65
	"												
2.0	0.3	0.6	0.9	1.2	1.5	1.9	2.3	2.7	3.2	3.7	4.3	5.1	6.0
2.5	0.6	1.2	1.8	2.4	3.0	3.7	4.5	5.3	6.2	7.3	8.5	10.0	11.9
3.0	0.8	1.7	2.5	3.4	4.4	5.4	6.5	7.7	9.1	10.6	12.4	14.6	17.3
3.5	1.1	2.2	3.3	4.5	5.7	7.0	8.5	10.0	11.8	13.8	16.2	19.0	22.5
4.0	1.3	2.7	4.0	5.5	7.0	8.6	10.3	12.2	14.3	16.8	19.7	23.1	27.4
4.5	1.6	3.1	4.7	6.4	8.2	10.0	12.1	14.3	16.8	19.7	23.1	27.1	32.1
5.0	1.8	3.5	5.4	7.3	9.3	11.4	13.7	16.3	19.1	22.4	26.2	30.8	36.6
5.5	2.0	3.9	6.0	8.1	10.3	12.7	15.3	18.1	21.3	24.9	29.2	34.3	40.6
6.0	2.1	4.3	6.6	8.9	11.3	13.9	16.7	19.8	23.3	27.3	32.0	37.6	44.5
6.5	2.3	4.7	7.1	9.6	12.2	15.0	18.1	21.4	25.2	29.5	34.5	40.6	48.1
7.0	2.5	5.0	7.6	10.3	13.1	16.1	19.4	23.0	27.0	31.6	37.0	43.5	51.6
7.5	2.6	5.3	8.1	10.9	13.9	17.1	20.6	24.4	28.7	33.6	39.3	46.2	54.8
8.0	2.8	5.6	8.5	11.5	14.7	18.0	21.7	25.7	30.2	35.4	41.4	48.7	57.8
8.5	2.9	5.9	8.9	12.1	15.4	18.9	22.7	27.0	31.7	37.1	43.4	51.1	60.5
9.0	3.0	6.1	9.3	12.6	16.0	19.7	23.7	28.1	33.1	38.7	45.3	53.3	63.2
9.5	3.2	6.4	9.6	13.0	16.6	20.4	24.6	29.1	34.2	40.1	47.0	55.2	65.4
10.0	3.3	6.6	10.0	13.5	17.2	21.1	25.4	30.2	35.4	41.5	48.6	57.1	67.7

Photogrammetric refraction at altitudes above a ground level of:

2.0 km.

km	5°	10	15	20	25	30	35	40	45	50	55	60	65
	"												
2.5	0.3	0.6	0.9	1.2	1.5	1.8	2.2	2.6	3.1	3.6	4.2	5.0	5.9
3.0	0.6	1.1	1.7	2.3	2.9	3.6	4.3	5.1	6.0	7.0	8.2	9.6	11.4
3.5	0.8	1.6	2.4	3.3	4.2	5.2	6.3	7.4	8.7	10.2	11.9	14.0	16.6
4.0	1.0	2.1	3.2	4.3	5.5	6.8	8.2	9.7	11.4	13.3	15.6	18.3	21.7
4.5	1.3	2.6	3.9	5.3	6.7	8.3	9.9	11.8	13.8	16.2	19.0	22.3	26.4
5.0	1.5	3.0	4.5	6.1	7.8	9.6	11.6	13.7	16.1	18.9	22.1	26.0	30.8
5.5	1.7	3.4	5.2	7.0	8.9	11.0	13.2	15.6	18.4	21.5	25.2	29.6	35.1
6.0	1.9	3.8	5.7	7.8	9.9	12.2	14.6	17.4	20.4	23.9	28.0	32.9	39.0
6.5	2.1	4.1	6.3	8.5	10.9	13.3	16.1	19.0	22.4	26.2	30.7	36.1	42.8
7.0	2.2	4.5	6.8	9.2	11.7	14.4	17.3	20.6	24.2	28.3	33.1	39.0	46.2
7.5	2.4	4.8	7.3	9.8	12.6	15.4	18.6	22.0	25.9	30.3	35.5	41.7	49.4
8.0	2.5	5.1	7.7	10.5	13.3	16.4	19.7	23.4	27.5	32.2	37.7	44.3	52.5
8.5	2.7	5.4	8.1	11.0	14.0	17.3	20.8	24.6	29.0	33.9	39.7	46.7	55.3
9.0	2.8	5.6	8.5	11.6	14.7	18.1	21.8	25.9	30.4	35.6	41.7	49.0	58.1
9.5	2.9	5.9	8.9	12.0	15.3	18.9	22.7	26.9	31.6	37.0	43.3	50.9	60.4
10.0	3.0	6.1	9.2	12.5	15.9	19.6	23.5	27.9	32.8	38.4	45.0	52.9	62.7

2.5 km.

km	5°	10	15	20	25	30	35	40	45	50	55	60	65
	"												
3.0	0.3	0.6	0.8	1.1	1.4	1.8	2.1	2.5	3.0	3.5	4.1	4.8	5.7
3.5	0.5	1.1	1.6	2.2	2.8	3.4	4.1	4.9	5.7	6.7	7.8	9.2	10.9
4.0	0.8	1.6	2.4	3.2	4.1	5.0	6.0	7.1	8.4	9.8	11.5	13.5	16.0
4.5	1.0	2.0	3.1	4.2	5.3	6.5	7.8	9.3	10.9	12.8	15.0	17.6	20.9
5.0	1.2	2.5	3.7	5.1	6.5	7.9	9.6	11.3	13.3	15.6	18.3	21.5	25.5
5.5	1.4	2.9	4.4	5.9	7.5	9.3	11.2	13.2	15.5	18.2	21.3	25.1	29.7
6.0	1.6	3.3	4.9	6.7	8.5	10.5	12.6	15.0	17.6	20.6	24.1	28.4	33.6
6.5	1.8	3.6	5.5	7.5	9.5	11.7	14.1	16.7	19.6	23.0	26.9	31.7	37.5
7.0	2.0	4.0	6.0	8.2	10.4	12.8	15.4	18.2	21.4	25.1	29.4	34.5	41.0
7.5	2.1	4.3	6.5	8.8	11.3	13.9	16.7	19.8	23.2	27.2	31.8	37.4	44.4
8.0	2.3	4.6	7.0	9.5	12.1	14.8	17.8	21.1	24.9	29.1	34.1	40.1	47.5
8.5	2.4	4.9	7.4	10.0	12.8	15.7	18.9	22.4	26.3	30.8	36.1	42.4	50.3
9.0	2.6	5.1	7.8	10.6	13.5	16.6	19.9	23.6	27.8	32.5	38.1	44.7	53.0
9.5	2.7	5.4	8.2	11.0	14.1	17.3	20.8	24.7	29.0	34.0	39.8	46.8	55.5
10.0	2.8	5.6	8.5	11.5	14.7	18.1	21.8	25.8	30.3	35.5	41.6	48.9	57.9

Ground refraction, ground level at 0.0 km.

km	5°	10	15	20	25	30	35	40	45	50	55	60	65
	"												
0.0	0.0	0.0	0.0	0.0	0.0	0.0	0.0	0.0	0.0	0.0	0.0	0.0	0.0
0.5	0.3	0.7	1.0	1.4	1.7	2.1	2.6	3.1	3.6	4.2	4.9	5.8	6.9
1.0	0.7	1.3	2.0	2.7	3.5	4.3	5.1	6.1	7.2	8.4	9.8	11.6	13.7
1.5	1.0	2.0	3.0	4.0	5.1	6.3	7.6	9.0	10.6	12.4	14.5	17.1	20.2
2.0	1.3	2.6	3.9	5.3	6.8	8.3	10.0	11.8	13.9	16.3	19.1	22.4	26.6
2.5	1.6	3.2	4.8	6.6	8.4	10.3	12.4	14.7	17.3	20.2	23.7	27.8	33.0
3.0	1.9	3.8	5.7	7.8	9.9	12.2	14.6	17.4	20.4	23.9	28.0	32.9	39.0
3.5	2.2	4.4	6.6	8.9	11.4	14.0	16.9	20.0	23.5	27.5	32.2	37.9	44.9
4.0	2.4	4.9	7.5	10.1	12.9	15.8	19.1	22.6	26.6	31.1	36.4	42.8	50.8
4.5	2.7	5.5	8.3	11.2	14.3	17.6	21.2	25.1	29.6	34.6	40.5	47.6	56.5
5.0	3.0	6.0	9.1	12.3	15.7	19.3	23.2	27.5	32.4	37.9	44.4	52.2	61.8
5.5	3.2	6.5	9.9	13.4	17.1	21.0	25.2	29.9	35.2	41.2	48.2	56.7	67.2
6.0	3.5	7.0	10.7	14.4	18.4	22.6	27.2	32.3	37.9	44.4	52.0	61.1	72.5
6.5	3.7	7.5	11.4	15.5	19.7	24.3	29.2	34.6	40.7	47.6	55.7	65.5	77.7
7.0	4.0	8.0	12.1	16.4	21.0	25.8	31.0	36.8	43.2	50.6	59.2	69.6	82.6
7.5	4.2	8.5	12.9	17.4	22.2	27.3	32.8	38.9	45.8	53.6	62.8	73.8	87.5
8.0	4.4	8.9	13.5	18.3	23.4	28.7	34.6	41.0	48.2	56.4	66.0	77.6	92.0
8.5	4.7	9.4	14.2	19.3	24.6	30.2	36.3	43.1	50.6	59.3	69.4	81.6	96.8
9.0	4.9	9.8	14.9	20.1	25.7	31.6	38.0	45.0	53.0	62.0	72.6	85.3	101.2
9.5	5.1	10.2	15.5	21.0	26.8	33.0	39.6	47.0	55.3	64.7	75.8	89.1	105.6
10.0	5.3	10.6	16.1	21.8	27.8	34.2	41.2	48.8	57.4	67.2	78.7	92.5	109.7

Effect of curvature.

The secondary effect of curvature in refraction is disregarded, as in section I. The primary effect, however, has to be regarded as much larger than refraction, and of the opposite sign.

It can readily be derived geometrically that the effect in height of curvature seen from ground can be written

$$\Delta h = \frac{h^2 \operatorname{tg}^2 z}{2(R+h)},$$

and the effect in height (seen from aircraft) of photogrammetric curvature

$$\Delta h = \frac{h^2 \operatorname{tg}^2 n}{2R},$$

where R is the radius of curvature of the earth at the surface of the ellipsoid of reference, and n = nadir distance.

The corresponding angular effects, o_g and o_f

$$o_g = \frac{h}{2(R+h)} \cdot \frac{\sin^3 z}{\cos z}$$

and

$$o_f = \frac{h}{2R} \cdot \frac{\sin^3 n}{\cos n}.$$

Using Hayford's [20] constants,

$$a = 6\,378.388 \text{ km}$$
$$b = 6\,356.912 \text{ km}$$

we get the following limits of R:

	North—South	East—West
Pole	6 399.937 km	6 399.937 km
Equator	6 335.508 km	6 378.388 km
Averages	6 367.722	6 389.162
Final average	6 378.442	

and the largest differences from the final average:

Pole	21.495 km
Equator, north—south	42.934 km.

The difference in the radius of curvature between ground and a height of 10 km is then only 25 % of the last-mentioned difference.

At 50° nadir distance and a height of 10 km the largest amount of difference in o_f, caused by latitude, is 1."7, since $(o_f)_{\substack{Eq \\ N-S}} = 251."2$ and $(o_f)_{R\,med} = 249."5$. This is only 7 ‰ of the total curvature effect.

Considering these facts, we assume $o_g = o_f$ and $R = 6\,378.442$ km.

Ground curvature ≈ Photogrammetric curvature.

km	5°	10	15	20	25	30	35	40	45	50	55	60	65
	"												
0.5	0.0	0.1	0.3	0.8	1.5	2.6	4.2	6.3	9.0	12.5	16.9	22.5	29.6
1.0	0.0	0.2	0.7	1.5	3.0	5.2	8.3	12.5	18.0	25.0	33.8	45.0	59.2
1.5	0.0	0.3	1.0	2.3	4.5	7.9	12.5	18.8	27.0	37.4	50.7	67.4	88.8
2.0	0.0	0.4	1.3	3.1	6.1	10.5	16.7	25.1	36.0	49.9	67.6	89.9	118.4
2.5	0.1	0.5	1.6	3.9	7.6	13.1	20.9	31.3	44.9	62.4	84.5	112.4	148.0
3.0	0.1	0.6	2.0	4.6	9.1	15.7	25.0	37.6	53.9	74.9	101.4	134.9	177.6
3.5	0.1	0.7	2.3	5.4	10.6	18.3	29.2	43.8	62.9	87.3	118.2	157.3	207.2
4.0	0.1	0.8	2.6	6.2	12.1	21.0	33.4	50.1	71.9	99.8	135.1	179.8	236.8
4.5	0.1	0.9	2.9	7.0	13.6	23.6	37.6	56.4	80.9	112.3	152.0	202.3	266.4
5.0	0.1	1.0	3.3	7.7	15.1	26.2	41.7	62.6	89.9	124.8	168.9	224.8	296.0
5.5	0.1	1.1	3.6	8.5	16.6	28.8	45.9	68.9	98.9	137.2	185.8	247.3	325.6
6.0	0.1	1.2	3.9	9.3	18.2	31.4	50.1	75.2	107.9	149.7	202.7	269.7	355.2
6.5	0.2	1.3	4.2	10.1	19.7	34.1	54.3	81.1	116.9	162.2	219.6	292.2	384.8
7.0	0.2	1.4	4.6	10.8	21.2	36.7	58.4	87.8	125.8	174.7	236.5	314.7	414.4
7.5	0.2	1.5	4.9	11.6	22.7	39.3	62.6	93.9	134.8	187.1	253.4	337.2	444.0
8.0	0.2	1.5	5.2	12.4	24.2	41.9	66.8	100.2	143.8	199.6	270.3	359.7	473.6
8.5	0.2	1.6	5.6	13.2	25.7	44.5	71.0	106.5	152.8	212.1	287.2	382.1	503.2
9.0	0.2	1.7	5.9	13.9	27.2	47.2	75.1	112.7	161.8	224.6	304.1	404.6	532.8
9.5	0.2	1.8	6.2	14.7	28.8	49.8	79.3	119.0	170.8	237.0	321.0	427.1	562.4
10.0	0.2	1.9	6.5	15.5	30.3	52.4	83.5	125.3	179.8	249.5	337.9	449.6	592.0

Ground refraction and curvature.

km	5°	10	15	20	25	30	35	40	45	50	55	60	65
	"												
0.5	+ 0.3	+ 0.6	+ 0.7	+ 0.6	+ 0.2	— 0.5	— 1.6	— 3.2	— 5.4	— 8.3	— 12.0	— 16.7	— 22.7
1.0	+ 0.7	+ 1.1	+ 1.3	+ 1.2	+ 0.5	— 0.9	— 3.2	— 6.4	— 10.8	— 16.6	— 24.0	— 33.4	— 45.5
1.5	+ 1.0	+ 1.7	+ 2.0	+ 1.7	+ 0.6	— 1.6	— 4.9	— 9.8	— 16.4	— 25.0	— 36.2	— 50.3	— 68.6
2.0	+ 1.3	+ 2.2	+ 2.6	+ 2.2	+ 0.7	— 2.2	— 6.7	— 13.3	— 22.1	— 33.6	— 48.5	— 67.5	— 91.8
2.5	+ 1.5	+ 2.7	+ 3.2	+ 2.7	+ 0.8	— 2.8	— 8.5	— 16.6	— 27.6	— 42.2	— 60.3	— 84.6	— 115.0
3.0	+ 1.8	+ 3.2	+ 3.7	+ 3.2	+ 0.8	— 3.5	— 10.4	— 20.2	— 33.5	— 51.0	— 73.4	— 102.0	— 138.6
3.5	+ 2.1	+ 3.7	+ 4.3	+ 3.5	+ 0.8	— 4.3	— 12.3	— 23.8	— 39.4	— 59.8	— 86.0	— 119.4	— 162.3
4.0	+ 2.3	+ 4.1	+ 4.9	+ 3.9	+ 0.8	— 5.2	— 14.3	— 27.5	— 45.3	— 68.7	— 98.7	— 137.0	— 186.0
4.5	+ 2.6	+ 4.6	+ 5.4	+ 4.2	+ 0.7	— 6.0	— 16.4	— 31.3	— 51.3	— 77.7	— 111.5	— 154.7	— 209.9
5.0	+ 2.9	+ 5.0	+ 5.8	+ 4.6	+ 0.6	— 6.9	— 18.5	— 35.1	— 57.5	— 86.9	— 124.5	— 172.6	— 234.2
5.5	+ 3.1	+ 5.4	+ 6.3	+ 4.9	+ 0.5	— 7.8	— 20.7	— 39.0	— 63.7	— 96.0	— 137.6	— 190.6	— 258.4
6.0	+ 3.4	+ 5.8	+ 6.8	+ 5.1	+ 0.2	— 8.8	— 22.9	— 42.9	— 70.0	— 105.3	— 150.7	— 208.6	— 282.7
6.5	+ 3.5	+ 6.2	+ 7.2	+ 5.4	0.0	— 9.8	— 25.1	— 46.8	— 76.2	— 114.6	— 163.9	— 226.7	— 307.1
7.0	+ 3.8	+ 6.6	+ 7.5	+ 5.6	— 0.2	— 10.9	— 27.4	— 51.0	— 82.6	— 124.1	— 177.3	— 245.1	— 331.8
7.5	+ 4.0	+ 7.0	+ 8.0	+ 5.8	— 0.5	— 12.0	— 29.8	— 55.0	— 89.0	— 133.5	— 190.6	— 263.4	— 356.5
8.0	+ 4.2	+ 7.4	+ 8.3	+ 5.9	— 0.8	— 13.2	— 32.2	— 59.2	— 95.6	— 143.2	— 204.3	— 282.1	— 381.6
8.5	+ 4.5	+ 7.8	+ 8.6	+ 6.1	— 1.1	— 14.3	— 34.7	— 63.4	— 102.2	— 152.8	— 217.8	— 300.5	— 406.4
9.0	+ 4.7	+ 8.1	+ 9.0	+ 6.2	— 1.5	— 15.6	— 37.1	— 67.7	— 108.8	— 162.6	— 231.5	— 319.3	— 431.6
9.5	+ 4.9	+ 8.4	+ 9.3	+ 6.3	— 2.0	— 16.8	— 39.7	— 72.0	— 115.5	— 172.3	— 245.2	— 338.0	— 456.8
10.0	+ 5.1	+ 8.7	+ 9.6	+ 6.3	— 2.5	— 18.2	— 42.3	— 76.5	— 122.4	— 182.3	— 259.2	— 357.1	— 482.3

Schütte [19], Bachmann [21], Zeller [22] and Blum [23] do not make any difference for variation in R.

Aschenbrenner [18] does not discuss curvature in his treatise on refraction, and thus obtains a deformation of the ground of illusional character, as an elevation with increasing nadir distance.

Cancellation effect.

Refraction and curvature cancel each other at certain zones, as seen from the following table and the tables in the appendix.

These are the definitive values for the result of the two effects, in the I.C.A.N. atmosphere.

The zones of cancellation are drawn in fig. 10.

Effect of variation in conditions.

For the study of atmospheric conditions for photogrammetric refraction the same intervals are used as in chapter I.

To use the formula

$$r = \left[R - 636\,620 \, \frac{\frac{\cos z}{\operatorname{tg} z} (P_f - P_g)}{h_f - h_g} \right] \operatorname{tg} z$$

derived above we need the extremes in parameter.

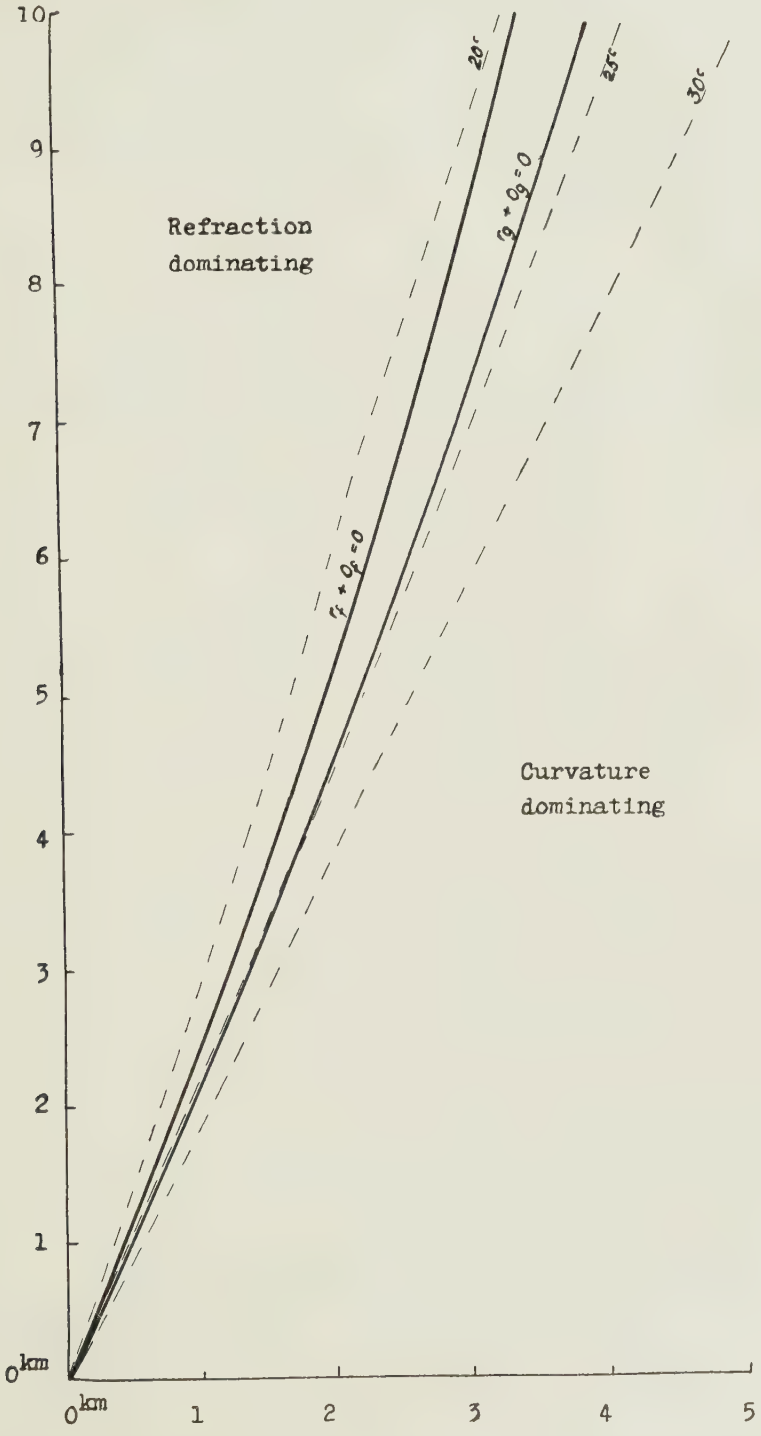
10
9
8
7
6
5
4
3
2
1
0km
0km
1
2
3
4
5
Refraction
dominating
Curvature
dominating
20°
25°
30°
f + Q = 0
g + Q = 0

Fig. 10.

According to normal refraction and parameter

$$K'' = 57.82 - 5.554\,h + 0.2040\,h^2 - 0.00347\,h^3 + 0.000025\,h^4$$

$$P^{km} = 10^{-7\,\frac{\operatorname{tg} z}{\cos z}}[2\,803.114\,h - 134.6290\,h^2 + 3.29664\,h^3 - 0.042056\,h^4 + 0.0002424\,h^5]$$

we can form

Pressure extremes

730 mm
$$\begin{cases} 55.54 - 5.335\,h + 0.1960\,h^2 - 0.00333\,h^3 + 0.000025\,h^4 \\ 2\,692.579\,h - 129.3204\,h^2 + 3.16736\,h^3 - 0.040360\,h^4 + 0.0002424\,h^5 \end{cases}$$

790 mm
$$\begin{cases} 60.10 - 5.773\,h + 0.2122\,h^2 - 0.00360\,h^3 + 0.000025\,h^4 \\ 2\,913.648\,h - 139.9375\,h^2 + 3.42915\,h^3 - 0.043632\,h^4 + 0.0002424\,h^5 \end{cases}$$

Temperature extremes

258° A
$$\begin{cases} 64.54 - 6.919\,h + 0.2838\,h^2 - 0.00538\,h^3 + 0.000042\,h^4 \\ 3\,128.899\,h - 167.7166\,h^2 + 4.58621\,h^3 - 0.065206\,h^4 + 0.0004072\,h^5 \end{cases}$$

318° A
$$\begin{cases} 52.36 - 4.555\,h + 0.1516\,h^2 - 0.00233\,h^3 + 0.000017\,h^4 \\ 2\,538.413\,h - 110.4132\,h^2 + 2.44986\,h^3 - 0.028240\,h^4 + 0.0001648\,h^5 \end{cases}$$

Lapse-rate extremes

0.35°
$$\begin{cases} 57.82 - 6.154\,h + 0.2902\,h^2 - 0.00795\,h^3 + 0.000138\,h^4 \\ 2\,803.114\,h - 149.1730\,h^2 + 4.68963\,h^3 - 0.096354\,h^4 + 0.0013380\,h^5 \end{cases}$$

0.95°
$$\begin{cases} 57.82 - 4.951\,h + 0.1304\,h^2 - 0.00085\,h^3 \\ 2\,803.114\,h - 120.0122\,h^2 + 2.10726\,h^3 - 0.010302\,h^4 \end{cases}$$

Humidity extremes ($\mu_2 = 1.000257$)

318° A, 0 %
$$\begin{cases} 52.36 - 4.555\,h + 0.1516\,h^2 - 0.00233\,h^3 + 0.000017\,h^4 \\ 2\,538.413\,h - 110.4132\,h^2 + 2.44986\,h^3 - 0.028240\,h^4 + 0.0001648\,h^5 \end{cases}$$

318° A, 100 %
$$\begin{cases} 51.77 - 4.453\,h + 0.1465\,h^2 - 0.00223\,h^3 + 0.000012\,h^4 \\ 2\,509.810\,h - 107.9407\,h^2 + 2.36744\,h^3 - 0.027028\,h^4 + 0.0001164\,h^5 \end{cases}$$

r_f-extrems over a ground level of 0.0 km

Cond.	h	R''_{50^c}	$10^{+3}\frac{\cos z}{\operatorname{tg} z}P$	$\times \frac{\varrho}{h}$	r_f
730 mm	1	155.56	0.256639	163.38	7.82
	4	114.60	0.889382	141.55	26.95
	10	57.75	1.678175	106.84	49.09
790 mm	1	168.33	0.277710	176.80	8.47
	4	124.01	0.962414	153.17	29.16
	10	62.47	1.815980	115.61	53.14
258° A	1	178.70	0.296570	188.80	10.10
	4	126.76	1.010937	160.90	34.14
	10	57.93	1.849220	117.73	59.80
318° A	1	147.99	0.243038	154.72	6.73
	4	112.41	0.853677	135.87	23.46
	10	61.14	1.652675	105.21	44.07
0.35° C	1	160.34	0.265854	168.61	8.27
	4	115.34	0.910253	144.87	29.53
	10	57.81	1.697373	108.06	50.25
0.95° C	1	163.58	0.268520	170.95	7.37
	4	123.61	0.942449	150.00	26.39
	10	63.27	1.803416	114.81	51.54
0 % at 318° A	1	147.99	0.243038	154.72	6.73
	4	112.41	0.853677	135.87	23.46
	10	61.14	1.652675	105.21	44.07
100 % at 318° A	1	146.48	0.240421	153.06	6.58
	4	111.60	0.845690	134.60	23.00
	10	61.05	1.641283	104.49	43.44

From these extremes we compute the amplitudes, as follows.

Comparison between amplitudes r_f.

Conditions	h	Ampl. total	Ampl. unit.
730—790 mm	1 km	0.65	0.011 per mm
	4	2.21	0.037
	10	4.05	0.068
258—318° A	1	3.37	0.056 per °A
	4	10.68	0.178
	10	15.73	0.262
0.35—0.95 C	1	0.90	0.015 per 0°.01 C
	4	3.14	0.052
	10	1.29	0.022
0—100 % at +318° A....	1	0.15	0.002 per %
	4	0.46	0.005
	10	0.63	0.006

It is clearly evident that the lapse-rate has the largest influence upon refraction.

The effect of a variation of 1 mm, 1° A or 1 % relative humidity can only be compared with that of a few hundredths of 1° C in variation of the lapse-rate.

The sole effect that exceeds 10 % of lapse-rate is that of absolute temperature at 10 km, 12 %.

At the altitude of 1 km the influence of absolute temperature is 3.7 % of that of lapse-rate, while pressure causes only 0.2 % and humidity at 318° less.

Errors at 4 000 m and relative errors.

The tables in the appendix give data for various errors at each half km from 0 to 10 km.

For the work in the Geographical Survey Office of Sweden, the errors at 4 000 m are of special interest.

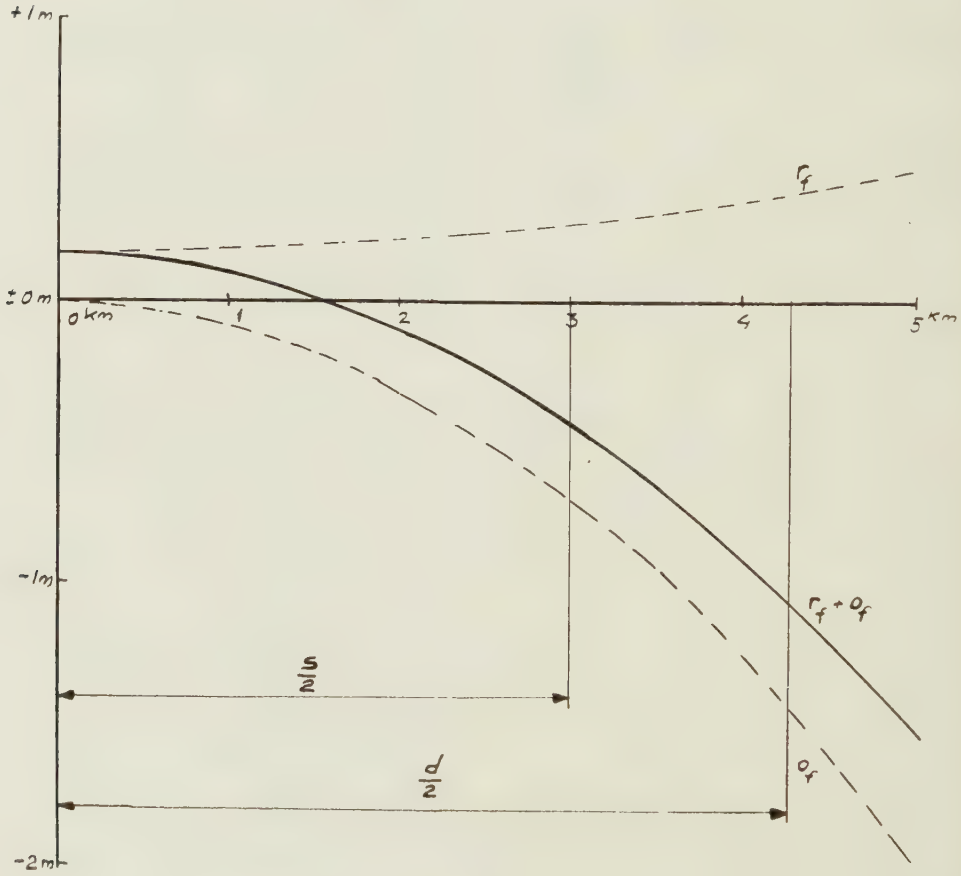

Fig. 11.

Height and lateral errors at this altitude are shown in fig. 11 and 12. Errors are counted positively upwards and outwards from nadir. The horizontal axis gives distance from nadir in km.

The deformation of the ground in one picture is shown in fig. 13, where the outward side is 6 km, and the numbers give lateral error in m. The circle marks the section between elimination zone and photoplane.

Two final diagrams showing relative errors (fig. 14 and 15).

These diagrams can be used for a swift computation of the errors at any flight level below 10 km and with any type of camera.

The only operation is to multiply the relative error obtained in diagrams with the actual flight level.

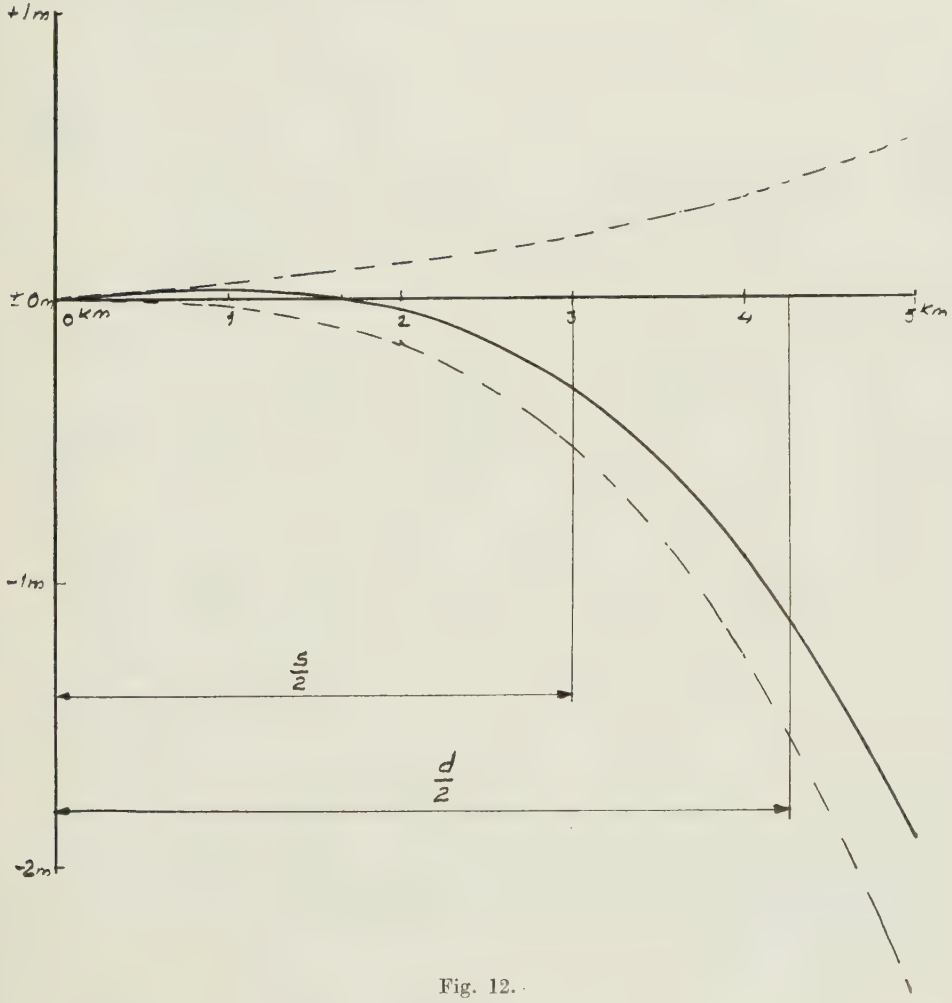

Fig. 12.

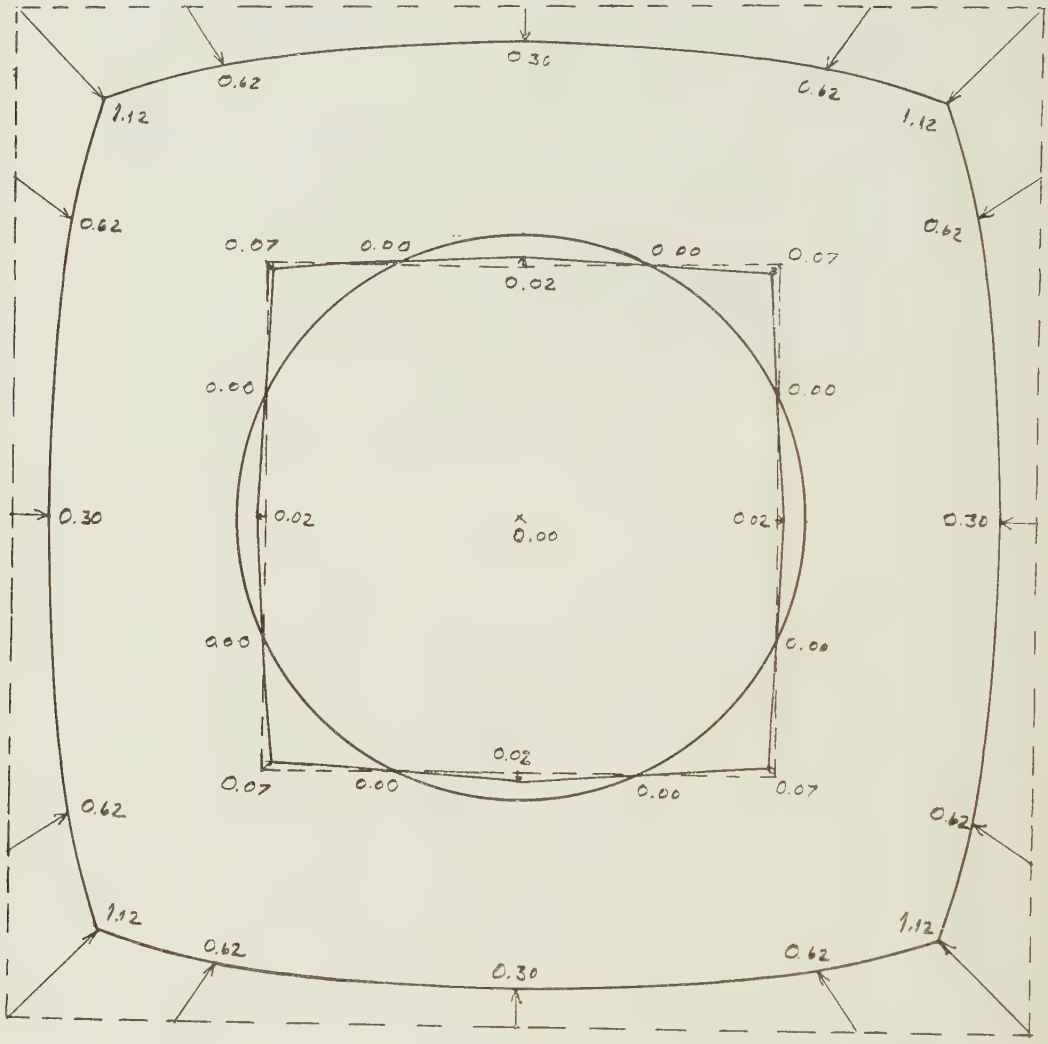

Fig. 13.

The shaded zone marks the range of the Zeiss RMK 20/30 30 surveying cameras used in the Geographical Survey Office of Sweden.

The mean error for Multiplex in the diagrams is the one internationally known for this instrument, and the mean error for Stereoplanigraph is the one given by Hallert [24] for a stereomodel with an average density of 4—5 points per model.

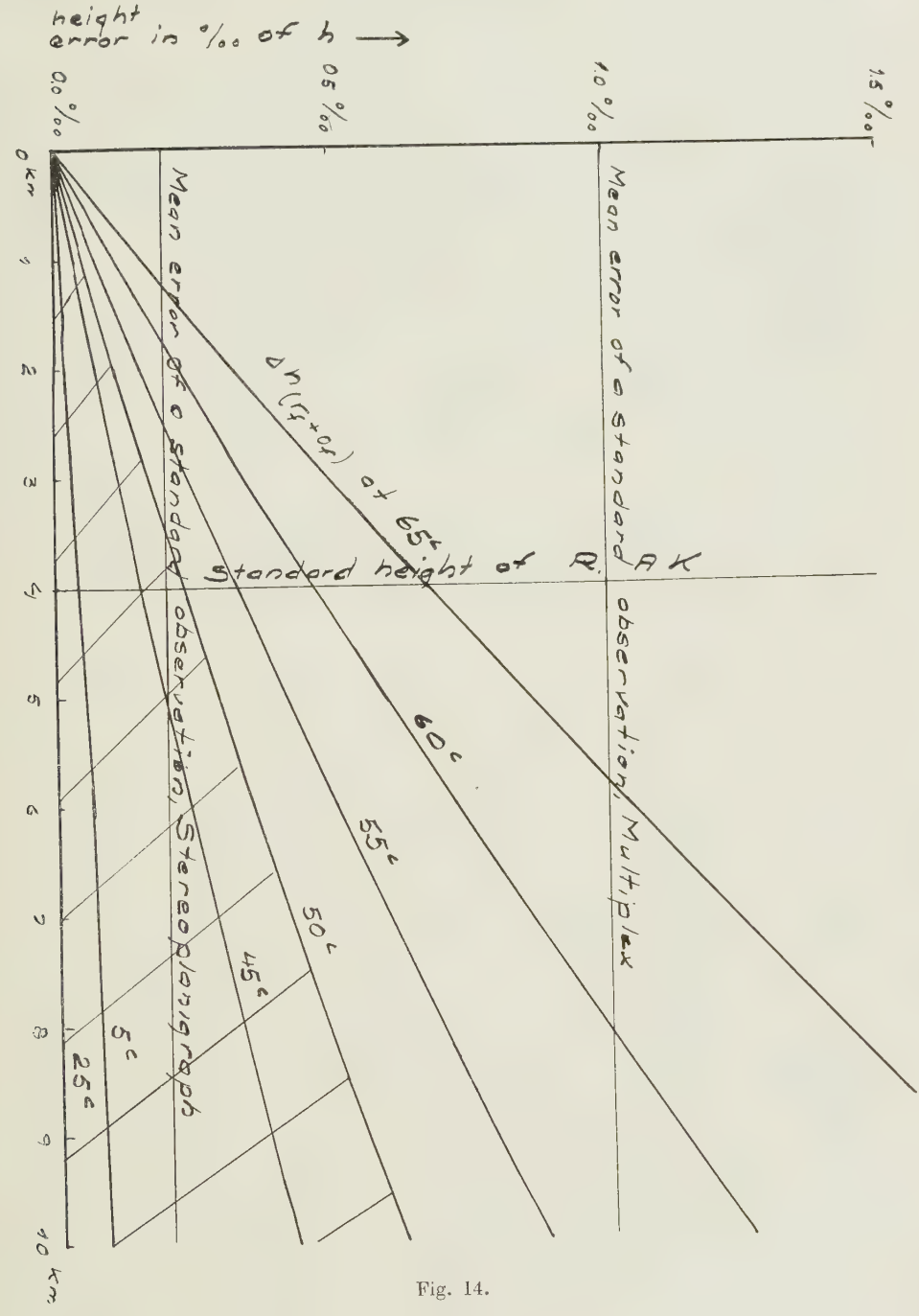
height error in ‰ of h →
0.0 ‰
0.5 ‰
1.0 ‰
1.5 ‰
h →
0 km
1
2
3
4
5
6
7
8
9
10 km
Mean error of a standard observation, Stereoplanigraph
Mean error of a standard observation, Multiplex
Standard height of R. AK
Δh (f+of) at 65°
60°
55°
50°
45°
25°
5°

Fig. 14.

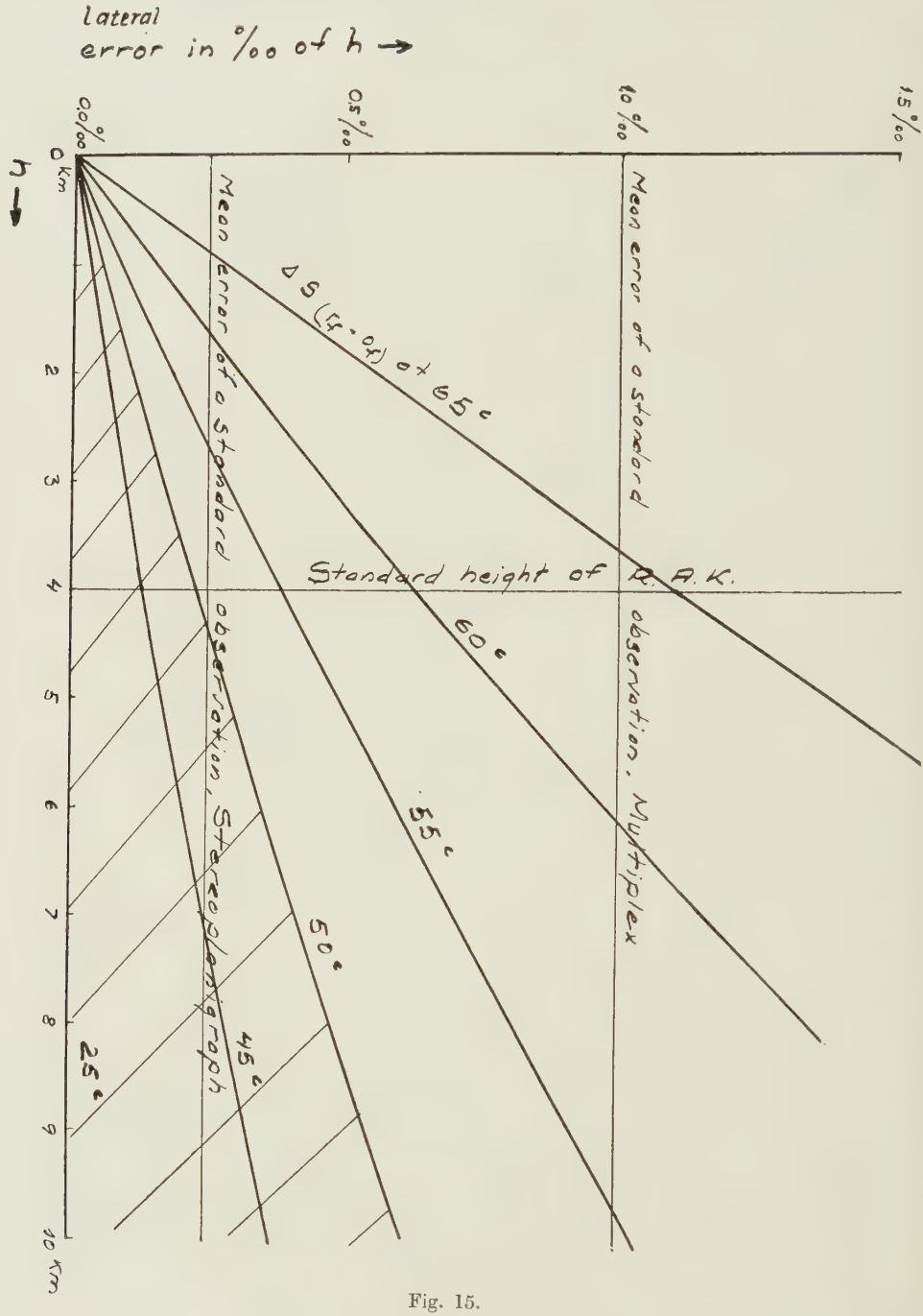
lateral
error in ‰ of h →
0,0‰
0,5‰
1,0‰
1,5‰
h →
0 km
2
3
4
5
6
7
8
9
10 km
Mean error of a standard observation, Stereokomparator
Mean error of a standard observation, Multiplex
Δ S (ζ - 0ζ) at 65°
Standard height of R. A. K.
60°
55°
50°
45°
25°

Fig. 15.

A method for measurements.

During the winter of 1948—49 a method for direct investigation of these errors was prepared. A lot of work was completely lost when the last possible instrument, after final laboratory tests, proved to be unsatisfactory.

The principle was to ascend up to at least 10 km of height and make exposures of an extremely long straight stretch of railway in southern Sweden. With known nivellements and positions of electric power posts along this stretch it would be possible to study both the relative deformation and the absolute values of errors, when the exposures are made at different angles.

The demands on an instrument for this purpose are great. A glass plate-camera with wide angle lens and sufficient focal length and opening must be used. The conventional target cameras have sufficient focal length and opening, but small angle lens. The cameras used in photogrammetric surveying are for use with film and the photogrammetric hand cameras are too small.

A camera exceptionally well-adapted to such observations is the newly-designed Wild RC 7, which was not available at that time.

III. Trigonometric refraction.

The term »trigonometric refraction» is used in analogy with the expressions »photogrammetric refraction» and »nivellitic refraction» already used by other writers, and means the effect of refraction on the trigonometric determination of the heights of the stations.

A. Hypothesis based upon known observations of surface inversion.

Initial formulae.

To get a first impression of the effect of surface inversion, we use the following recent expressions for pressure:

$$p_h = p_o \left(\frac{T_o - \beta h}{T_o} \right)^{\frac{1}{0.293}}$$

at decreasing temperature upwards, and (with p in millibars)

$$\log p_h = \log p_o - \frac{h}{67.4\ T_o}$$

at uniform temperature, used by Brunt [3], and for refraction R_1 in the layer 1, with known refraction coefficients K_1 and K_2 and distance $S \cdot 10\,000$ m.,

$$R_1 = \frac{1}{2} \cdot \frac{S}{637.8442} \cdot \frac{3\,K_1 + K_2}{4}$$

when for each layer (p in mb)

$$K = 17.19 \frac{p}{T^2} (1 - 0.2925\ \beta)$$

both constructed by Brocks [32].

Lapse-rates at Leafield.

The investigations of surface inversion made by Johnson and Heywood [33] at Leafield seem to be very useful for this purpose and are used here for analysis of the effects upon refraction.

The Leafield measurements are made over grassland up to about 100 m over a five-year period, and the inclination of the upper parts of the temperature curves give the tendency as well for the lowest three hundred meters, the zone of common height intervals in surveying.

With these measurements it is possible to distinguish three typical stages of surface inversion in the summer semester.

The first of these stages appears two hours after sunrise, is linear, and has the value of 0.°00 C/100 m.

The second appears at noon and is linear only down to the lowest 8 or 10 meters. The value of the lapse-rate is about 1.°10 C/100 m.

The third appears two hours before sunset, is linear, and has the value of 0.°80 C/100 m.

Discussion of surface inversion.

The investigations by Kukkamäki [34], made with the Wheatstone bridge, which was first used by Best [35], show the influence of surface inversion in the nivellement. Brocks' [32] investigations show the effect, at greater heights in the Alps, of variations in lapse-rate.

In the previous chapter the effects of such variations are also derived. In trigonometric refraction, however, we find the most difficult forms of inversion. Both nivellitic and photogrammetric refraction are computed on approximately linear lapse-rates, as seen from the following schematical figure:

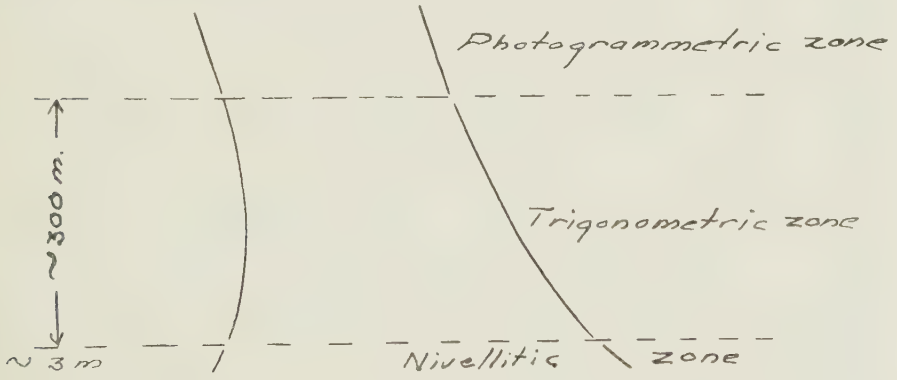

The curved forms of inversion give the immediate impression, that the influence of ground profile will be greater than for the linear forms.

For the computations of typical stages, however, we have to begin with the three types of lapse-rates, combined with the normal lapse-rate in the I.C.A.N. athmosphere, tentatively presumed to be valid for overcast sky, but probably too high.

Computation of typical stages.

Using the formulae above on the four types of lapse-rates and distances of 5, 10, 15 and 20 km, we get the data for each type:

$\beta = 0.°00.$

Distance, km	5		10		15	20
Height diff., m	50	200	100	400	100	100
p_o mm	760.00	760.00	760.00	760.00	760.00	760.00
p_o mb	1 013.33	1 013.33	1 013.33	1 013.33	1 013.33	1 013.33
log p_o	3.005755	3.005755	3.005755	3.005755	3.005755	3.005755
67.4 T_o	19 411.2	19 411.2	19 411.2	19 411.2	19 411.2	19 411.2
$\frac{h}{67.4\ T_o}$	0.002576	0.010303	0.005152	0.020607	0.005152	0.005152
log p_h	3.003180	2.995452	3.000603	2.985148	3.000603	3.000603
p_h mb	1 007.35	989.58	1 001.39	966.38	1 001.39	1 001.39
$\frac{p_o}{T_o^2}$	0.012217	0.012217	0.012217	0.012217	0.012217	0.012217
T_h^2	82 944	82 944	82 944	82 944	82 944	82 944
$\frac{p_h}{T_h^2}$	0.012145	0.011931	0.012073	0.011651	0.012073	0.012073
0.2925 β	0.000000	0.000000	0.000000	0.000000	0.000000	0.000000
17.19 (1—0.2925 β)	17.19	17.19	17.19	17.19	17.19	17.19
K_o	0.210010	0.210010	0.210010	0.210010	0.210010	0.210010
K_h	0.208773	0.205094	0.207535	0.200281	0.207535	0.207535
$3\ K_o + K_h$	0.838803	0.835124	0.837565	0.830311	0.837565	0.837565
$3\ K_h + K_o$	0.836329	0.825292	0.832615	0.810853	0.832615	0.832615
$\frac{1}{8}\ S/637.8442$	20.2125	20.2125	40.4250	40.4250	60.6375	80.8500
R_o'' "	16.95 52.3	16.88 52.1	33.86 104.5	33.57 103.6	50.79 156.8	67.72 209.0
R_h'' "	16.90 52.2	16.68 51.5	33.66 103.9	32.78 101.2	50.49 155.8	67.32 207.8
R_o m at object	0.41	0.41	1.64	1.63	3.69	6.57
R_h m at object	0.41	0.40	1.63	1.59	3.67	6.53

$\beta = 1.°10.$

Distance, km	5		10		15	20
Height diff., m	50	200	100	400	100	100
$\log p_o$	3.005755	3.005755	3.005755	3.005755	3.005755	3.005755
$\frac{3.413}{\beta}$	3.102727	3.102727	3.102727	3.102727	3.102727	3.102727
$T_o - \beta_h$	287.450	285.800	286.900	283.600	286.900	286.900
$\frac{T_o - \beta_h}{T_o}$	0.998090	0.992361	0.996181	0.984722	0.996181	0.996181
$\log \frac{T_o - \beta_h}{T_o}$	0.999170–1	0.996670–1	0.998338–1	0.993314–1	0.998338–1	0.998338–1
$\log p_h$	3.003180	2.995423	3.000598	2.985010	3.000598	3.000598
p_h	1 007.35	989.52	1 001.38	966.07	1 001.38	1 001.38
$\frac{p_o}{T_o^2}$	0.012217	0.012217	0.012217	0.012217	0.012217	0.012217
T_h^2	82 627.5	81 681.6	82 311.6	80 429.0	82 311.6	82 311.6
$\frac{p_h}{T_h^2}$	0.012191	0.012114	0.012166	0.012011	0.012166	0.012166
$0.2925\ \beta$	0.321750	0.321750	0.321750	0.321750	0.321750	0.321750
$17.19\ (1—0.2925\ \beta)$	11.659118	11.659118	11.659118	11.659118	11.659118	11.659118
K_o	0.142439	0.142439	0.142439	0.142439	0.142439	0.142439
K_h	0.142136	0.141239	0.141845	0.140038	0.141845	0.141845
$3\,K_o + K_h$	0.569453	0.568556	0.569162	0.567355	0.569162	0.569162
$3\,K_h + K_o$	0.568847	0.566156	0.567974	0.562553	0.567974	0.567974
$\frac{1}{8}\ S/637.8442$	20.2125	20.2125	40.4250	40.4250	60.6375	80.8500
R_o'' "	11.51 35.5	11.49 35.5	23.01 71.0	22.94 70.8	34.51 106.5	46.02 142.0
R_h'' "	11.50 35.5	11.44 35.3	22.96 70.9	22.74 70.2	34.44 106.3	45.92 141.7
R_o m. at object	0.28	0.28	1.12	1.11	2.51	4.46
R_h m. at object	0.28	0.28	1.11	1.10	2.50	4.45

$\beta = 0.°80.$

Distance, km	5		10		15	20
Height diff., m	50	200	100	400	100	100
$\log p_o$	3.005755	3.005755	3.005755	3.005755	3.005755	3.005755
$\frac{3.413}{\beta}$	4.266250	4.266250	4.266250	4.266250	4.266250	4.266250
$T_o - \beta_h$	287.600	286.400	287.200	284.800	287.200	287.200
$\frac{T_o - \beta_h}{T_o}$	0.998611	0.994444	0.997222	0.988889	0.997222	0.997222
$\log \frac{T_o - \beta_h}{T_o}$	0.999396–1	0.997581–1	0.998792–1	0.995148–1	0.998792–1	0.998792–1
$\log p_h$	3.003178	2.995435	3.000601	2.985055	3.000601	3.000601
p_h	1 007.35	989.54	1 001.38	966.17	1 001.38	1 001.38
$\frac{p_o}{T_o^2}$	0.012217	0.012217	0.012217	0.012217	0.012217	0.012217
T_h^2	82 713.8	82 025.0	82 483.8	81 111.0	82 483.8	82 483.8
$\frac{p_h}{T_h^2}$	0.012179	0.012064	0.012140	0.011912	0.012140	0.012140
$0.2925\ \beta$	0.234000	0.234000	0.234000	0.234000	0.234000	0.234000
$17.19\ (1—0.2925\ \beta)$	13.167540	13.167540	13.167540	13.167540	13.167540	13.167540
K_o	0.160868	0.160868	0.160868	0.160868	0.160868	0.160868
K_h	0.160367	0.158853	0.159854	0.156852	0.159854	0.159854
$3\,K_o + K_h$	0.642971	0.641457	0.642458	0.639456	0.642458	0.642458
$3\,K_h + K_o$	0.641969	0.637427	0.640430	0.631424	0.640430	0.640430
$\frac{1}{8}\ S/637.8442$	20.2125	20.2125	40.4250	40.4250	60.6375	80.8500
R_o'' "	13.00 40.1	12.97 40.0	25.97 80.2	25.85 79.8	38.96 120.2	51.94 160.3
R_h'' "	12.98 40.1	12.88 39.8	25.89 79.9	25.53 78.8	38.83 119.8	51.78 159.8
R_o m., at object	0.31	0.31	1.26	1.25	2.83	5.04
R_h m., at object	0.31	0.31	1.26	1.24	2.82	5.02

$\beta = 0.°65.$

Distance, km	5		10		15	20
Height diff., m	50	200	100	400	100	100
$\log p_o$	3.005755	3.005755	3.005755	3.005755	3.005755	3.005755
$\frac{3.413}{\beta}$	5.250769	5.250769	5.250769	5.250769	5.250769	5.250769
$T_o - \beta_h$	287.675	286.700	287.350	285.400	287.350	287.350
$\frac{T_o - \beta_h}{T_o}$	0.998872	0.995486	0.997743	0.990972	0.997743	0.997743
$\log \frac{T_o - \beta_h}{T_o}$	0.999510–1	0.998035–1	0.999019–1	0.996062–1	0.999019–1	0.999019–1
$\log p_h$	3.003182	2.995437	3.000604	2.985077	3.000604	3.000604
p_h	1 007.35	989.55	1 001.39	966.22	1 001.39	1 001.39
$\frac{p_o}{T_o^2}$	0.012217	0.012217	0.012217	0.012217	0.012217	0.012217
T_h^2	82 756.9	82 196.9	82 570.0	81 453.2	82 570.0	82 570.0
$\frac{p_h}{T_h^2}$	0.012172	0.012039	0.012128	0.011862	0.012128	0.012128
$0.2925\ \beta$	0.190125	0.190125	0.190125	0.190125	0.190125	0.190125
$17.19\ (1—0.2925\ \beta)$	13.921751	13.921751	13.921751	13.921751	13.921751	13.921751
K_o	0.170082	0.170082	0.170082	0.170082	0.170082	0.170082
K_h	0.169456	0.167604	0.168843	0.165140	0.168843	0.168843
$3\ K_o + K_h$	0.679702	0.677850	0.679089	0.675386	0.679089	0.679089
$3\ K_h + K_o$	0.678450	0.672894	0.676611	0.665502	0.676611	0.676611
$\frac{1}{8}\ S/637.8442$	20.2125	20.2125	40.4250	40.4250	60.6375	80.8500
R_o'' "	13.74 42.4	13.70 42.3	27.45 84.7	27.30 84.3	41.18 127.1	54.90 169.4
R_h'' "	13.71 42.3	13.60 42.0	27.35 84.4	26.90 83.0	41.03 126.6	54.70 168.8
R_o m., at object	0.33	0.33	1.33	1.32	2.99	5.32
R_h m., at object	0.33	0.33	1.33	1.30	2.98	5.30

Result.

The result of these computations is given in figures 16—19, showing the effects at 5, 10, 15, and 20 km respectively, all hypothetical.

The dotted lines mark the assumed overcast constant refraction throughout the day.

This assumption is based upon examination of the records from Johnson-Heywood's [33], Best's [35] and Johnson's own first [36] measurements.

As refraction primarily depends upon the lapse-rate of temperature, (as we have already seen in chapters I and II), and the lapse-rate according to the material in Geophys. Mem. varies with insolation, it appears that insolation is much more important than, for example, temperature and pressure at ground level.

Brocks [32] has clearly described earlier dependable measurements of diurnal variation:

Baeyers (Derenburg) [37],

U. S. Coast and Geodetic Survey's (Ross Mountain, Sacramento, San Fransisco) [38, 39, 40, 41, 42],

Bauernfeinds (Döbra, Höhensteig) [43, 44, 45],

Venturi-Soler (Palermo) [47],

Reina-Cicconetti (Rom) [48].

Cicconetti-Pierpaoli (Udine) [49].

None of these, including his own, give any relation to cloudiness, latitude or day-length, all important factors in insolation.

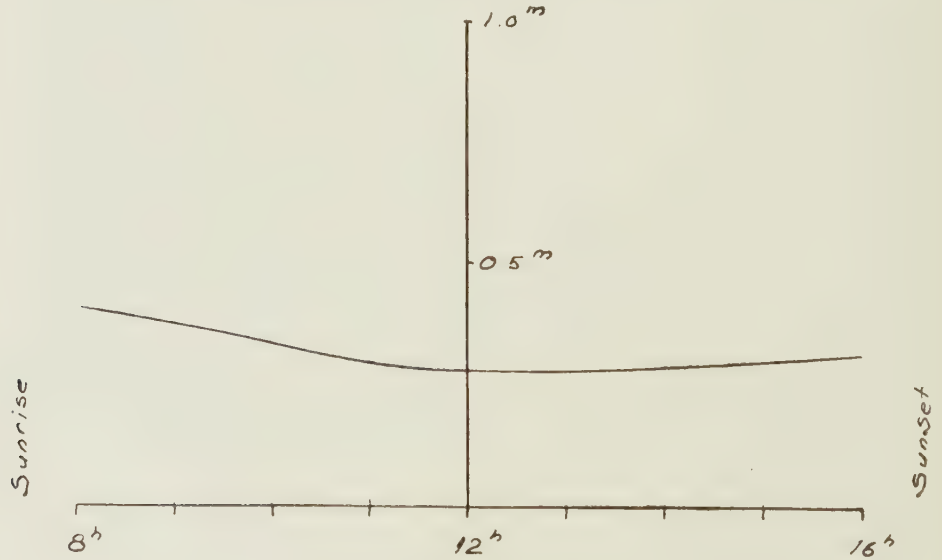

Fig. 16.

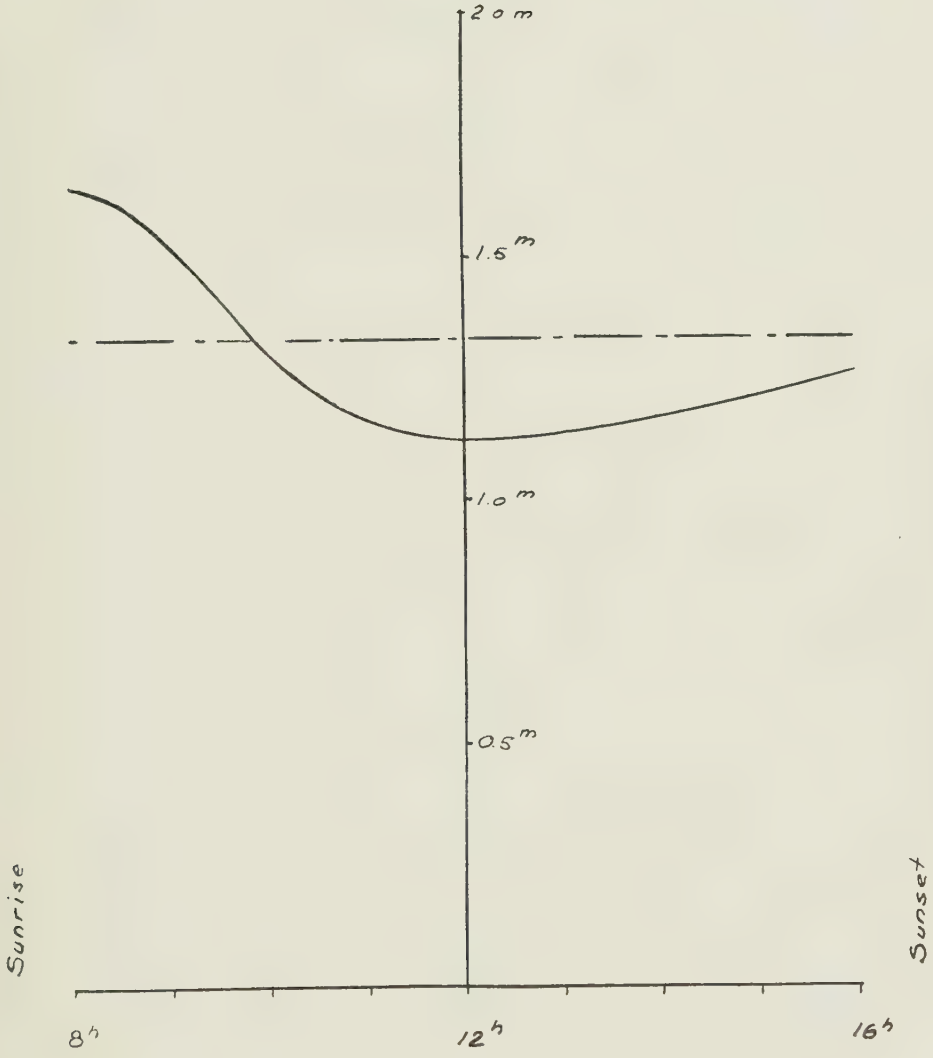

Fig. 17.

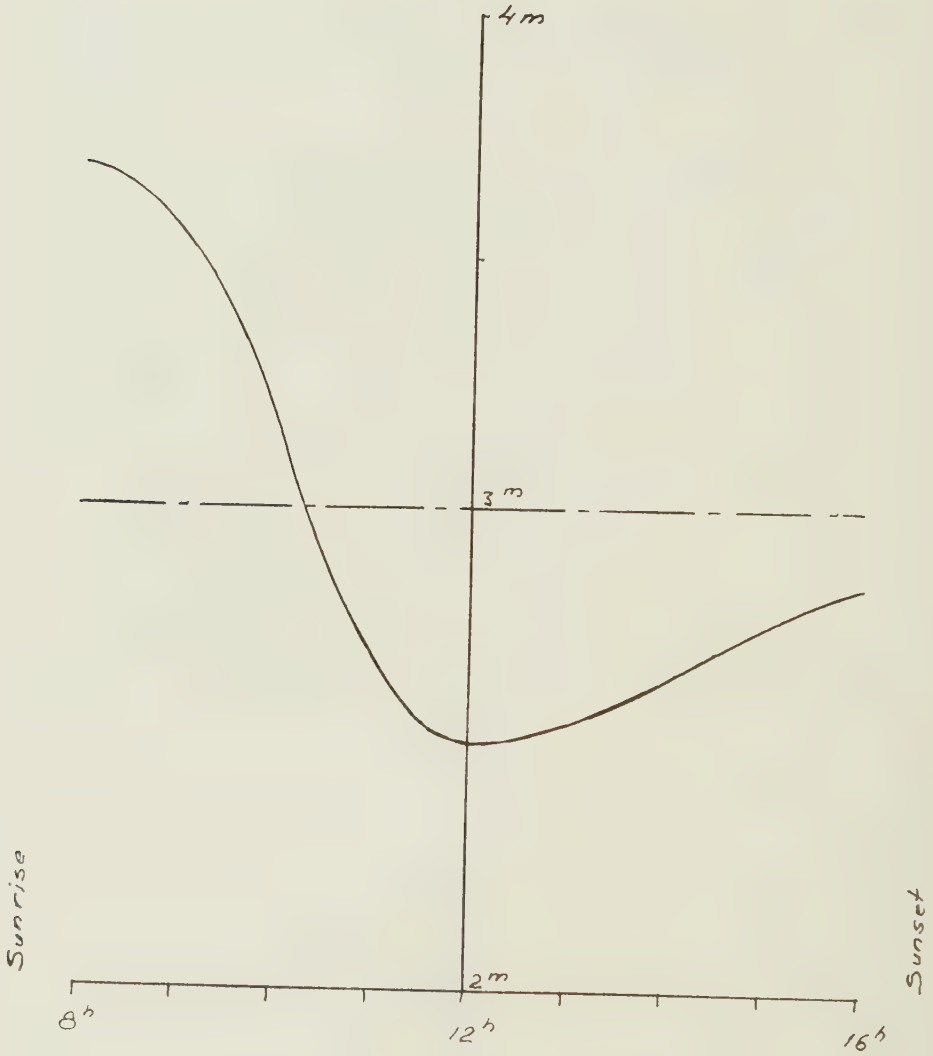

Fig. 18.

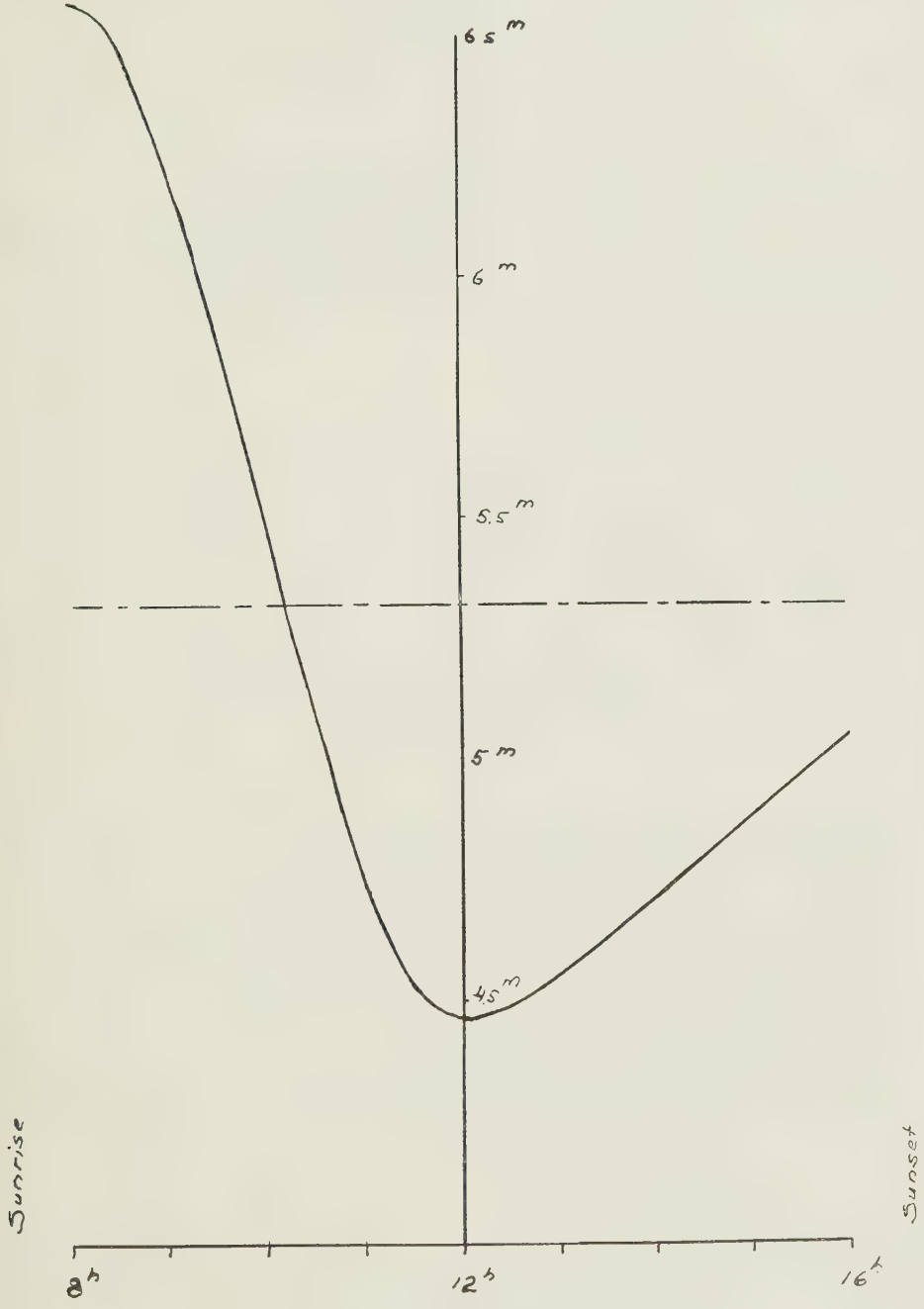

Fig. 19.

B. Theory based on measurements.

Experiment stations.

The instrument, a Wild T3 with the most powerful ocular, 40×, was situated at the tower of the Royal Institute of Technology at Stockholm.

To avoid the effects of »town-climate», objects in the country to the north of the city were used, as the Institute is situated on the north side of Stockholm.

The instrument was placed in total shadow, 62.39 m. over the reference level surface.

Seven objects were used:	Dist.	Height diff.
Paleontol. Museum, Frescati	2.6 km.	3 m.
Watertower of Bergshamra	4.6	12
Tower at station 658 in the Danderyd net.	8.8	9
Southern wireless mast at Spånga	10.6	99
Tower at the Töjnan station, Stockholm net	10.8	5
Tureberg church	11.7	1
Station Löttingekullen, Stockholm net	14.9	5

The rays to these objects had to pass over varying configurations of the ground below. The corresponding ground-profiles are shown in fig. 20.

Taking measurements.

The measurements were taken in a sequence of days in clear, cloudy and overcast weather, with varying ground pressure and temperature, to which no attention was given. Only the factors affecting insolation, such as cloudiness, time of day, and day of year, were taken into account.

Unfortunately, there has been no opportunity to get larger measurements nor to compute some material observed later in surveying, but the given material allows a very rough construction of the variation with insolation. Days of observation, April 22 to May 2, 1949.

Fig. 21—27 show the variations for each object.

The axes give angle from horizon and time of day.

Signs

× = Clear

⊗ = 1/4 overcast

⊗ = 2/4 overcast

⊗ = 3/4 overcast

⊗ = overcast

→ = increasing cloudiness

← = decreasing »

- - - - - - - = curve for clear sky

——— = » » overcast sky.

Profiles.

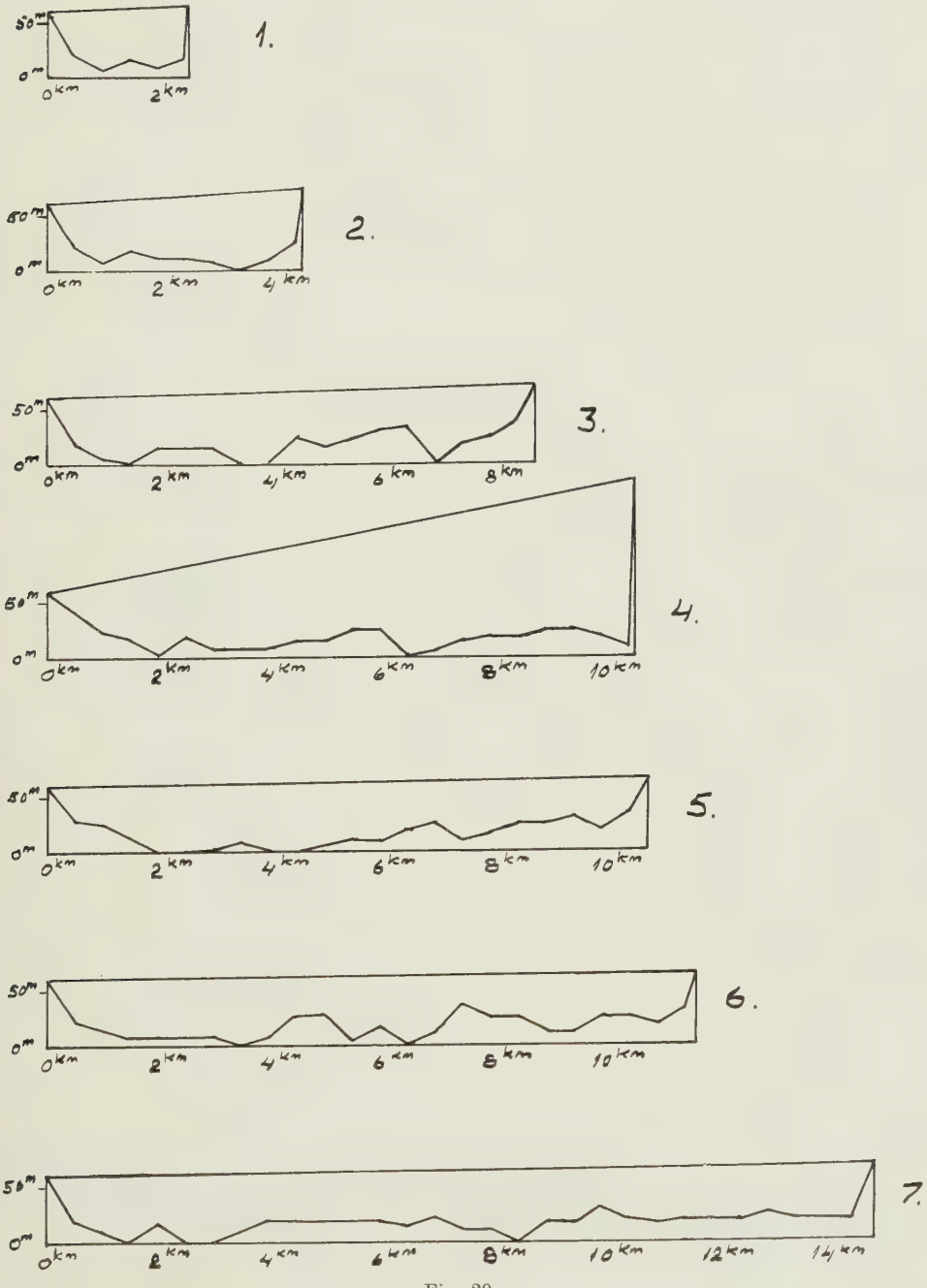

Fig. 20.

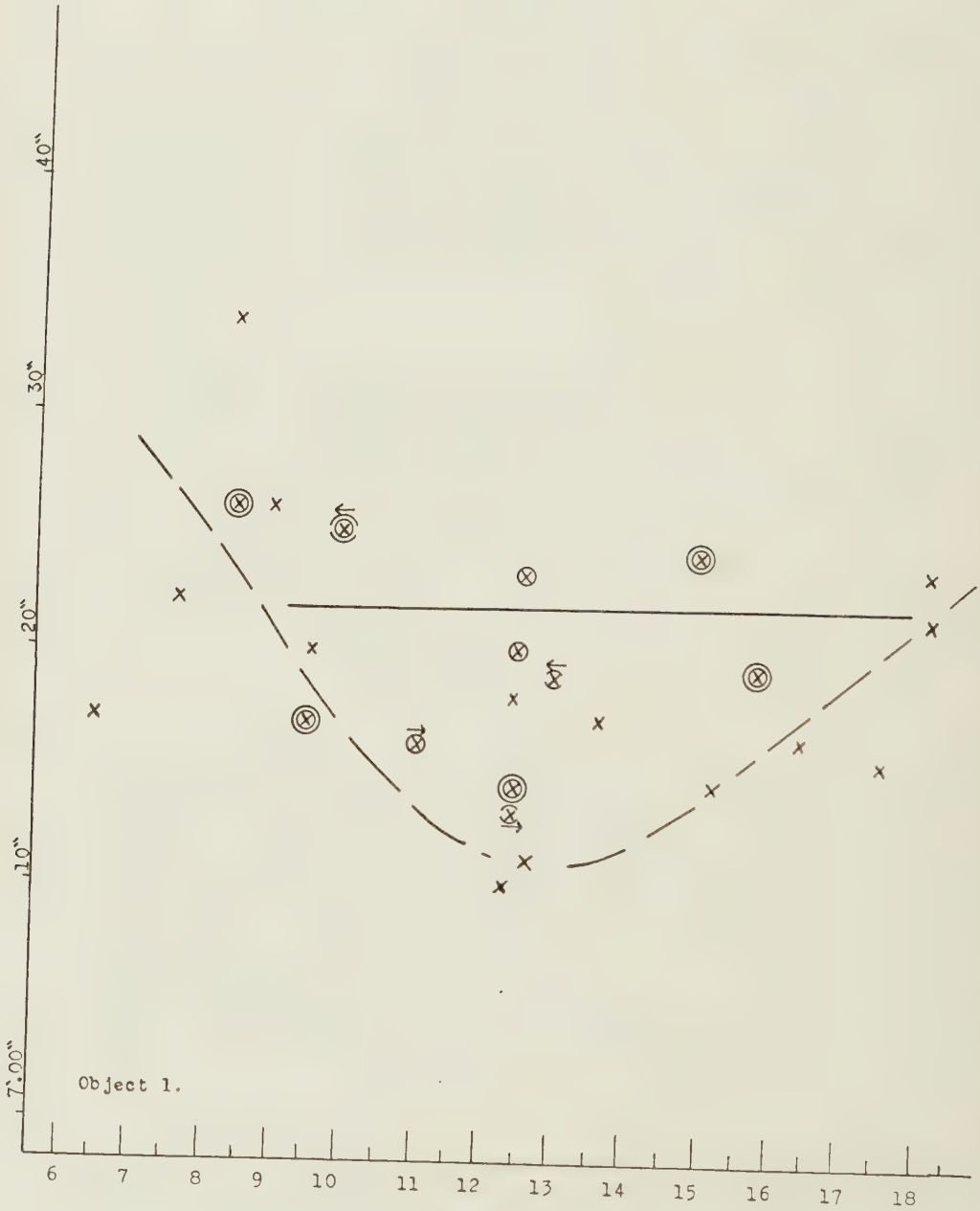

Fig. 21.

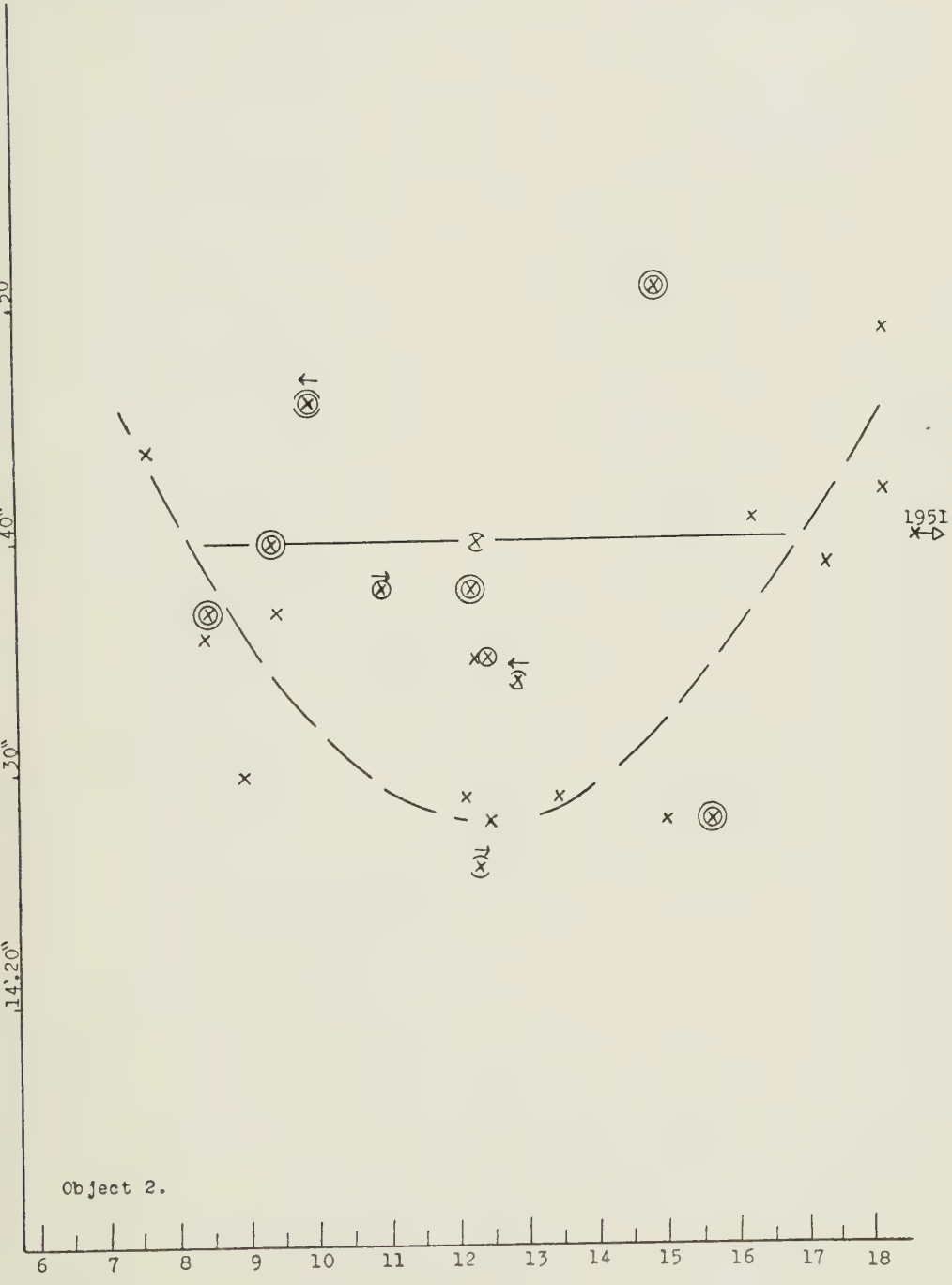

Fig. 22.

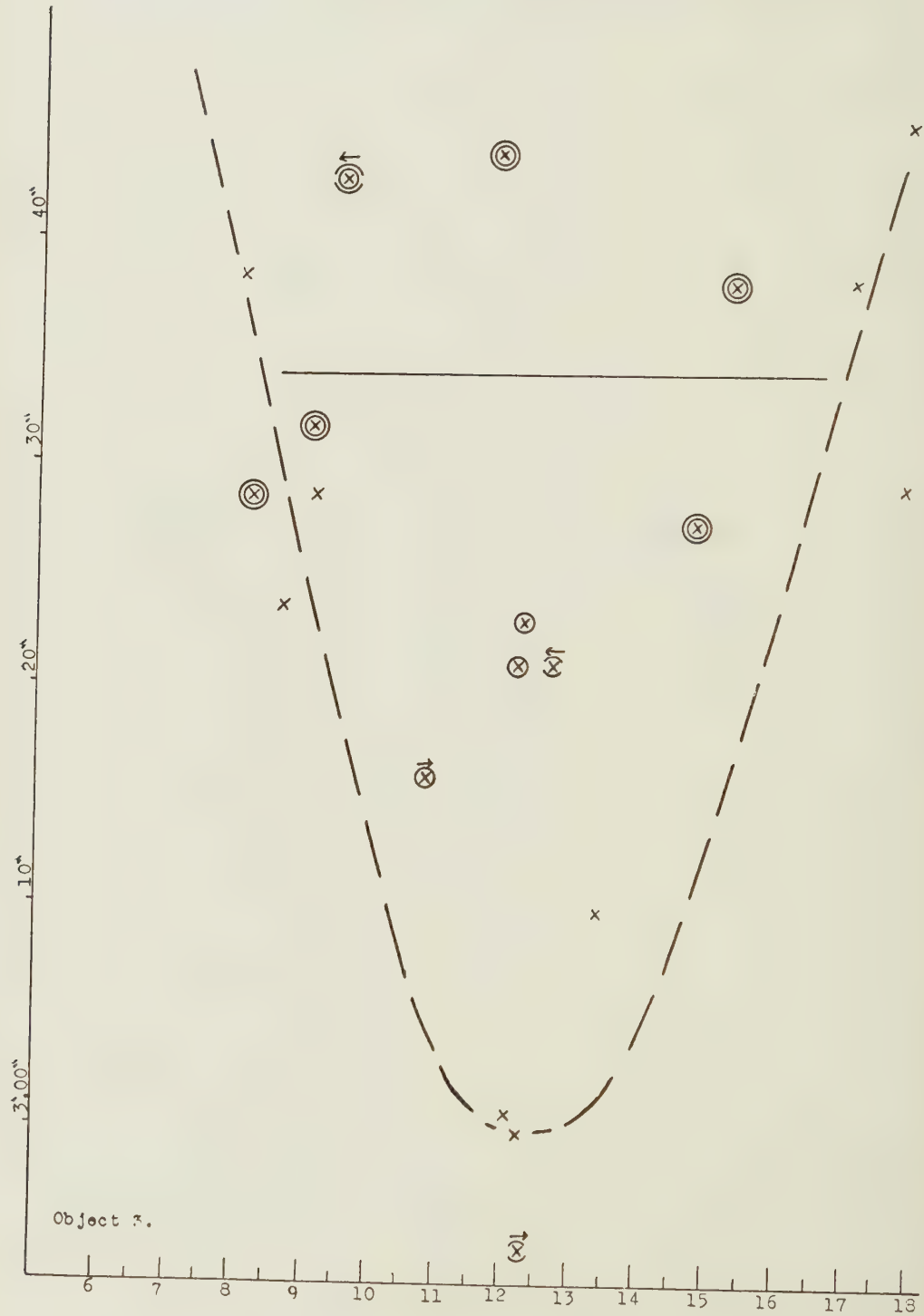

Fig. 23.

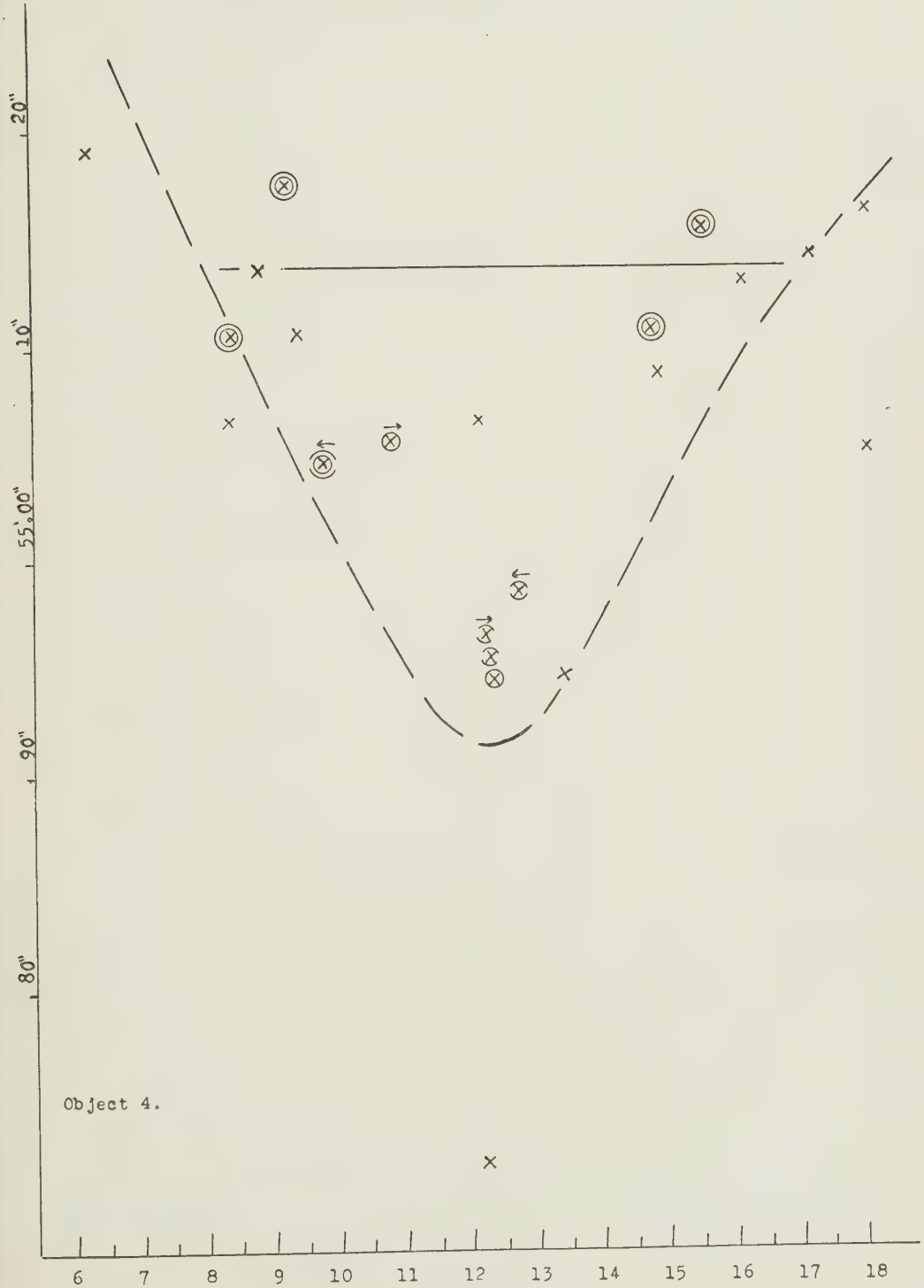

Fig. 24.

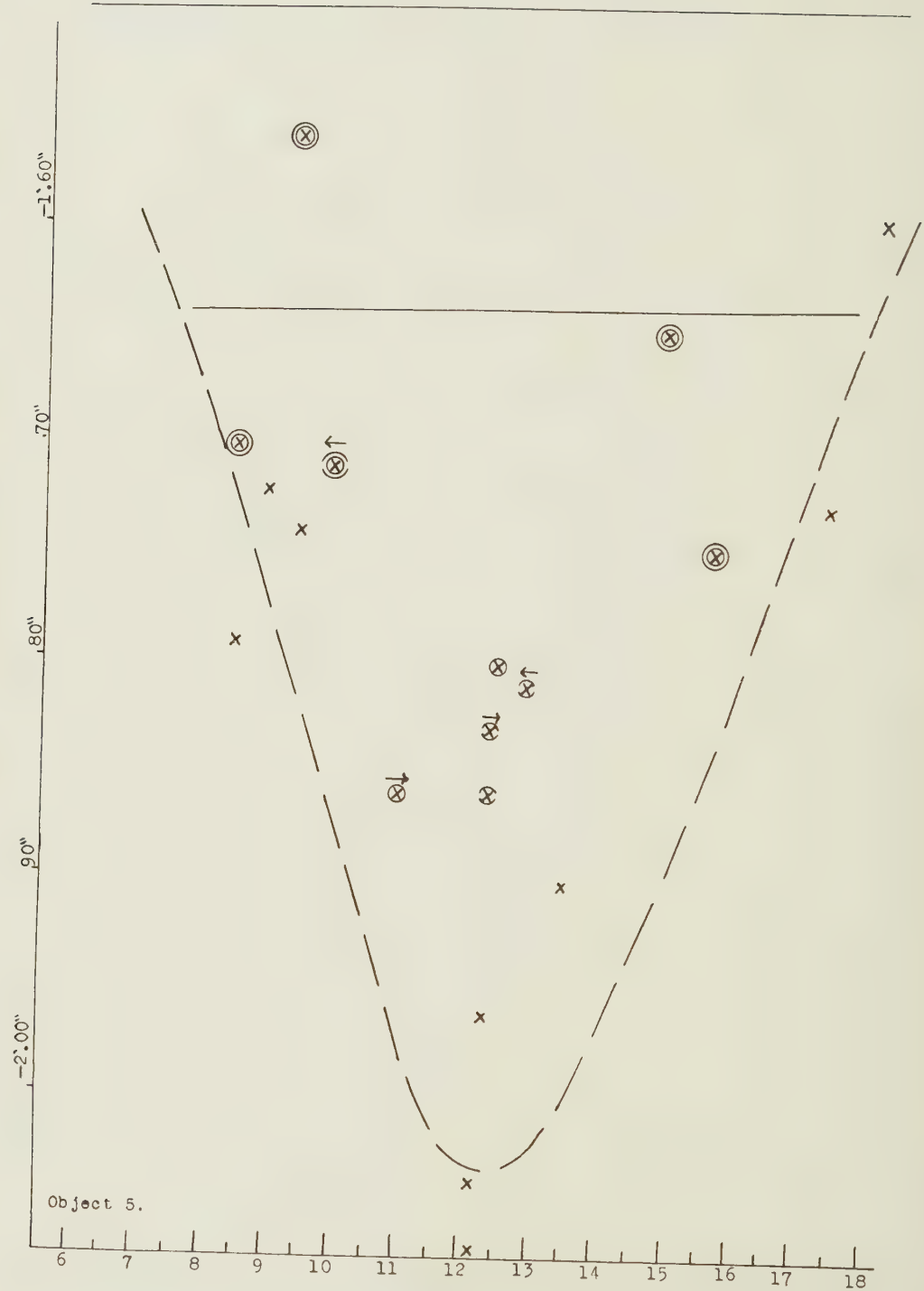

Fig. 25.

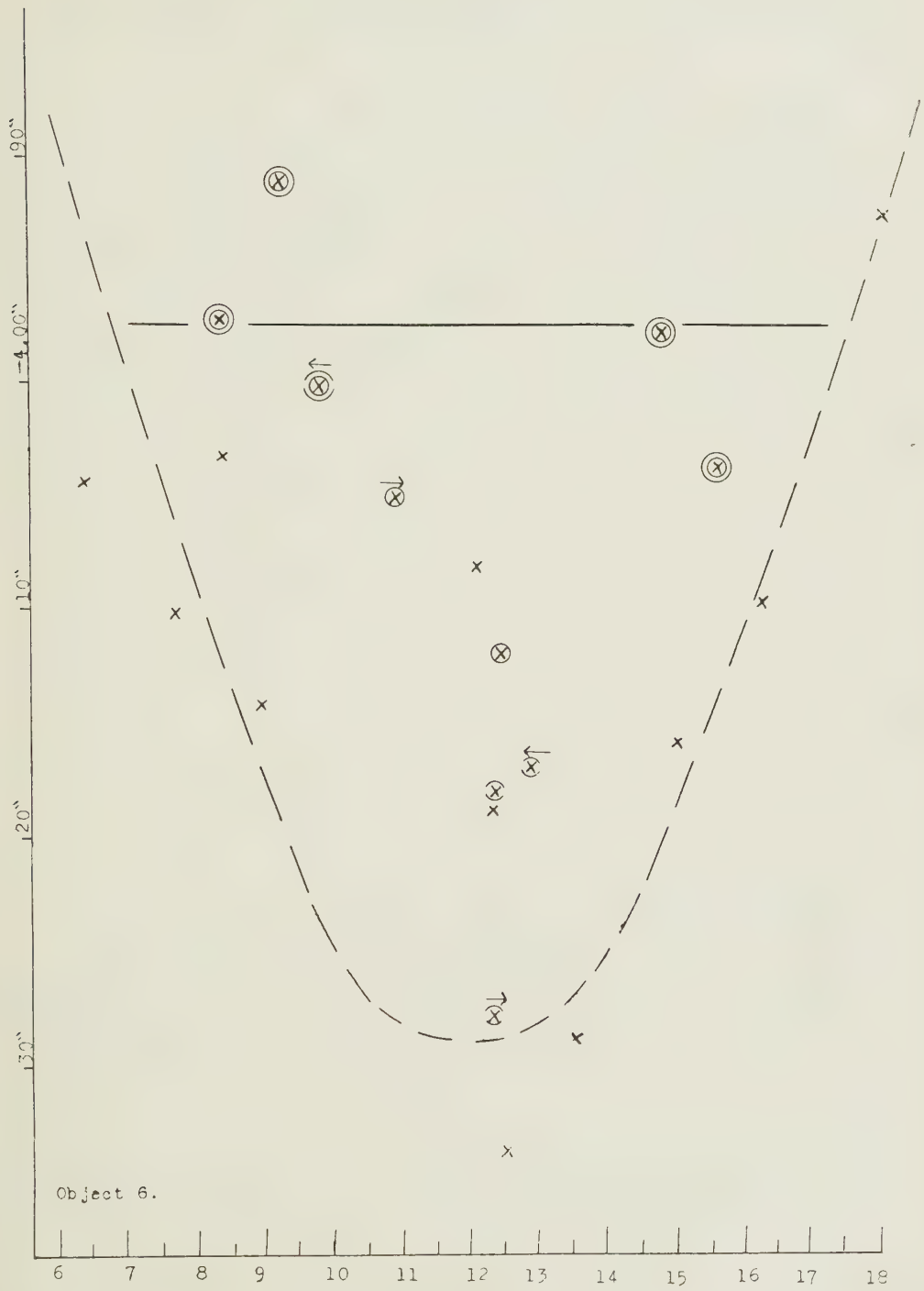

Fig. 26.

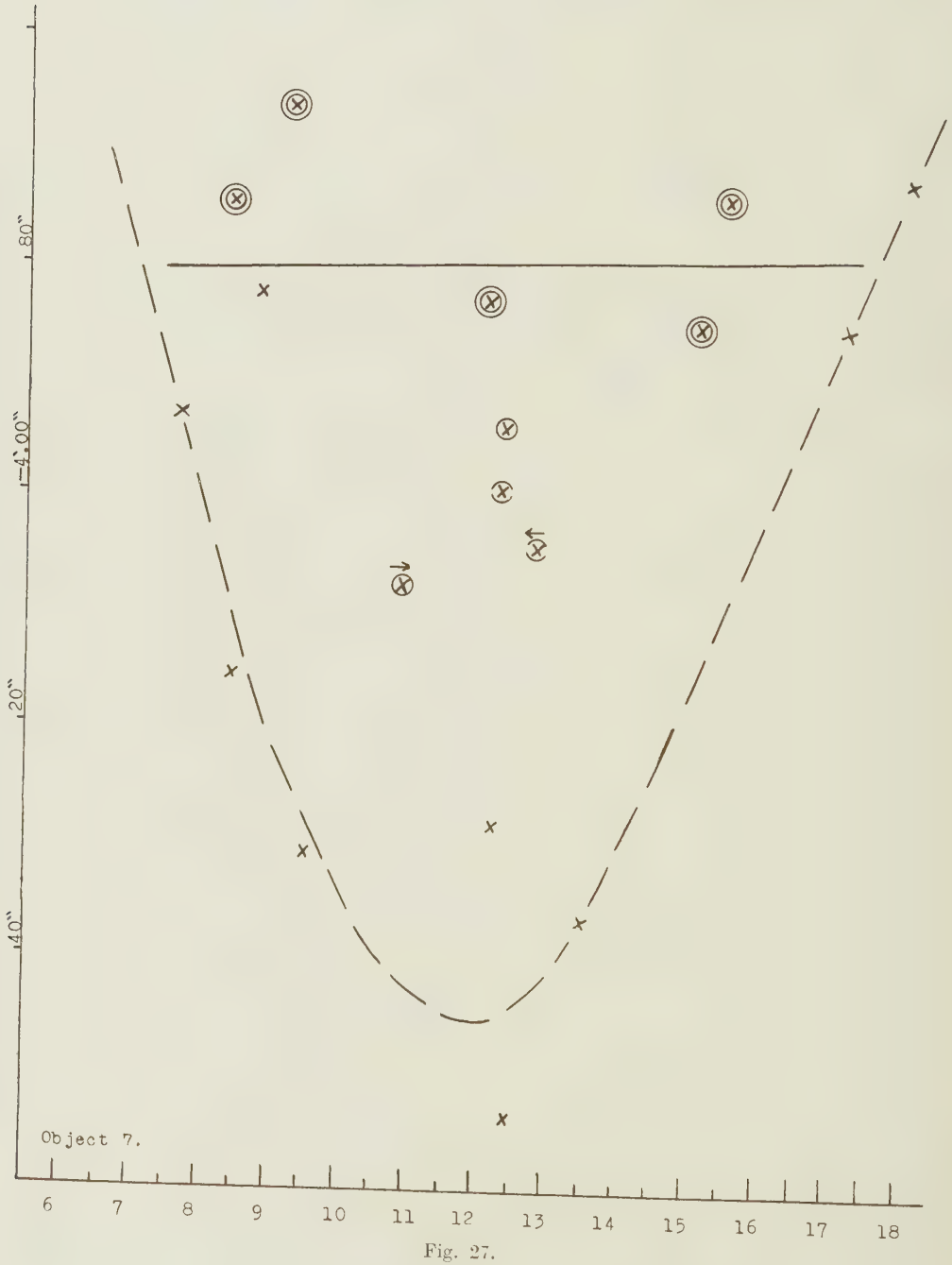

Fig. 27.

Effective height.

The topographical profile is very important, as ground inversion varies with height above ground level.

Brocks [32] gives the mean height over sea-level of the ray as the most significant factor in, for instance, diurnal amplitude, considering it to be more valid than the distance from ground!

This probably results from the fact that obviously the *average* absolute heights and topographical heights have been compared.

On the contrary, Brocks [32] himself has very clearly given the dependance of refraction on the distance from the instrument. He thus defines the first quarter of the ray as being of 43.8 % weight for refraction at the instrument, while the last quarter has a weight of only 6.2 %.

These facts give the impression that average heights should not be used as they give disproportional weights to the parts of the ray.

In this essay a conception containing the correct proportions in weight by concentrating the numerical points near the instrument is used. This height is called »effective height», h_e, and is the mean of the heights of the ray above ground level at the instrument, and at the first, third and sixth eighths of the slope,

$$h_e = \frac{2h_{\text{instr.}} + h_{\text{obj.}} - h_{1/8} - h_{3/8} - h_{6/8}}{4}.$$

over 50 m. height difference to be added with

$$\frac{h_{\text{obj.}} - h_{\text{instr.}}}{16}$$

In this formula the heights in the numerator are computed from sea level and the instrument height above ground level is assumed to be 0 m, which could be allowed in practice when the instrument is mounted on a tripod which rests on the ground. If the height over ground of the instrument is greater, it has to be added to the numerator.

Fig. 28 shows the four points in the ray, of which h_e is the average.

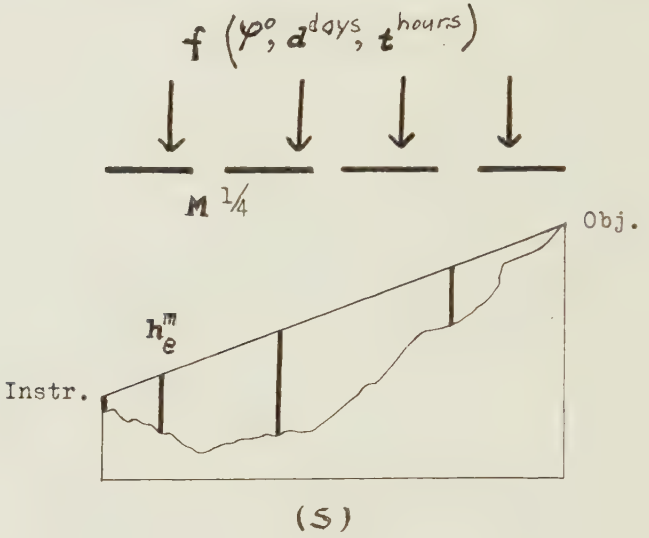

Fig. 28.

Amplitudes.

The amplitude *clear-overcast* is obvious even with the scarce material available. The diurnal amplitude can only be estimated, as no night observations were made.

Using effective height, the expression for the amplitude *clear-overcast* becomes simply $0.136\,\frac{s}{h_c}$, where s is the distance in meters.

The diurnal amplitude according to Brocks [32] has to be multiplied by about 0.42 to be of approximately the same magnitude.

Clear-overcast amplitudes.

Objects	S m	$h_{\text{aver.}}$ m	$h_{\text{eff.}}$ m	$\text{ampl.}''_{\text{meas.}}$	$0.42\left(9.6+27.8\,\frac{S^2}{h_{\text{aver.}}}-\right)''$	$0.136\,\frac{S''}{h_e}$
1	2 634	41	32	10	6.0	11.2
2	4 586	50	40	12	8.9	15.6
3	8 815	47	34	34	23.4	35.2
4	10 584	92	60	22	18.3	23.9
5	10 842	45	38	39	34.6	38.8
6	11 670	44	33	32	40.1	48.1
7	14 934	47	34	62	59.4	59.7

Absolute refraction.

The overcast line for each object seems to be firm enough for a reference value, where we can fix the absolute refraction.

Thus, a formula based on this principle will contain two terms, one constant overcast and one variable, depending upon insolation, the latter becoming 0 in overcast weather.

The objects N:ris 2, 4 and 6 were nivellated and could be used for absolute measurements. Unfortunately, object 2 showed a mistake in the detail measurement at the station, made by the author, and very difficult to evaluate, partly depending upon object phases with steep rays.

Object 4, South wireless mast at Spånga

$S = 10\,584.4$ m. $h_e = 60$ m

h diff. $= + 99.44$ m $\pm$ 0.04 m

angle of obs. $+ 55' 14''$ = overcast line

Curvature, height effect $- 8.78$ m

angular » $- 5' 28''$

Trigonometric height $+ 59' 81''$ (corresp. to height diff.)

Refr. observed $= 5' 28'' + 55' 14'' - 59' 81'' = + 0' 61''$

$$\frac{R \cdot h_e}{S} = 0.346$$

$$R_{\text{obj. 4}} = 0.346 \frac{S}{h_e}$$

Object 6, Tureberg church

$S = 11\,669.5$ m. $h_e = 33$ m

h diff. $= + 1.31$ m $\pm$ 0.06 m

angle of obs. $= - 3' 94''$ = overcast line

curvature, height effect $= - 10.68$ m

angular » $= - 5' 82''$

trigonometric height $= + 0' 71''$ (corresp. to height diff.)

refr. observed $= 5' 82'' - 3' 94'' - 0' 71'' = 1' 17''$

$$\frac{R \cdot h_e}{S} = 0.331$$

$$R_{\text{obj. 6}} = 0.331 \frac{S}{h_e}$$

We obtain $R = 0.34 \frac{S}{h_e}$ as an acceptable value with this material.

Insolation functions.

The day-length can be obtained out of any almanac. The day-length of Stockholm has here been treated as two linear functions, crossing at a maximum 174 days from Jan. 1.

As the max. day-length for these purposes can be approximated to 19.7 hours, we can write

$$D = 19.7 - 0.083 \left| 172 - d \right| , \text{ in hours}$$

where D means day-length and d day of the year, numbered from Jan. 1.

But this is only the day-length for the latitude of Stockholm, $\varphi = 59.^{\circ}5$. To obtain a function for day-length correction according to latitude will be a matter of empirical tests to get the most convenient trigonometric function. The expression

$$K_D = 0.5 \, (\varphi - 59.5) \sin^{|2|}(d - 82) , \text{ in hours,}$$

where

K_D = correction for latitude

and

$$\sin^{|2|}(d - 82) = \sin (d - 82) \left| \sin (d - 82) \right|$$

seems to follow the real corrections acceptably.

The overcast line always makes a chord in the clear curve. This chord is of about the same length for all objects, which could be expected, and about 64 % of the day-length.

The centre of this curve seems to be at about 12.8 o'clock. The explanation of this is possibly the speed of reaction from insolation to lapse-rate.

As the lowest parts of the clear curves are sharply bowed, it would not require excessively large approximations to treat them as two crossing lines.

The position of an observation on the clear curve will then be a certain part of the amplitude below overcast, a linear function of the observation time $\left| t - 12.8 \right|$ divided through the half-chord, i. e. $0.32 \, (D + K_D)$. The position of an observation is within the time-chord always below the overcast line and thus of negative sign, a subtraction by 1. At the ends of the chord this binominal

$$0.136 \frac{S}{h_e} \left\{ \frac{\left| t - 12.8 \right|}{0.32 \left[19.7 - 0.083 \left| 172 - d \right| + 0.5 \, (\varphi - 59.5) \sin^{|2|}(d - 82) \right]} - 1 \right|$$

becomes 0. The effect of cloudiness is reached by multiplying the binomial with the factor $\frac{4 - M}{4}$, which is 0 at overcast. M is the cloudiness in quarters.

General formulae.

We obtain

$$R = 0.34\,\frac{S}{h_e} + 0.136\,\frac{S}{h_e}\left[\frac{3.12\,|t-12.8|}{19.7-0.083\,|172-d|+0.5\,(\varphi-59.5)\sin^{|2|}(d-82)} - 1\right]\frac{4-M}{4},$$

or

$$R = \frac{S}{h_e}\left[0.34 + \frac{4-M}{29.4}\left(\frac{3.12\,|t-12.8|}{19.7-0.083\,|172-d|+0.5\,(\varphi-59.5)\sin^{|2|}(d-82)} - 1\right)\right].$$

If the variable term in the brackets is called V, we can write the combined effects of refraction and curvature in the expression

$$S\left(\frac{0.34+V}{h_e} - 0.0499\right)''.$$

The signs used are, repeated,

Time of the day = t hours.
Day of the year = d days from Jan. 1.
Latitude = φ°
Distance = S m.
Effective height = h_e m.
Cloudiness = M quarters
Refraction = R''.

Diagrams for solution.

These formulae cannot be used for each ray with numerical computations, since they would be too tedious for surveying.

The diagrams in fig. 29—33 give a graphical solution of both trigonometric refraction and curvature, which will be much faster.

These diagrams are only schematical, to show the principles. Diagrams for practical use have to be made on larger scales and cross-ruled.

Finally, the constants in the obtained formulae have to be regarded as primary, experimental values for the rough formation of the theory.

The principles of this are illustrated in fig. 28.

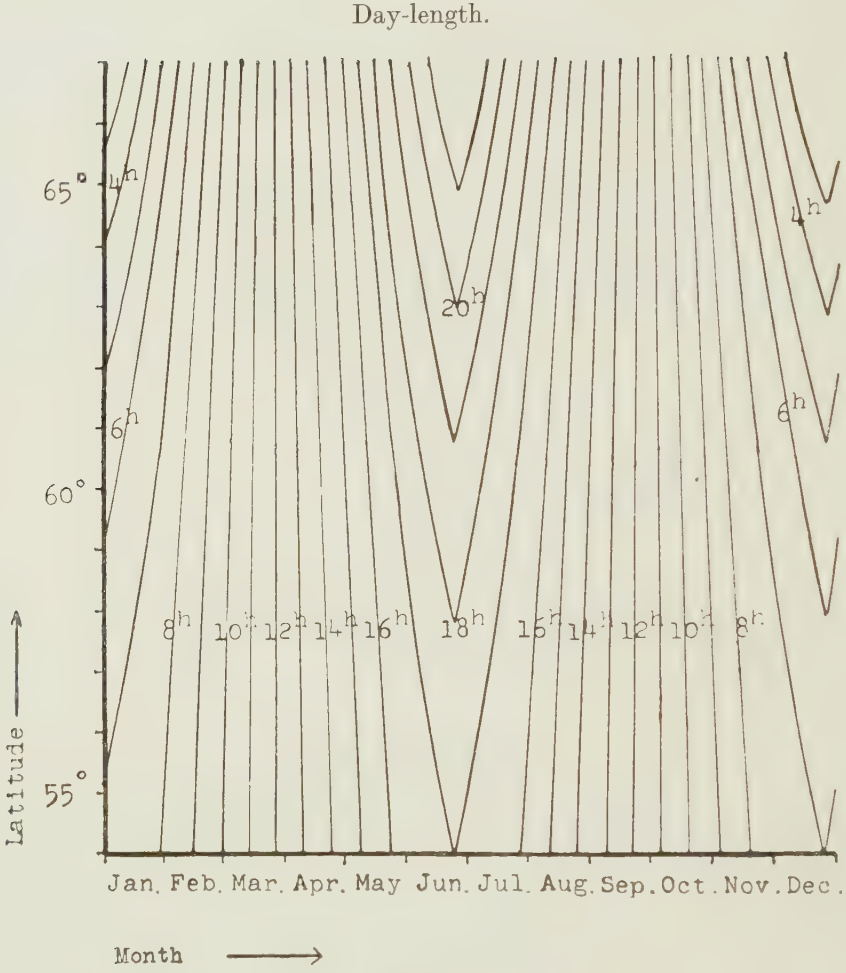
Day-length.
65°
60°
55°
4h
6h
8h
10h
12h
14h
16h
18h
20h
Latitude
Jan. Feb. Mar. Apr. May Jun. Jul. Aug. Sep. Oct. Nov. Dec.
Month

Fig. 29.

Time-quotient.
0.1
0.2
0.3
0.4
0.5
0.6
0.7
0.8
0.9
1,0
1.1
1.2
1.3
1.4
1.5
Day-length
21 20 19 18 17 16 15 14 13 12 11 10 9 8 7 6 5 4 3
12 11 10 9 8 7 6 5 4
13 14 15 16 17 18 19 20 21
Hour

Fig. 30.

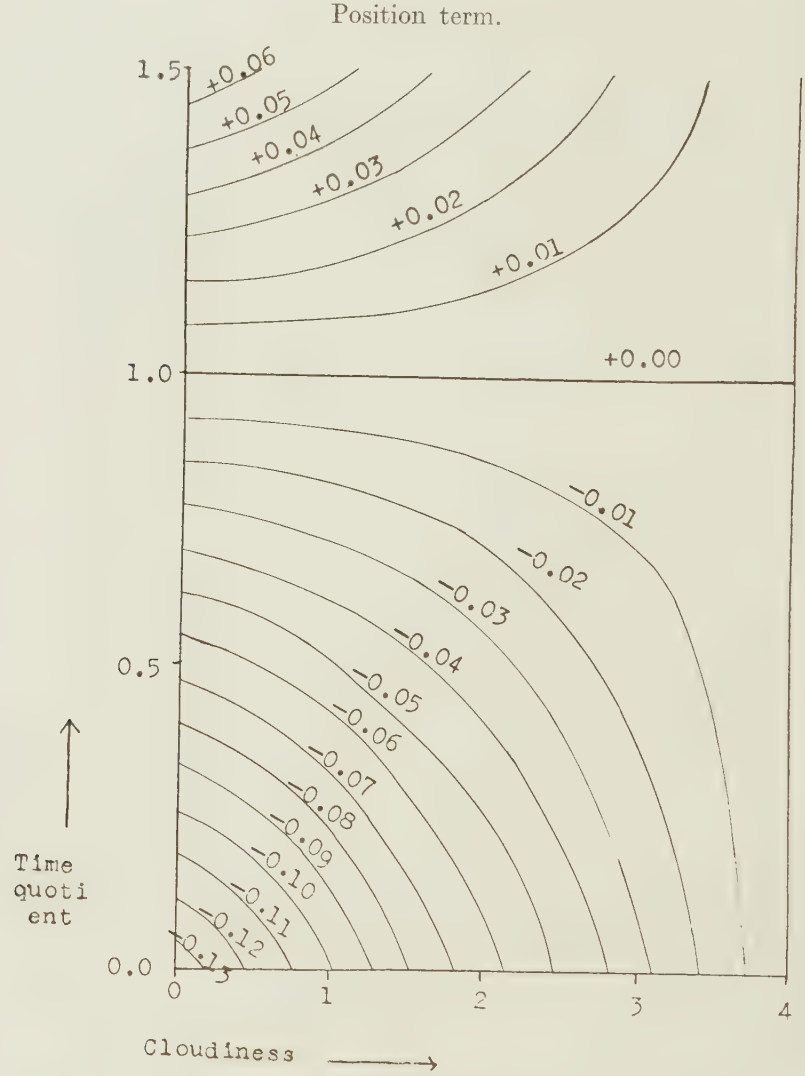
Position term.
1.5
1.0
0.5
0.0
+0.06
+0.05
+0.04
+0.03
+0.02
+0.01
+0.00
−0.01
−0.02
−0.03
−0.04
−0.05
−0.06
−0.07
−0.08
−0.09
−0.10
−0.11
−0.12
−0.13
Time quotient
0
1
2
3
4
Cloudiness

Fig. 31.

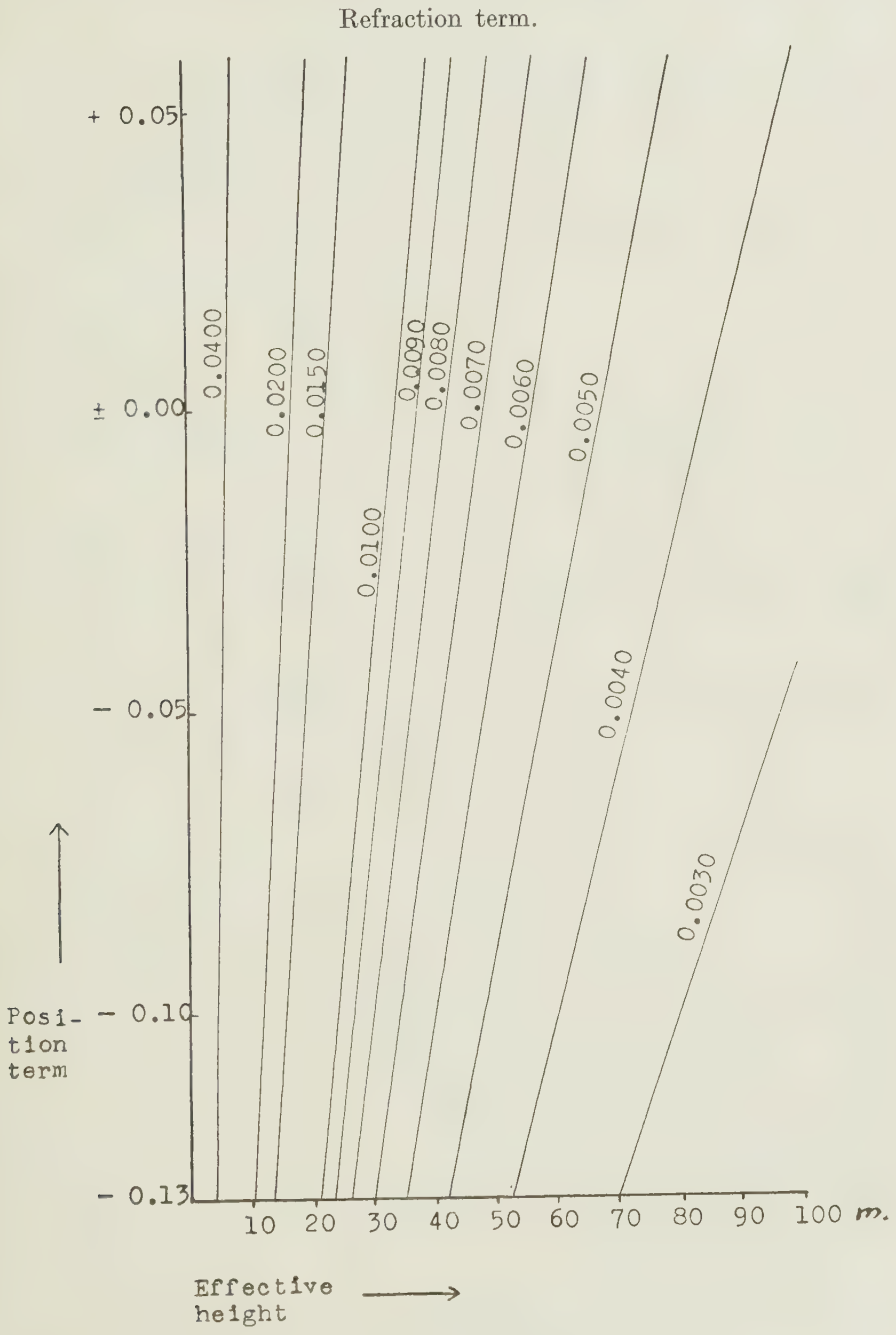
Refraction term.
+ 0.05
± 0.00
− 0.05
− 0.10
− 0.13
0.0400
0.0200
0.0150
0.0100
0.0090
0.0080
0.0070
0.0060
0.0050
0.0040
0.0030
Posi-
tion
term
10 20 30 40 50 60 70 80 90 100 m.
Effective
height

Fig. 32.

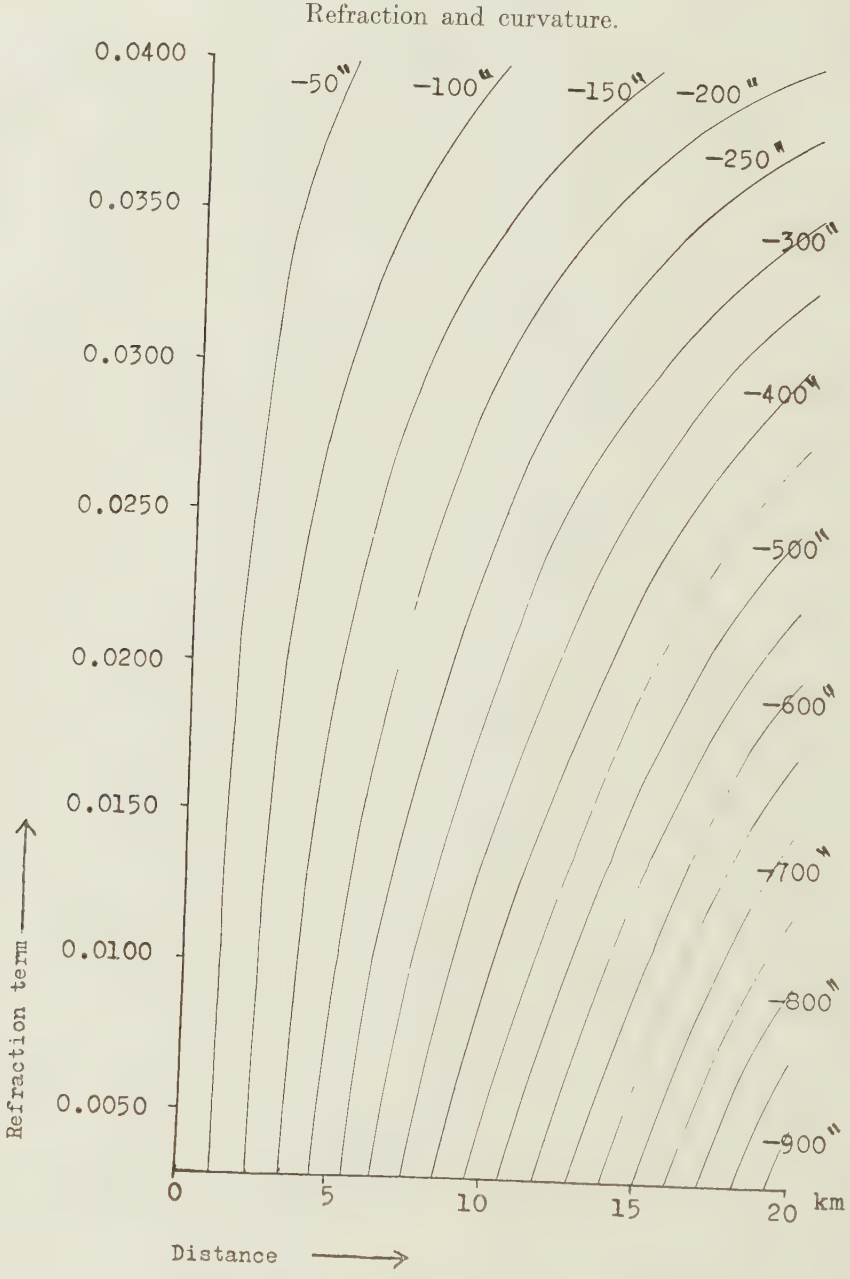
Refraction and curvature.
0.0400
0.0350
0.0300
0.0250
0.0200
0.0150
0.0100
0.0050
Refraction term
−50″
−100″
−150″
−200″
−250″
−300″
−400″
−500″
−600″
−700″
−800″
−900″
0
5
10
15
20
km
Distance

Fig. 33.

LITERATURE.

([ ] in the text.)

1. Meteorologische Optik, Wien 1910.
2. Refraction Tables of Poulkovo Observatory, Moskau 1930.
3. Physical and Dynamical Meteorology, Cambridge 1934.
4. Beiträge zur Geophysik, V. 50, 1937.
5. Bildmessung und Luftbildwesen, 1937, 3.
6. Tables for Sea and Air Navigation, London 1938.
7. Photogrammetria, 1942, 3.
8. Quarterly Journal, R. M. S. 55, 1929.
9. Phil. Trans. R. Soc., 1863.
10. Ann. Chim. phys., 55, Paris 1858.
11. Wiedemanns Ann. Physik., 9, 1880.
12. Physical Review, 14, 1902.
13. Kaye and Laby's Tables, 1911.
14. Neue Annalen der K. Sternwarte in München, 3, 1898.
15. Veröffentlichungen der Grossherzogl. Sternw. zu Heidelberg, 3, 1904.
16. Veröffentl. der Badischen Sternw. zu Heidelberg (Königsstuhl) 8, 1932.

17 a. A comp. of spher. astr., Cambridge 1906.

17 b. L. der Sphärischen Astronomie, Leipzig 1912.

18. Bildmessung und Luftbildwesen, 1937, 1.
19. Zeitschr. f. Vermessungswesen, 1937, 17.
20. Union Géodés. et Geophys. Intern., l'Ellipsoide de Réf. Int., Paris 1928.
21. Zeitschr. f. Verm.wesen u. Kaulturtechnik, Schweizisch. Geometerver., jan. 1945.
22. D:o febr. 1945.
23. Photogrammetric Engineering, 1946, 2.
23. Über die Herstellung Photogrammetrischer Pläne, Esselte, 1944.
25. Geophysical Memoirs, No:s 2 and 13.
26. Ann. de l'Observatoire de Paris, Tome XVI, 1882.
27. Publikation der Sternw. in Kiel, XIII, 1922—24.
28. Bull. of the Astr. Institutes of the Netherlands, Vol. IV, 1928.
29. Royal Inst. of Great Britain, nov. 1936.
30. Monthly Notices, Royal Astr. Soc., Vol. 92, 1931.
31. Ann. Reg. Scientiarum Soc. Upsaliensis, 1938.
32. Veröffentl. d. Meteor. Inst. d. Univ. Berlin, 1939.
33. Geophysical Memoirs, No 77, London 1938.
34. Suomen Geodeettisen Laitoksen Julkaisuja, Helsinki 1939.
35. Geophysical Memoirs, No 65, London 1935.
36. D:o , No 46, London 1929.
37. Mém. de L'Academie impériale des Sciences de S:t Petersb. T. 3, N. 5, 1860.
38. U. S. Coast and Geodetic Survey, Reports 1871, Davidson-Schott.
39. D:o , Reports 1876, D:o.
40. D:o , Reports 1883, Appendix 12.
41. D:o , Reports 1884, Appendix 10.
42. D:o , Special Publication Nr 4, 1900.
43. 1. Mitteilung. Abh. d. Kgl. Bayer. Akad. d. Wiss., Bd. XIII, München 1880.
44. 2. Mitteilung. D:o , Bd. XV, München 1886.
45. 3. Mitteilung. D:o , Bd. XVI, 1888.
46. Nachtrag D:o , Bd. XVII, 1889.
47. Atti d. Acad. de Sc. de Palermo, 3 Serie, Vol. 13, Palermo 1895.
48. Mem. d. mat. e d. fis. d. soc. ital. d. sc., Serie III, Tome X, Roma 1896.
49. Tipografia della R. Ac. di Lincei, Roma 1902.
50. A comp. of spher. astr.

APPENDIX.

Photogrammetric refraction and curvature.

Ground level 0 km.

km	5°	10	15	20	25	30	35	40	45	50	55	60	65
	"												
0.5	+ 0.3	+ 0.6	+ 0.7	+ 0.6	+ 0.2	— 0.5	— 1.6	— 3.2	— 5.4	— 8.3	— 12.0	— 16.7	— 22.7
1.0	+ 0.6	+ 1.1	+ 1.3	+ 1.2	+ 0.4	— 1.0	— 3.3	— 6.5	— 11.0	— 16.8	— 24.2	— 33.7	— 45.8
1.5	+ 0.9	+ 1.6	+ 1.9	+ 1.6	+ 0.4	— 1.8	— 5.2	— 10.2	— 16.8	— 25.5	— 36.8	— 51.0	— 69.4
2.0	+ 1.2	+ 2.1	+ 2.4	+ 1.9	+ 0.3	— 2.6	— 7.2	— 13.8	— 22.8	— 34.4	— 49.5	— 68.6	— 93.1
2.5	+ 1.4	+ 2.5	+ 2.9	+ 2.2	+ 0.2	— 3.5	— 9.3	— 17.6	— 28.8	— 43.5	— 62.4	— 86.4	— 117.2
3.0	+ 1.6	+ 2.9	+ 3.3	+ 2.6	+ 0.1	— 4.4	— 11.4	— 21.5	— 34.9	— 52.7	— 75.4	— 104.3	— 141.4
3.5	+ 1.9	+ 3.3	+ 3.7	+ 2.8	— 0.2	— 5.5	— 13.8	— 25.5	— 41.4	— 62.1	— 88.7	— 122.6	— 166.1
4.0	+ 2.1	+ 3.7	+ 4.1	+ 2.9	— 0.5	— 6.7	— 16.2	— 29.7	— 47.9	— 71.7	— 102.2	— 141.1	— 190.9
4.5	+ 2.3	+ 4.0	+ 4.5	+ 3.0	— 0.8	— 7.9	— 18.7	— 34.0	— 54.6	— 81.5	— 115.9	— 159.9	— 216.1
5.0	+ 2.5	+ 4.3	+ 4.7	+ 3.1	— 1.3	— 9.2	— 21.3	— 38.4	— 61.5	— 91.5	— 129.9	— 179.0	— 241.7
5.5	+ 2.7	+ 4.6	+ 5.0	+ 3.1	— 1.8	— 10.6	— 24.0	— 43.0	— 68.4	— 101.5	— 144.0	— 198.2	— 267.3
6.0	+ 2.9	+ 4.8	+ 5.2	+ 3.0	— 2.5	— 12.0	— 26.8	— 47.6	— 75.4	— 111.7	— 158.2	— 217.4	— 293.2
6.5	+ 3.0	+ 5.1	+ 5.4	+ 2.9	— 3.1	— 13.7	— 29.7	— 52.3	— 82.7	— 122.1	— 172.6	— 237.0	— 319.4
7.0	+ 3.1	+ 5.3	+ 5.5	+ 2.8	— 3.8	— 15.3	— 32.7	— 57.3	— 89.9	— 132.7	— 187.3	— 256.9	— 345.9
7.5	+ 3.3	+ 5.5	+ 5.6	+ 2.7	— 4.5	— 16.9	— 35.7	— 62.0	— 97.3	— 143.2	— 202.0	— 276.8	— 372.4
8.0	+ 3.4	+ 5.7	+ 5.7	+ 2.4	— 5.3	— 18.7	— 38.9	— 67.1	— 104.9	— 154.0	— 216.9	— 296.9	— 399.2
8.5	+ 3.5	+ 5.9	+ 5.7	+ 2.1	— 6.2	— 20.5	— 42.1	— 72.3	— 112.6	— 165.0	— 232.1	— 317.3	— 426.3
9.0	+ 3.6	+ 6.0	+ 5.8	+ 1.9	— 7.1	— 22.4	— 45.3	— 77.4	— 120.3	— 176.0	— 247.2	— 337.7	— 453.5
9.5	+ 3.7	+ 6.1	+ 5.8	+ 1.5	— 8.1	— 24.4	— 48.7	— 82.7	— 128.2	— 187.1	— 262.6	— 358.4	— 481.0
10.0	+ 3.8	+ 6.2	+ 5.8	+ 1.1	— 9.1	— 26.3	— 52.1	— 88.1	— 136.1	— 198.3	— 278.0	— 379.1	— 508.4

Ground level 0.5 km.

km	5°	10	15	20	25	30	35	40	45	50	55	60	65
	"												
1.0	+ 0.3	+ 0.5	+ 0.7	+ 0.5	+ 0.2	— 0.6	— 1.7	— 3.4	— 5.6	— 8.5	— 12.2	— 17.0	— 23.1
1.5	+ 0.6	+ 1.1	+ 1.2	+ 1.1	+ 0.3	— 1.2	— 3.5	— 6.8	— 11.3	— 17.1	— 24.6	— 34.1	— 46.3
2.0	+ 0.9	+ 1.5	+ 1.8	+ 1.4	+ 0.3	— 2.0	— 5.5	— 10.4	— 17.2	— 25.9	— 37.2	— 51.6	— 70.0
2.5	+ 1.2	+ 2.0	+ 2.3	+ 1.7	+ 0.1	— 2.9	— 7.6	— 14.3	— 23.3	— 35.0	— 50.2	— 69.4	— 94.1
3.0	+ 1.3	+ 2.4	+ 2.8	+ 2.0	— 0.1	— 3.8	— 9.7	— 18.1	— 29.4	— 44.2	— 63.2	— 87.3	— 118.3
3.5	+ 1.5	+ 2.8	+ 3.1	+ 2.3	— 0.3	— 4.8	— 11.9	— 22.1	— 35.7	— 53.6	— 76.5	— 105.6	— 142.8
4.0	+ 1.8	+ 3.1	+ 3.5	+ 2.5	— 0.6	— 6.0	— 14.4	— 26.2	— 42.2	— 63.1	— 89.9	— 124.0	— 167.7
4.5	+ 2.0	+ 3.5	+ 3.9	+ 2.6	— 0.9	— 7.2	— 16.9	— 30.5	— 48.8	— 72.8	— 103.5	— 142.6	— 192.7
5.0	+ 2.2	+ 3.8	+ 4.2	+ 2.6	— 1.3	— 8.5	— 19.5	— 34.9	— 55.6	— 82.7	— 117.3	— 161.6	— 218.1
5.5	+ 2.4	+ 4.1	+ 4.4	+ 2.7	— 1.8	— 9.9	— 22.1	— 39.4	— 62.6	— 92.8	— 131.4	— 180.8	— 243.8
6.0	+ 2.6	+ 4.3	+ 4.6	+ 2.6	— 2.4	— 11.3	— 24.9	— 44.0	— 69.6	— 102.9	— 145.6	— 200.1	— 269.6
6.5	+ 2.8	+ 4.6	+ 4.9	+ 2.6	— 3.1	— 12.5	— 27.7	— 48.7	— 76.7	— 113.2	— 160.0	— 219.5	— 295.6
7.0	+ 2.8	+ 4.8	+ 5.0	+ 2.4	— 3.8	— 14.5	— 30.7	— 53.4	— 84.0	— 123.7	— 174.5	— 239.2	— 322.0
7.5	+ 3.0	+ 5.0	+ 5.1	+ 2.3	— 4.5	— 16.2	— 33.7	— 58.5	— 91.4	— 134.4	— 189.3	— 259.2	— 348.6
8.0	+ 3.1	+ 5.2	+ 5.2	+ 2.1	— 5.3	— 17.8	— 36.8	— 63.3	— 98.8	— 145.0	— 204.1	— 279.3	— 375.3
8.5	+ 3.2	+ 5.4	+ 5.3	+ 1.8	— 6.1	— 19.6	— 40.0	— 68.5	— 106.5	— 155.9	— 219.1	— 299.6	— 402.3
9.0	+ 3.4	+ 5.6	+ 5.3	+ 1.5	— 7.0	— 21.5	— 43.3	— 73.7	— 114.2	— 166.9	— 234.3	— 319.9	— 429.4
9.5	+ 3.5	+ 5.7	+ 5.3	+ 1.2	— 7.9	— 23.5	— 46.5	— 78.8	— 122.0	— 178.0	— 249.5	— 340.5	— 456.8
10.0	+ 3.6	+ 5.8	+ 5.3	+ 0.8	— 9.0	— 25.4	— 50.0	— 84.3	— 130.0	— 159.0	— 265.0	— 361.3	— 484.4

Photogrammetric refraction and curvature.

Ground level 1.0 km.

km	5°	10	15	20	25	30	35	40	45	50	55	60	65
	"												
1.5	+ 0.3	+ 0.5	+ 0.6	+ 0.5	+ 0.1	— 0.6	— 1.8	— 3.5	— 5.7	— 8.6	— 12.3	— 17.1	— 23.2
2.0	+ 0.6	+ 1.0	+ 1.1	+ 1.0	+ 0.1	— 1.3	— 3.6	— 7.0	— 11.5	— 17.4	— 24.9	— 34.5	— 46.8
2.5	+ 0.9	+ 1.5	+ 1.7	+ 1.3	+ 0.1	— 2.2	— 5.7	— 10.7	— 17.5	— 26.3	— 37.7	— 52.1	— 70.7
3.0	+ 1.1	+ 1.9	+ 2.2	+ 1.6	— 0.1	— 3.2	— 7.9	— 14.6	— 23.7	— 35.5	— 50.9	— 70.1	— 94.9
3.5	+ 1.3	+ 2.3	+ 2.6	+ 1.8	— 0.4	— 4.2	— 10.2	— 18.6	— 30.0	— 44.9	— 64.0	— 88.3	— 119.4
4.0	+ 1.5	+ 2.6	+ 2.9	+ 2.1	— 0.6	— 5.3	— 12.4	— 22.7	— 36.4	— 54.4	— 77.4	— 106.7	— 144.1
4.5	+ 1.7	+ 3.0	+ 3.3	+ 2.2	— 0.9	— 6.4	— 14.9	— 26.9	— 43.0	— 64.0	— 90.9	— 125.2	— 169.2
5.0	+ 1.9	+ 3.3	+ 3.6	+ 2.2	— 1.4	— 7.8	— 17.5	— 31.3	— 49.8	— 73.9	— 104.8	— 144.2	— 194.5
5.5	+ 2.1	+ 3.6	+ 3.9	+ 2.2	— 1.8	— 9.1	— 20.2	— 35.8	— 56.6	— 83.9	— 118.7	— 163.2	— 220.1
6.0	+ 2.3	+ 3.9	+ 4.1	+ 2.3	— 2.3	— 10.5	— 22.8	— 40.2	— 63.6	— 94.0	— 132.8	— 182.4	— 245,7
6.5	+ 2.5	+ 4.1	+ 4.3	+ 2.2	— 2.9	— 12.0	— 25.7	— 44.9	— 70.7	— 104.2	— 147.2	— 201.9	— 271.7
7.0	+ 2.7	+ 4.3	+ 4.5	+ 2.1	— 3.7	— 13.6	— 28.7	— 49.8	— 78.0	— 114.7	— 161.7	— 221.5	— 298.1
7.5	+ 2.7	+ 4.5	+ 4.7	+ 1.9	— 4.4	— 15.3	— 31.7	— 54.6	— 85.4	— 125.3	— 176.4	— 241.4	— 324.6
8.0	+ 2.8	+ 4.7	+ 4.7	+ 1.8	— 5.2	— 17.0	— 34.7	— 59.7	— 92.7	— 136.0	— 191.3	— 261.4	— 351.2
8.5	+ 3.0	+ 4.9	+ 4.8	+ 1.5	— 6.0	— 18.7	— 37.8	— 64.5	— 100.3	— 146.7	— 206.1	— 281.6	— 378.1
9.0	+ 3.1	+ 5.1	+ 4.9	+ 1.2	— 6.8	— 20.6	— 41.1	— 69.8	— 108.0	— 157.7	— 221.2	— 302.0	— 405.2
9.5	+ 3.2	+ 5.3	+ 4.8	+ 0.9	— 7.8	— 22.4	— 44.5	— 75.0	— 115.8	— 168.8	— 236.5	— 322.5	— 432.5
10.0	+ 3.3	+ 5.4	+ 4.8	+ 0.6	— 8.7	— 24.5	— 47.8	— 80.3	— 123.7	— 180.0	— 251.9	— 343.2	— 460.0

Ground level 1.5 km.

km	5°	10	15	20	25	30	35	40	45	50	55	60	65
	"												
2.0	+ 0.3	+ 0.5	+ 0.6	+ 0.4	0.0	— 0.7	— 1.9	— 3.6	— 5.8	— 8.8	— 12.6	— 17.4	— 23.6
2.5	+ 0.6	+ 1.0	+ 1.1	+ 0.9	0.0	— 1.5	— 3.8	— 7.2	— 11.8	— 17.7	— 25.3	— 35.0	— 47.3
3.0	+ 0.8	+ 1.4	+ 1.5	+ 1.1	— 0.1	— 2.5	— 6.0	— 11.1	— 17.9	— 26.8	— 38.3	— 52.8	— 71.5
3.5	+ 1.1	+ 1.8	+ 2.0	+ 1.4	— 0.4	— 3.5	— 8.2	— 15.1	— 24.2	— 36.1	— 51.4	— 70.9	— 95.9
4.0	+ 1.2	+ 2.2	+ 2.4	+ 1.6	— 0.6	— 4.5	— 10.6	— 19.1	— 30.6	— 45.6	— 64.8	— 89.3	— 120.6
4.5	+ 1.5	+ 2.5	+ 2.7	+ 1.8	— 0.9	— 5.7	— 12.9	— 23.3	— 37.1	— 55.2	— 78.3	— 107.8	— 145.5
5.0	+ 1.7	+ 1.0	+ 3.1	+ 1.9	— 1.3	— 6.9	— 15.5	— 27.5	— 43.8	— 64.9	— 92.0	— 126.5	— 170.6
5.5	+ 1.9	+ 3.1	+ 3.4	+ 1.9	— 1.8	— 8.3	— 18.1	— 32.0	— 50.6	— 74.9	— 105.9	— 145.5	— 196.2
6.0	+ 2.0	+ 3.4	+ 3.7	+ 1.9	— 2.3	— 9.7	— 20.9	— 36.6	— 57.6	— 85.0	— 120.0	— 164.7	— 221.9
6.5	+ 2.2	+ 3.7	+ 3.8	+ 1.9	— 2.9	— 11.2	— 23.6	— 41.2	— 64.7	— 95.3	— 134.4	— 184.2	— 247.9
7.0	+ 2.4	+ 3.9	+ 4.0	+ 1.8	— 3.5	— 12.7	— 26.5	— 45.9	— 71.9	— 105.6	— 148.8	— 203.8	— 274.0
7.5	+ 2.5	+ 4.1	+ 4.2	+ 1.6	— 4.3	— 14.3	— 29.5	— 50.8	— 79.2	— 116.1	— 163.4	— 223.5	— 300.4
8.0	+ 2.6	+ 4.3	+ 4.3	+ 1.4	— 5.0	— 16.1	— 32.6	— 55.7	— 86.7	— 126.8	— 178.2	— 243.5	— 327.0
8.5	+ 2.7	+ 4.5	+ 4.3	+ 1.3	— 5.8	— 17.8	— 35.7	— 60.8	— 94.1	— 137.6	— 193.1	— 263.6	— 353.9
9.0	+ 2.8	+ 4.6	+ 4.4	+ 1.0	— 6.7	— 19.6	— 38.9	— 65.8	— 101.7	— 148.4	— 208.1	— 283.9	— 380.8
9.5	+ 3.0	+ 4.9	+ 4.4	+ 0.6	— 7.6	— 21.5	— 42.2	— 71.1	— 109.6	— 159.5	— 223.3	— 304.5	— 408.2
10.0	+ 3.1	+ 5.0	+ 4.4	+ 0.3	— 8.5	— 23.4	— 45.6	— 76.3	+ 117.4	— 170.6	— 238.6	— 325.0	— 435.5

Photogrammetric refraction and curvature.

Ground level 2.0 km.

km	5°	10	15	20	25	30	35	40	45	50	55	60	65
	"												
2.5	+ 0.3	+ 0.5	+ 0.6	+ 0.4	0.0	— 0.8	— 2.0	— 3.7	— 5.9	— 8.9	— 12.7	— 17.5	— 23.7
3.0	+ 0.6	+ 0.9	+ 1.0	+ 0.8	— 0.1	— 1.6	— 4.0	— 7.4	— 12.0	— 18.0	— 25.6	— 35.4	— 47.8
3.5	+ 0.8	+ 1.3	+ 1.4	+ 1.0	— 0.3	— 2.7	— 6.2	— 11.4	— 18.3	— 27.2	— 38.8	— 53.4	— 72.2
4.0	+ 1.0	+ 1.7	+ 1.9	+ 1.2	— 0.6	— 3.7	— 8.5	— 15.4	— 24.6	— 36.0	— 52.0	— 71.6	— 96.7
4.5	+ 1.2	+ 2.1	+ 2.3	+ 1.4	— 0.9	— 4.8	— 11.0	— 19.5	— 31.1	— 46.2	— 65.5	— 90.1	— 121.6
5.0	+ 1.4	+ 2.4	+ 2.5	+ 1.5	— 1.3	— 6.1	— 13.4	— 23.9	— 37.8	— 56.0	— 79.4	— 108.9	— 146.8
5.5	+ 1.6	+ 2.7	+ 2.9	+ 1.6	— 1.7	— 7.3	— 16.0	— 28.2	— 44.5	— 65.8	— 93.0	— 127.7	— 172.1
6.0	+ 1.8	+ 3.0	+ 3.1	+ 1.6	— 2.2	— 8.8	— 18.8	— 32.7	— 51.5	— 75.9	— 107.1	— 146.9	— 197.8
6.5	+ 2.0	+ 3.2	+ 3.4	+ 1.5	— 2.7	— 10.3	— 21.5	— 37.4	— 58.5	— 86.1	— 121.3	— 166.2	— 223.6
7.0	+ 2.1	+ 3.5	+ 3.5	+ 1.5	— 3.4	— 11.8	— 24.4	— 42.0	— 65.7	— 96.5	— 135.8	— 185.8	— 249.8
7.5	+ 2.3	+ 3.7	+ 3.7	+ 1.3	— 4.0	— 13.4	— 27.3	— 46.9	— 73.0	— 106.9	— 150.3	— 205.6	— 276.2
8.0	+ 2.4	+ 3.9	+ 3.8	+ 1.2	— 4.9	— 15.0	— 30.4	— 51.8	— 80.4	— 117.5	— 165.0	— 225.4	— 302.7
8.5	+ 2.5	+ 4.1	+ 3.9	+ 0.9	— 5.7	— 16.8	— 33.5	— 56.8	— 87.9	— 128.3	— 179.9	— 245.5	— 329.5
9.0	+ 2.6	+ 4.2	+ 3.9	+ 0.8	— 6.5	— 18.6	— 36.6	— 61.9	— 95.4	— 139.1	— 194.8	— 265.7	— 356.3
9.5	+ 2.7	+ 4.4	+ 4.0	+ 0.4	— 7.4	— 20.4	— 39.9	— 67.0	— 103.2	— 150.1	— 210.1	— 286.3	— 383.6
10.0	+ 2.8	+ 4.6	+ 4.0	+ 0.1	— 8.3	— 22.3	— 43.3	— 72.3	— 111.0	— 161.2	— 225.3	— 306.8	— 410.9

Ground level 2.5 km.

km	5°	10	15	20	25	30	35	40	45	50	55	60	65
	"												
3.0	+ 0.3	+ 0.5	+ 0.5	+ 0.3	— 0.1	— 0.8	— 2.1	— 3.8	— 6.0	— 9.0	— 12.8	— 17.7	— 23.9
3.5	+ 0.5	+ 0.9	+ 0.9	+ 0.7	— 0.2	— 1.8	— 4.2	— 7.6	— 12.3	— 18.3	— 26.0	— 35.8	— 48.3
4.0	+ 0.8	+ 1.3	+ 1.4	+ 0.9	— 0.4	— 2.9	— 6.5	— 11.7	— 18.6	— 27.6	— 39.2	— 53.9	— 72.8
4.5	+ 1.0	+ 1.6	+ 1.8	+ 1.1	— 0.8	— 4.0	— 8.9	— 15.8	— 25.1	— 37.1	— 52.6	— 72.3	— 97.5
5.0	+ 1.1	+ 2.0	+ 2.1	+ 1.2	— 1.1	— 5.2	— 11.3	— 20.0	— 31.6	— 46.8	— 66.2	— 90.9	— 122.5
5.5	+ 1.3	+ 2.3	+ 2.4	+ 1.3	— 1.6	— 6.4	— 13.8	— 24.4	— 38.4	— 56.7	— 80.1	— 109.8	— 147.9
6.0	+ 1.5	+ 2.6	+ 2.6	+ 1.3	— 2.1	— 7.8	— 16.6	— 28.8	— 45.3	— 66.7	— 94.1	— 128.9	— 173.6
6.5	+ 1.7	+ 2.8	+ 2.9	+ 1.3	— 2.6	— 9.3	— 19.3	— 33.4	— 52.3	— 76.8	— 108.2	— 148.1	— 199.3
7.0	+ 1.9	+ 3.1	+ 3.1	+ 1.2	— 3.2	— 10.8	— 22.2	— 38.2	— 59.5	— 87.2	— 122.6	— 167.8	— 225.4
7.5	+ 2.0	+ 3.3	+ 3.2	+ 1.1	— 3.8	— 12.3	— 25.0	— 42.8	— 66.7	— 97.6	— 137.1	— 187.4	— 251.6
8.0	+ 2.2	+ 3.5	+ 3.4	+ 1.0	— 4.5	— 14.0	— 28.1	— 47.8	— 74.0	— 108.1	— 151.7	— 207.2	— 278.1
8.5	+ 2.3	+ 3.7	+ 3.5	+ 0.7	— 5.4	— 15.7	— 31.2	— 52.8	— 81.6	— 118.9	— 166.6	— 227.3	— 304.9
9.0	+ 2.4	+ 3.8	+ 3.6	+ 0.5	— 6.2	— 17.5	— 34.4	— 57.8	— 89.1	— 129.7	— 181.5	— 247.5	— 331.8
9.5	+ 2.5	+ 4.0	+ 3.6	+ 0.2	— 7.1	— 19.4	— 37.6	— 63.1	— 96.8	— 140.7	— 196.7	— 267.9	— 358.9
10.0	+ 2.6	+ 4.1	+ 3.6	— 0.1	— 8.0	— 21.2	— 40.8	— 68.1	— 104.5	— 151.6	— 211.8	— 288.3	— 386.1

Photogrammetric refraction and curvature above various ground levels from an altitude of:

10.0 km.

km	5°	10	15	20	25	30	35	40	45	50	55	60	65
	"												
0.0	+ 3.8	+ 6.2	+ 5.8	+ 1.1	— 9.1	— 26.3	— 52.1	— 88.1	— 136.1	— 198.3	— 278.0	— 379.1	— 508.4
0.5	+ 3.6	+ 5.8	+ 5.3	+ 0.8	— 9.0	— 25.4	— 50.0	— 84.3	— 130.0	— 159.0	— 265.0	— 361.3	— 484.4
1.0	+ 3.3	+ 5.4	+ 4.8	+ 0.6	— 8.7	— 24.5	— 47.8	— 80.3	— 123.7	— 180.0	— 251.9	— 343.2	— 460.0
1.5	+ 3.1	+ 5.0	+ 4.4	+ 0.3	— 8.5	— 23.4	— 45.6	— 76.3	— 117.4	— 170.6	— 238.6	— 325.0	— 435.5
2.0	+ 2.8	+ 4.6	+ 4.0	+ 0.1	— 8.3	— 22.3	— 43.3	— 72.3	— 111.0	— 161.2	— 225.3	— 306.8	— 410.9
2.5	+ 2.6	+ 4.1	+ 3.6	— 0.1	— 8.0	— 21.2	— 40.8	— 68.1	— 104.5	— 151.6	— 211.8	— 288.3	— 386.1

6 km.

km	5°	10	15	20	25	30	35	40	45	50	55	60	65
	"												
0.0	+ 2.9	+ 4.8	+ 5.2	+ 3.0	— 2.5	— 12.0	— 26.8	— 47.6	— 75.4	— 117.7	— 158.2	— 217.4	— 293.2
0.5	+ 2.6	+ 4.3	+ 4.6	+ 2.6	— 2.4	— 11.3	— 24.9	— 44.0	— 69.6	— 102.9	— 145.6	— 200.1	— 269.6
1.0	+ 2.3	+ 3.9	+ 4.1	+ 2.3	— 2.3	— 10.5	— 22.8	— 40.2	— 63.6	— 94.0	— 132.8	— 182.4	— 245.7
1.5	+ 2.0	+ 3.4	+ 3.7	+ 1.9	— 2.3	— 9.7	— 20.9	— 36.6	— 57.6	— 85.0	— 120.0	— 164.7	— 221.9
2.0	+ 1.8	+ 3.0	+ 3.1	+ 1.6	— 2.2	— 8.8	— 18.8	— 32.7	— 51.5	— 75.9	— 107.1	— 146.9	— 197.8
2.5	+ 1.5	+ 2.6	+ 2.6	+ 1.3	— 2.1	— 7.8	— 16.6	— 28.8	— 45.3	— 66.7	— 94.1	— 128.9	— 173.6

4.5 km.

km	5°	10	15	20	25	30	35	40	45	50	55	60	65
	"												
0.0	+ 2.3	+ 4.0	+ 4.5	+ 3.0	— 0.8	— 7.9	— 18.7	— 34.0	— 54.6	— 81.5	— 115.9	— 159.9	— 216.1
0.5	+ 2.0	+ 3.5	+ 3.9	+ 2.6	— 0.9	— 7.2	— 16.9	— 30.5	— 48.8	— 72.8	— 103.5	— 142.6	— 192.7
1.0	+ 1.7	+ 3.0	+ 3.3	+ 2.2	— 0.9	— 6.4	— 14.9	— 26.9	— 43.0	— 64.0	— 90.9	— 125.2	— 169.2
1.5	+ 1.5	+ 2.5	+ 2.7	+ 1.8	— 0.9	— 5.7	— 12.9	— 23.3	— 37.1	— 55.2	— 78.3	— 107.8	— 145.5
2.0	+ 1.2	+ 2.1	+ 2.3	+ 1.4	— 0.9	— 4.8	— 11.0	— 19.5	— 31.1	— 46.2	— 65.5	— 90.1	— 121.6
2.5	+ 1.0	+ 1.6	+ 1.8	+ 1.1	— 0.8	— 4.0	— 8.9	— 15.8	— 25.1	— 37.1	— 52.6	— 72.3	— 97.5

4.0 km.

km	5°	10	15	20	25	30	35	40	45	50	55	60	65
	"												
0.0	+ 2.1	+ 3.7	+ 4.1	+ 2.9	— 0.5	— 6.7	— 16.2	— 29.7	— 47.9	— 71.7	— 102.2	— 141.1	— 190.9
0.5	+ 1.8	+ 3.1	+ 3.5	+ 2.5	— 0.6	— 6.0	— 14.4	— 26.2	— 42.2	— 63.1	— 89.9	— 124.0	— 167.7
1.0	+ 1.5	+ 2.6	+ 2.9	+ 2.1	— 0.6	— 5.3	— 12.4	— 22.7	— 36.4	— 54.4	— 77.4	— 106.7	— 144.1
1.5	+ 1.2	+ 2.2	+ 2.4	+ 1.6	— 0.6	— 4.5	— 10.6	— 19.1	— 30.6	— 45.6	— 64.8	— 89.3	— 120.6
2.0	+ 1.0	+ 1.7	+ 1.9	+ 1.2	— 0.6	— 3.7	— 8.5	— 15.4	— 24.6	— 36.0	— 52.0	— 71.6	— 96.7
2.5	+ 0.8	+ 1.3	+ 1.4	+ 0.9	— 0.4	— 2.9	— 6.5	— 11.7	— 18.6	— 27.6	— 39.2	— 53.9	— 72.8

3.5 km.

km	5°	10	15	20	25	30	35	40	45	50	55	60	65
	"												
0.0	+ 1.9	+ 3.3	+ 3.7	+ 2.8	— 0.2	— 5.5	— 13.8	— 25.5	— 41.4	— 62.1	— 88.7	— 122.6	— 166.1
0.5	+ 1.5	+ 2.8	+ 3.1	+ 2.3	— 0.3	— 4.8	— 11.9	— 22.1	— 35.7	— 53.6	— 76.5	— 105.6	— 142.8
1.0	+ 1.3	+ 2.3	+ 2.6	+ 1.8	— 0.4	— 4.2	— 10.2	— 18.6	— 30.0	— 44.9	— 64.0	— 88.3	— 119.4
1.5	+ 1.1	+ 1.8	+ 2.0	+ 1.4	— 0.4	— 3.5	— 8.2	— 15.1	— 24.2	— 36.1	— 51.4	— 70.9	— 95.9
2.0	+ 0.8	+ 1.3	+ 1.4	+ 1.0	— 0.3	— 2.7	— 6.2	— 11.4	— 18.3	— 27.2	— 38.8	— 53.4	— 72.2
2.5	+ 0.5	+ 0.9	+ 0.9	+ 0.7	— 0.2	— 1.8	— 4.2	— 7.6	— 12.3	— 18.3	— 26.0	— 35.8	— 48.3

Photogrammetric refraction and curvature above various ground levels from an altitude of:

3.0 km.

km	5°	10	15	20	25	30	35	40	45	50	55	60	65
	"												
0.0	+1.6	+2.9	+3.3	+2.6	+0.1	−4.4	−11.4	−21.5	−34.9	−52.7	−75.4	−104.3	−141.4
0.5	+1.3	+2.4	+2.8	+2.0	−0.1	−3.8	−9.7	−18.1	−29.4	−44.2	−63.2	−87.3	−118.3
1.0	+1.1	+1.9	+2.2	+1.6	−0.1	−3.2	−7.9	−14.6	−23.7	−35.5	−50.9	−70.1	−94.9
1.5	+0.8	+1.4	+1.5	+1.1	−0.1	−2.5	−6.0	−11.1	−17.9	−26.8	−38.3	−52.8	−71.5
2.0	+0.6	+0.9	+1.0	+0.8	−0.1	−1.6	−4.0	−7.4	−12.0	−18.0	−25.6	−35.4	−47.8
2.5	+0.3	+0.5	+0.5	+0.3	−0.1	−0.8	−2.1	−3.8	−6.0	−9.0	−12.8	−17.7	−23.9

Alt. 2.5 km.

km	5°	10	15	20	25	30	35	40	45	50	55	60	65
	"												
0.0	+1.4	+2.5	+2.9	+2.2	+0.2	−3.5	−9.3	−17.6	−28.8	−43.5	−62.4	−86.4	−117.2
0.5	+1.2	+2.0	+2.3	+1.7	+0.1	−2.9	−7.6	−14.3	−23.3	−35.0	−50.2	−69.4	−94.1
1.0	+0.9	+1.5	+1.7	+1.3	+0.1	−2.2	−5.7	−10.7	−17.5	−26.3	−37.7	−52.1	−70.7
1.5	+0.6	+1.0	+1.1	+0.9	0.0	−1.5	−3.8	−7.2	−11.8	−17.7	−25.3	−35.0	−47.3
2.0	+0.3	+0.5	+0.6	+0.4	0.0	−0.8	−2.0	−3.7	−5.9	−8.9	−12.7	−17.5	−23.7

Alt. 2.0 km.

km	5°	10	15	20	25	30	35	40	45	50	55	60	65
	"												
0.0	+1.2	+2.1	+2.4	+1.9	+0.3	−2.6	−7.2	−13.8	−22.8	−34.4	−49.5	−68.6	−93.1
0.5	+0.9	+1.5	+1.8	+1.4	+0.3	−2.0	−5.5	−10.4	−17.2	−25.9	−37.2	−51.6	−70.0
1.0	+0.6	+1.0	+1.1	+1.0	+0.1	−1.3	−3.6	−7.0	−11.5	−17.4	−24.9	−34.5	−46.8
1.5	+0.3	+0.5	+0.6	+0.4	0.0	−0.7	−1.9	−3.6	−5.8	−8.8	−12.6	−17.4	−23.6

Alt. 1.5 km.

km	5°	10	15	20	25	30	35	40	45	50	55	60	65
	"												
0.0	+0.9	+1.6	+1.9	+1.6	+0.4	−1.8	−5.2	−10.2	−16.8	−25.5	−36.8	−51.0	−69.4
0.5	+0.6	+1.1	+1.2	+1.1	+0.3	−1.2	−3.5	−6.8	−11.3	−17.1	−24.6	−34.1	−46.3
1.0	+0.3	+0.5	+0.6	+0.5	+0.1	−0.6	−1.8	−3.5	−5.7	−8.6	−12.3	−17.1	−23.2

Alt. 1.0 km.

km	5°	10	15	20	25	30	35	40	45	50	55	60	65
	"												
0.0	+0.6	+1.1	+1.3	+1.2	+0.4	−1.0	−3.3	−6.5	−11.0	−16.8	−24.2	−33.7	−45.8
0.5	+0.3	+0.5	+0.7	+0.5	+0.2	−0.6	−1.7	−3.4	−5.6	−8.5	−12.2	−17.0	−23.1

$E_h = 0.0031416\, h\,(r + o)$ cosec $2N$ m.

Height error.

Alt. 10.0 km.

km	5°	10	15	20	25	30	35	40	45	50	55	60	65
	m												
0.0	+ 0.76	+ 0.63	+ 0.40	+ 0.06	— 0.40	— 1.02	— 1.84	— 2.91	— 4.33	— 6.23	— 8.84	—12.52	—17.93
0.5	+ 0.69	+ 0.56	+ 0.35	+ 0.04	— 0.38	— 0.94	— 1.67	— 2.65	— 3.93	— 4.75	— 8.01	—11.34	—16.23
1.0	+ 0.60	+ 0.49	+ 0.30	+ 0.03	— 0.35	— 0.86	— 1.52	— 2.39	— 3.54	— 5.09	— 7.21	—10.20	—14.60
1.5	+ 0.53	+ 0.43	+ 0.26	+ 0.01	— 0.32	— 0.77	— 1.37	— 2.14	— 3.17	— 4.56	— 6.45	— 9.13	—13.05
2.0	+ 0.45	+ 0.37	+ 0.22	0.00	— 0.30	— 0.69	— 1.22	— 1.91	— 2.82	— 4.05	— 5.73	— 8.11	—11.59
2.5	+ 0.39	+ 0.31	+ 0.19	0.00	— 0.27	— 0.62	— 1.08	— 1.69	— 2.49	— 3.57	— 5.05	— 7.06	—10.21

Alt. 6.0 km.

km	5°	10	15	20	25	30	35	40	45	50	55	60	65
	m												
0.0	+ 0.35	+ 0.29	+ 0.22	+ 0.10	— 0.07	— 0.28	— 0.57	— 0.94	— 1.44	— 2.11	— 3.02	— 4.31	— 6.20
0.5	+ 0.29	+ 0.24	+ 0.18	+ 0.08	— 0.06	— 0.24	— 0.48	— 0.80	— 1.22	— 1.78	— 2.55	— 3.64	— 5.23
1.0	+ 0.23	+ 0.20	+ 0.14	+ 0.06	— 0.05	— 0.20	— 0.40	— 0.66	— 1.01	— 1.48	— 2.11	— 3.01	— 4.33
1.5	+ 0.18	+ 0.16	+ 0.12	+ 0.05	— 0.05	— 0.17	— 0.33	— 0.54	— 0.82	— 1.20	— 1.72	— 2.45	— 3.52
2.0	+ 0.14	+ 0.12	+ 0.09	+ 0.03	— 0.04	— 0.14	— 0.27	— 0.43	— 0.66	— 0.95	— 1.36	— 1.94	— 2.79
2.5	+ 0.11	+ 0.09	+ 0.06	+ 0.02	— 0.03	— 0.11	— 0.20	— 0.33	— 0.50	— 0.73	— 1.05	— 1.49	— 2.14

Alt. 4.5 km.

km	5°	10	15	20	25	30	35	40	45	50	55	60	65
	m												
0.0	+ 0.21	+ 0.18	+ 0.14	+ 0.07	— 0.02	— 0.14	— 0.30	— 0.51	— 0.78	— 1.15	— 1.66	— 2.38	— 3.43
0.5	+ 0.16	+ 0.14	+ 0.11	+ 0.06	— 0.02	— 0.11	— 0.24	— 0.40	— 0.60	— 0.91	— 1.32	— 1.88	— 2.72
1.0	+ 0.12	+ 0.11	+ 0.08	+ 0.04	— 0.01	— 0.09	— 0.18	— 0.31	— 0.48	— 0.70	— 1.01	— 1.45	— 2.09
1.5	+ 0.09	+ 0.08	+ 0.06	+ 0.03	— 0.01	— 0.07	— 0.14	— 0.23	— 0.35	— 0.52	— 0.75	— 1.07	— 1.54
2.0	+ 0.06	+ 0.05	+ 0.04	+ 0.02	— 0.01	— 0.05	— 0.10	— 0.16	— 0.25	— 0.36	— 0.52	— 0.74	— 1.07
2.5	+ 0.04	+ 0.03	+ 0.02	+ 0.01	— 0.01	— 0.03	— 0.06	— 0.10	— 0.16	— 0.23	— 0.33	— 0.48	— 0.69

Alt. 4.0 km.

km	5°	10	15	20	25	30	35	40	45	50	55	60	65
	m												
0.0	+ 0.17	+ 0.15	+ 0.11	+ 0.06	— 0.01	— 0.10	— 0.23	— 0.39	— 0.61	— 0.90	— 1.30	— 1.86	— 2.69
0.5	+ 0.13	+ 0.11	+ 0.08	+ 0.05	— 0.01	— 0.08	— 0.18	— 0.30	— 0.47	— 0.69	— 1.00	— 1.43	— 2.07
1.0	+ 0.09	+ 0.08	+ 0.06	+ 0.03	— 0.01	— 0.06	— 0.13	— 0.22	— 0.35	— 0.51	— 0.74	— 1.06	— 1.52
1.5	+ 0.06	+ 0.06	+ 0.04	+ 0.02	— 0.01	— 0.04	— 0.09	— 0.16	— 0.24	— 0.36	— 0.52	— 0.74	— 1.06
2.0	+ 0.04	+ 0.03	+ 0.03	+ 0.01	— 0.01	— 0.03	— 0.06	— 0.10	— 0.16	— 0.23	— 0.33	— 0.47	— 0.68
2.5	+ 0.02	+ 0.02	+ 0.01	+ 0.01	0.00	— 0.02	— 0.03	— 0.06	— 0.09	— 0.13	— 0.19	— 0.27	— 0.39

Alt. 3.5 km.

km	5°	10	15	20	25	30	35	40	45	50	55	60	65
	m												
0.0	+ 0.13	+ 0.12	+ 0.09	+ 0.05	0.00	— 0.07	— 0.17	— 0.29	— 0.46	— 0.68	— 0.99	— 1.42	— 2.05
0.5	+ 0.09	+ 0.09	+ 0.06	+ 0.04	0.00	— 0.06	— 0.13	— 0.22	— 0.34	— 0.51	— 0.73	— 1.05	— 1.51
1.0	+ 0.07	+ 0.06	+ 0.04	+ 0.02	0.00	— 0.04	— 0.09	— 0.15	— 0.24	— 0.35	— 0.51	— 0.73	— 1.05
1.5	+ 0.04	+ 0.04	+ 0.03	+ 0.01	0.00	— 0.03	— 0.06	— 0.10	— 0.15	— 0.23	— 0.33	— 0.47	— 0.68
2.0	+ 0.02	+ 0.02	+ 0.01	+ 0.01	0.00	— 0.02	— 0.03	— 0.06	— 0.09	— 0.13	— 0.19	— 0.26	— 0.38
2.5	+ 0.01	+ 0.01	+ 0.01	0.00	0.00	— 0.01	— 0.01	— 0.03	— 0.04	— 0.06	— 0.08	— 0.12	— 0.17

$$E_h = 0.0031416\, h\,(r + o)\ \text{cosec}\ 2N \text{ m.}$$

Height error.

Alt. 3.0 km.

km	5°	10	15	20	25	30	35	40	45	50	55	60	65
	m												
0.0	+ 0.10	+ 0.09	+ 0.07	+ 0.04	0.00	— 0.05	— 0.12	— 0.21	— 0.33	— 0.50	— 0.72	— 1.03	— 1.50
0.5	+ 0.07	+ 0.06	+ 0.05	+ 0.03	0.00	— 0.04	— 0.09	— 0.15	— 0.23	— 0.35	— 0.50	— 0.72	— 1.04
1.0	+ 0.04	+ 0.04	+ 0.03	+ 0.02	0.00	— 0.02	— 0.06	— 0.10	— 0.15	— 0.22	— 0.32	— 0.46	— 0.67
1.5	+ 0.02	+ 0.02	+ 0.02	+ 0.01	0.00	— 0.01	— 0.03	— 0.06	— 0.09	— 0.13	— 0.18	— 0.26	— 0.38
2.0	+ 0.01	+ 0.01	+ 0.01	0.00	0.00	— 0.01	— 0.01	— 0.02	— 0.04	— 0.06	— 0.08	— 0.12	— 0.17
2.5	0.00	0.00	0.00	0.00	0.00	0.00	0.00	— 0.01	— 0.01	— 0.01	— 0.02	— 0.03	— 0.04

Alt. 2.5 km.

km	5°	10	15	20	25	30	35	40	45	50	55	60	65
	m												
0.0	+0.070	+0.064	+0.050	+0.029	+0.002	—0.034	—0.082	—0.145	—0.229	—0.342	—0.496	—0.713	—1.033
0.5	+0.048	+0.041	+0.032	+0.018	+0.001	—0.023	—0.054	—0.094	—0.148	—0.220	—0.319	—0.459	—0.664
1.0	+0.027	+0.023	+0.018	+0.010	+0.001	—0.013	—0.030	—0.053	—0.083	—0.124	—0.180	—0.258	—0.374
1.5	+0.012	+0.010	+0.008	+0.005	0.000	—0.006	—0.013	—0.024	—0.038	—0.056	—0.080	—0.116	—0.167
2.0	+0.003	+0.003	+0.002	+0.001	0.000	—0.002	—0.004	—0.006	—0.009	—0.014	—0.020	—0.029	—0.042

Alt. 2.0 km.

km	5°	10	15	20	25	30	35	40	45	50	55	60	65
	m												
0.0	+0.048	+0.043	+0.033	+0.020	+0.003	—0.020	—0.051	—0.091	—0.145	—0.216	—0.315	—0.453	—0.657
0.5	+0.027	+0.023	+0.019	+0.011	+0.002	—0.012	—0.029	—0.052	—0.082	—0.122	—0.177	—0.256	—0.370
1.0	+0.012	+0.010	+0.008	+0.005	0.000	—0.005	—0.013	—0.023	—0.037	—0.055	—0.079	—0.114	—0.165
1.5	+0.003	+0.003	+0.002	+0.001	0.000	—0.001	—0.003	—0.006	—0.009	—0.014	—0.020	—0.029	—0.042

Alt. 1.5 km.

km	5°	10	15	20	25	30	35	40	45	50	55	60	65
	m												
0.0	+0.027	+0.024	+0.020	+0.013	+0.003	—0.010	—0.028	—0.051	—0.080	—0.120	—0.176	—0.253	—0.367
0.5	+0.012	+0.011	+0.008	+0.006	+0.001	—0.005	—0.012	—0.022	—0.036	—0.054	—0.078	—0.113	—0.163
1.0	+0.003	+0.003	+0.002	+0.001	0.000	—0.001	—0.003	—0.006	—0.009	—0.014	—0.020	—0.028	—0.041

Alt. 1.0 km.

km	5°	10	15	20	25	30	35	40	45	50	55	60	65
	m												
0.0	+0.012	+0.011	+0.009	+0.006	+0.002	—0.004	—0.012	—0,021	—0.035	—0.053	—0.077	—0.111	—0.161
0.5	+0.003	+0.003	+0.002	+0.001	0.000	—0.001	—0.003	—0.006	—0.009	—0.013	—0.019	—0.028	—0.041

$$E_s = E_h \operatorname{tg} N.$$

Lateral error.

Alt. 10.0 km.

km	5°	10	15	20	25	30	35	40	45	50	55	60	65
	m												
0.0	+ 0.06	+ 0.10	+ 0.10	+ 0.02	— 0.17	— 0.52	— 1.13	— 2.11	— 3.70	— 6.23	—10.35	—17.23	—29.26
0.5	+ 0.05	+ 0.09	+ 0.08	+ 0.01	— 0.16	— 0.48	— 1.02	— 1.93	— 3.36	— 4.75	— 9.38	—15.61	—26.48
1.0	+ 0.05	+ 0.08	+ 0.07	+ 0.01	— 0.14	— 0.44	— 0.93	— 1.74	— 3.02	— 5.09	— 8.44	—14.04	—23.83
1.5	+ 0.04	+ 0.07	+ 0.06	0.00	— 0.13	— 0.39	— 0.84	— 1.55	— 2.71	— 4.56	— 7.55	—12.57	—21.30
2.0	+ 0.04	+ 0.06	+ 0.05	0.00	— 0.12	— 0.35	— 0.75	— 1.39	— 2.41	— 4.05	— 6.71	—11.16	—18.91
2.5	+ 0.03	+ 0.05	+ 0.05	0.00	— 0.11	— 0.32	— 0.66	— 1.23	— 2.13	— 3.57	— 5.91	— 9.72	—16.66

Alt. 6.0 km.

km	5°	10	15	20	25	30	35	40	45	50	55	60	65
	m												
0.0	+ 0.03	+ 0.05	+ 0.05	+ 0.03	— 0.03	— 0.14	— 0.35	— 0.68	— 1.23	— 2.11	— 3.54	— 5.93	—10.12
0.5	+ 0.02	+ 0.04	+ 0.04	+ 0.03	— 0.02	— 0.12	— 0.29	— 0.58	— 1.04	— 1.78	— 2.99	— 5.01	— 8.53
1.0	+ 0.02	+ 0.03	+ 0.03	+ 0.02	— 0.02	— 0.10	— 0.25	— 0.48	— 0.86	— 1.48	— 2.47	— 4.14	— 7.07
1.5	+ 0.01	+ 0.03	+ 0.03	+ 0.02	— 0.02	— 0.09	— 0.20	— 0.39	— 0.70	— 1.20	— 2.01	— 3.37	— 5.74
2.0	+ 0.01	+ 0.02	+ 0.02	+ 0.01	— 0.02	— 0.07	— 0.17	— 0.31	— 0.56	— 0.95	— 1.59	— 2.67	— 4.55
2.5	+ 0.01	+ 0.01	+ 0.01	+ 0.01	— 0.01	— 0.06	— 0.12	— 0.24	— 0.43	— 0.73	— 1.23	— 2.05	— 3.49

Alt. 4.5 km.

km	5°	10	15	20	25	30	35	40	45	50	55	60	65
	m												
0.0	+ 0.02	+ 0.03	+ 0.03	+ 0.02	— 0.01	— 0.07	— 0.18	— 0.37	— 0.67	— 1.15	— 1.94	— 3.28	— 5.60
0.5	+ 0.01	+ 0.02	+ 0.03	+ 0.02	— 0.01	— 0.06	— 0.15	— 0.29	— 0.51	— 0.91	— 1.55	— 2.59	— 4.44
1.0	+ 0.01	+ 0.02	+ 0.02	+ 0.01	0.00	— 0.05	— 0.11	— 0.23	— 0.41	— 0.70	— 1.18	— 2.00	— 3.41
1.5	+ 0.01	+ 0.01	+ 0.01	+ 0.01	0.00	— 0.04	— 0.09	— 0.17	— 0.30	— 0.52	— 0.88	— 1.47	— 2.51
2.0	0.00	+ 0.01	+ 0.01	+ 0.01	0.00	— 0.03	— 0.06	— 0.12	— 0.21	— 0.36	— 0.61	— 1.02	— 1.75
2.5	0.00	0.00	0.00	0.00	0.00	— 0.02	— 0.04	— 0.07	— 0.14	— 0.23	— 0.39	— 0.66	— 1.13

Alt. 4.0 km.

km	5°	10	15	20	25	30	35	40	45	50	55	60	65
	m												
0.0	+ 0.01	+ 0.02	+ 0.03	+ 0.02	0.00	— 0.05	— 0.14	— 0.28	— 0.52	— 0.90	— 1.52	— 2.56	— 4.39
0.5	+ 0.01	+ 0.02	+ 0.02	+ 0.02	0.00	— 0.04	— 0.11	— 0.22	— 0.40	— 0.69	— 1.17	— 1.97	— 3.38
1.0	+ 0.01	+ 0.01	+ 0.01	+ 0.01	0.00	— 0.03	— 0.08	— 0.16	— 0.30	— 0.51	— 0.87	— 1.46	— 2.48
1.5	0.00	+ 0.01	+ 0.01	+ 0.01	0.00	— 0.02	— 0.06	— 0.12	— 0.20	— 0.36	— 0.61	— 1.02	— 1.73
2.0	0.00	0.00	+ 0.01	0.00	0.00	— 0.02	— 0.04	— 0.07	— 0.14	— 0.23	— 0.39	— 0.65	— 1.11
2.5	0.00	0.00	0.00	0.00	0.00	— 0.01	— 0.02	— 0.04	— 0.08	— 0.13	— 0.22	— 0.37	— 0.64

$$E_s = E_h \operatorname{tg} N.$$

Lateral error.

Alt. 3.5 km.

km	5°	10	15	20	25	30	35	40	45	50	55	60	65
	m												
0.0	+ 0.01	+ 0.02	+ 0.02	+ 0.02	0.00	— 0.04	— 0.10	— 0.21	— 0.39	— 0.68	— 1.16	— 1.95	— 3.35
0.5	+ 0.01	+ 0.01	+ 0.01	+ 0.01	0.00	— 0.03	— 0.08	— 0.16	— 0.29	— 0.51	— 0.85	— 1.45	— 2.46
1.0	+ 0.01	+ 0.01	+ 0.01	+ 0.01	0.00	— 0.02	— 0.06	— 0.11	— 0.20	— 0.35	— 0.60	— 1.00	— 1.71
1.5	0.00	+ 0.01	+ 0.01	0.00	0.00	— 0.02	— 0.04	— 0.07	— 0.13	— 0.23	— 0.39	— 0.65	— 1.11
2.0	0.00	0.00	0.00	0.00	0.00	— 0.01	— 0.02	— 0.04	— 0.08	— 0.13	— 0.22	— 0.36	— 0.62
2.5	0.00	0.00	0.00	0.00	0.00	— 0.01	— 0.01	— 0.02	— 0.03	— 0.06	— 0.09	— 0.17	— 0.28

Alt. 3.0 km.

km	5°	10	15	20	25	30	35	40	45	50	55	60	65
	m												
0.0	+ 0.01	+ 0.01	+ 0.02	+ 0.01	0.00	— 0.03	— 0.07	— 0.15	— 0.28	— 0.50	— 0.84	— 1.42	— 2.45
0.5	+ 0.01	+ 0.01	+ 0.01	+ 0.01	0.00	— 0.02	— 0.06	— 0.11	— 0.20	— 0.35	— 0.59	— 0.99	— 1.70
1.0	0.00	+ 0.01	+ 0.01	+ 0.01	0.00	— 0.01	— 0.04	— 0.07	— 0.13	— 0.22	— 0.37	— 0.63	— 1.09
1.5	0.00	0.00	0.00	0.00	0.00	— 0.01	— 0.02	— 0.04	— 0.08	— 0.13	— 0.21	— 0.36	— 0.62
2.0	0.00	0.00	0.00	0.00	0.00	— 0.01	— 0.01	— 0.01	— 0.03	— 0.06	— 0.09	— 0.17	— 0.27
2.5	0.00	0.00	0.00	0.00	0.00	0.00	0.00	— 0.01	— 0.01	— 0.01	— 0.02	— 0.04	— 0.07

Alt. 2.5 km.

km	5°	10	15	20	25	30	35	40	45	50	55	60	65
	m												
0.0	+0.006	+0.010	+0.012	+0.009	+0.001	—0.017	—0.050	—0.105	—0.196	—0.342	—0.581	—0.981	—1.686
0.5	+0.004	+0.006	+0.008	+0.006	0.000	—0.012	—0.033	—0.068	—0.126	—0.220	—0.374	—0.632	—1.084
1.0	+0.002	+0.004	+0.004	+0.003	0.000	—0.007	—0.018	—0.039	—0.071	—0.124	—0.211	—0.355	—0.610
1.5	+0.001	+0.002	+0.002	+0.002	0.000	—0.003	—0.008	—0.017	—0.032	—0.056	—0.094	—0.160	—0.273
2.0	0.000	0.000	0.000	0.000	0.000	—0.001	—0.002	—0.004	—0.008	—0.014	—0.023	—0.040	—0.069

Alt. 2.0 km.

km	5°	10	15	20	25	30	35	40	45	50	55	60	65
	m												
0.0	+0.004	+0.007	+0.008	+0.006	+0.001	—0.010	—0.031	—0.066	0.124	—0.216	—0.369	—0.624	—1.072
0.5	+0.002	+0.004	+0.005	+0.004	+0.001	—0.006	—0.018	—0.038	—0.070	—0.122	—0.207	—0.352	—0.604
1.0	+0.001	+0.002	+0.002	+0.002	0.000	—0.003	—0.008	—0.017	—0.032	—0.055	—0.092	—0.157	—0.269
1.5	0.000	0.000	0.000	0.000	0.000	—0.001	—0.002	—0.004	—0.008	—0.014	—0.023	—0.040	—0.069

$$E_s = E_h \operatorname{tg} N.$$

Lateral error.

Alt. 1.5 km.

km	5°	10	15	20	25	30	35	40	45	50	55	60	65
	m												
0.0	+0.002	+0.004	+0.005	+0.004	+0.001	—0.005	—0.017	—0.037	—0.068	—0.120	—0.206	—0.318	—0.599
0.5	+0.001	+0.002	+0.002	+0.002	0.000	—0.003	—0.007	—0.016	—0.031	—0.054	—0.091	—0.156	—0.266
1.0	0.000	0.000	0.000	0.000	0.000	—0.001	—0.002	—0.004	—0.008	—0.014	—0.023	—0.039	—0.067

Alt. 1.0 km.

km	5°	10	15	20	25	30	35	40	45	50	55	60	65
	m												
0.0	+0.001	+0.002	+0.002	+0.002	+0.001	—0.002	—0.007	—0.015	—0.030	—0.053	—0.090	—0.153	—0.263
0.5	0.000	0.000	0.000	0.000	0.000	—0.001	—0.002	—0.004	—0.008	—0.013	—0.022	—0.039	—0.067

Alt. 0.5 km.

	5°	10	15	20	25	30	35	40	45	50	55	60	65
	w												
0.0 km	+0.3	+0.6	+0.7	+0.6	+0.2	—0.5	—1.6	—3.2	—5.4	—8.3	—12.0	—16.7	—22.7
Height	m												
error	+0.003	+0.003	+0.002	+0.002	0.000	—0.001	—0.003	—0.005	—0.009	—0.013	—0.019	—0.028	—0.040
Lateral													
error	0.000	0.000	0.000	+0.001	0.000	—0.001	—0.002	—0.004	—0.008	—0.013	—0.022	—0.039	—0.065